Synthesis and Characterization of Some Triphenylamine (TPA) Based Polyimides with Pendant *N*-Alkoxy Chains

A dissertation submitted to the Department of Chemistry, Quaid-i-Azam University, Islamabad, Pakistan, in partial fulfillment of the requirement for the degree of

Master of Philosophy

In

Organic Chemistry

By

Kinza Shabbir

Department of Chemistry

Quaid-i-Azam University

Islamabad, Pakistan

2023

DECLARATION

This is to certify that this dissertation entitled " **Synthesis and Characterization of Some Triphenylamine Based Polyimides with Pendant n-alkoxy Chains**" submitted by ***Ms. Kinza Shabbir***, is accepted in its present form by the Department of Chemistry, Quaid-i-Azam University, Islamabad, as satisfying the dissertation requirements for the degree of ***Master of Philosophy in Organic Chemistry.***

External Examiner:

Prof. Dr. Zahid Shafiq
Institute of Chemical Sciences
Bahauddin Zakariya University
Multan.

Supervisor & Head of Section:

Prof. Dr. Mrs. Humaira Masood Siddisi
Department of Chemistry
Quaid-i-Azam University
Islamabad

Chairman:

Prof. Dr. Aamer Saeed Bhatti (TI)
Department of Chemistry
Quaid-i-Azam University
Islamabad

The Word of Allah:

"As We have sent unto you a messenger among you,

to recite unto you Our revelations and purify you,

and to teach you the Book and the Wisdom,

and to teach you what you know not"

(Al Baqarah: 151)

Dedicated

To

My Loving Parents

Whose Prayers, Affection, Vigilance, and Inspiration

Helped Me at Every Stage of Life

Acknowledgment

All praises and gratitude to the **ALLAH ALMIGHTY**, the most merciful and the most beneficent who showered His countless blessings upon me and gave me the courage and knowledge to complete my research work. Countless Durood on **PROPHET HAZRAT MUHAMMAD (PBUH)** whose life is the best source of guidance for us.

I extend my deepest appreciation to my discerning supervisor, **Prof. Dr. Mrs. Humaira Masood Siddiqi** for her thought-provoking guidance, patience, motivation, and calm behavior. My sincere thanks to Chairman, **Prof. Dr. Aamer Saeed Bhatti** for providing the necessary research facilities. Special thanks to all faculty members of the Department of Chemistry. I would like to acknowledge my seniors **Alia Manzoor** and **Amna Bibi** and **Javeria** for guiding and encouraging me to achieve this goal. I would also like to pay my thanks to my friend and roommate **Saira Arshad** for her moral support and my lab fellows **Faiqa Sabih and Syeda Iqra Kazmi**, as well as **Rushba Saman, Zartasha Nadeem, Sadia and Rafia** for their cooperation and nice company.

I owe my deepest sense of gratitude to my **Ami** and **Abu**, but no words could be a substitute for their efforts, sacrifices, lot of prayers, and love. A very warm thanks to my sister **Izza Shabbir** my brother, **M. Abdul Wahab** for their caring and supportive company.

Kinza Shabbir

Abstract

Polyimides are available in thermoset and thermoplastic forms, are frequently used in adhesives, coatings, laminates, and encapsulating materials. Their lower solubility, high glass transition temperature, and melting temperature which were attributed to the strong intermolecular interactions which limit their processing and fabrication. The goal of this research was to synthesize triphenylamine-based polyimides having flexible *n*-alkoxy pendant groups in their backbone. Both triphenylamine unit and methylene spacer are packing disruptive thus preventing the formation of strong interaction between polymer chains. For this purpose, three diamine monomers having *n*-alkoxy groups of various chain lengths were synthesized with high purity and yield. The newly synthesized monomer diamines were polymerized using commercially available four dianhydride, 4,4'-(hexafluoroisopropylidine)dipthalic anhydride (6-FDA), 4,4′-oxydipthalic anhydride(ODPA), 3,3′,4,4′-benzophenonetetracarboxylic dianhydride (BTDA), pyromellitic dianyhydride (PMDA), resulting in the formation of eight polyimide films. A two-step thermal imidization procedure was used to synthesize polyimides. The synthesized polyimides were analyzed using physical data, FTIR spectroscopy, NMR, XRD, UV-Vis spectroscopy, cyclic-voltammetry, and DSC techniques. The synthesized polyimide films have appreciable solubility in organic solvents such as NMP, m-Cresol, and DMAc facilitating their processing and fabrication. The optical and electrochemical properties of all the synthesized polyimide films were investigated. The high laying HOMO – (5.00-6.00) and low energy band gap (Eg values: 2.7-3.1) indicated that these polyimides can be employed in optoelectronics.

Table of Contents

Chapter 2: Experimental

Chapter 3: Results and discussions

List of Figures

List of Tables

List of Schemes

List of Abbreviations

BTDA	3,3',4,4'-Benzophenone tetracarboxylic anhydride
CV	Cyclic voltammetry
DMAc	*N,N'* -Dimethylacetamide
DMF	*N,N'* -Dimethylformamide
DSC	Differential scanning calorimetry
6-FDA	4,4'-(Hexafluoroisopropylidene)diphthalic anhydride
FTIR	Fourier transform infrared
HOMO	Highest occupied molecular orbital
LUMO	Lowest unoccupied molecular orbital
OPDA	4,4'-Oxydipthalic anhydride
PAA	Polyamic acid
PIs	Polyimides
PMDA	Pyromellitic anhydride
TPA	Triphenylamine

Chapter 1
INTRODUCTION

1 Introduction

This introduction provides a glimpse into the significance of polymer chemistry, polyimides, and a comprehensive exploration of properties of triphenylamine unit along with its significance in the polymer backbone.

1.1 Origin of Polymer Science

J. J. Berzelius, a Swedish chemist, used the term "polymer" in 1883 to refer the structures containing the ethyne (C_2H_2) unit. Polymers are often referred to as macromolecules because they are large molecules with a high molecular weight, composed of repeating monomeric units. Monomers can be identical or different as they are chemically bonded through covalent bonds to form a chain-like structure.[1] The word polymer is derived from the Greek word "poly" which means "many" and "meros" means "parts and units" reflecting the repeating nature of their structure. In the 19th century, the Polymer industries was widely acknowledged when certain modifications were made in natural polymers which involved the vulcanization of natural rubber by Thomas Hancock in 1820.[2]

1. 2 Polymer Chemistry

Hundreds, thousands, or more of monomer molecules may be bonded together during the polymerization process to generate a polymeric substance with high molecular weight.[3] These materials are studied in the field of polymer chemistry. The polymers show variation in terms of their hardness, flexibility, temperature at which they soften, solubility in water, and biodegradability. Different terminal functional groups also take part in polymer branching.[4] The polymer industry employs more than half of all chemists and chemical engineers on the planet, whose extensive use has been found in a variety of industries, including textiles, medical devices, automobiles, electronics, civil engineering, agriculture, and many others.[5]

The polymer macromolecules have high molecular weight ranging from 2000 to millions in grams/mole. Covalent bonds connect these structural units. Polymers are present in our surroundings. From the naturally occurring biopolymer, such as strand of our DNA to polypropylene, which is a used throughout the world as plastic.[6]

1.2.1 Classification of polymers

Molecular forces, origin, structure, and the mechanism of polymerization all play a role in categorizing polymers.[7]

1.2.1.1 Classification based on origin of source

Natural, semi-synthetic, and synthetic polymers fall in this category.

a) **Natural Polymers:**

These polymers are found in nature and can be extracted. Natural polymers are economical, readily available, and non-toxic. Capable of chemical modifications, potentially biodegradable, and with few exceptions, also have biocompatibility.[8] Different polymers of plant origin are cellulose, hemicellulose, glucomannan, agar, and starch, and from animal origin is chitin, alginates, psyllium, and xanthum gum. Cellulose was isolated from plant matter and discovered in 1838 by the French chemist Anselme Payen. Cellulose is an organic polysaccharide with the formula $(C_6H_{10}O_5)_n$, consisting of several hundred to over ten thousand β(1→4) linked D-glucose units.[9] General structure of cellulose is shown in (Figure 1.1).

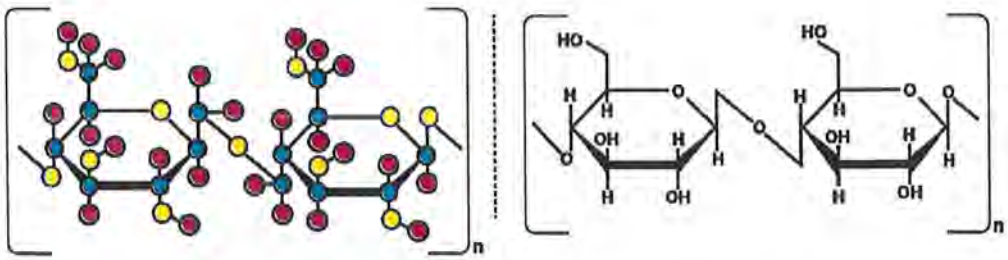

Fig 1.1: Structure of cellulose

Natural polymers play a vital role in drug delivery and drug manufacturing due to their lower toxicity and biocampatibility.[10]

b) **Semi-synthetic Polymers**

Altering the naturally occurring polymers, semi-synthetic polymers are produced. It contains cellulose acetate, cuprammonium silk, and viscous rayons, as well as cellulose nitrate and cellulose acetate. To examplify this, Vulcanization of rubber is shown in

(Figure 1.2). Formation of cross-links between long rubber molecules occurred to get improved elasticity, resilience, tensile strength, viscosity, hardness, and weather resistance.[11]

Fig 1.2: Vulcanization of rubber

c) Synthetic Polymers

Synthetic polymers are sometimes referred to as "Plastics". Bakelite was the first synthetic polymer invented by Baekland in 1907.[12] Although man-made synthetic polymers are virtually as diverse as natural ones, the development of these materials began after the Second World War. Some synthetic polymers, such as polyesters and polyamides used as artificial suture materials, and quickly found their use in medicine.[13] Synthetic polymers offer the achievement of a wide range of physical and chemical properties involving different concentrations of monomeric units, polymerization mechanisms, and structural activity relationships.[14] Synthetic polymers are preferable candidates for bioartificial organ manufacturing with excellent mechanical properties, tunable chemical structures, non-toxic degradation products.[15]

1.2.1.2 Classification based on structure

Subject to the intermolecular linkage, polymers are classified into linear, branched, and cross-linked polymers.

a) Linear Polymers

In this type, the monomer units are linked together linearly, one after the other, without significant side chains or structural deviations. Polymers chains are essentially straight and have minimal branching or cross-linking. Common examples include, Polyvinyl chloride, and polyvinyl acetate, used in electrical wires. A long continuous chain of carbon-carbon bonds linked together by weaker van der walls forces and hydrogen bonding.[16]

b) Branched-chain polymers

Regular or irregular attachment of side chains to a polymer's backbone chain give rise to branched chain polymers. They possess low tensile strength, melting points, and densities. They gained attention due to their wide range of applications in phase-separating systems, as an emulsifier and interfacial compatibilizers, resulting from a great diversity of polymer topologies, compositions, and morphologies.[17]

c) Cross-linked polymer

Long polymer chains are cross-linked through chemical linkage to create a 3D matrix of interconnected polymer chains that have more rigid and potentially better-defined shapes. These polymers have elastic behavior and good mechanical properties such as Bakelite and melamine.[18]

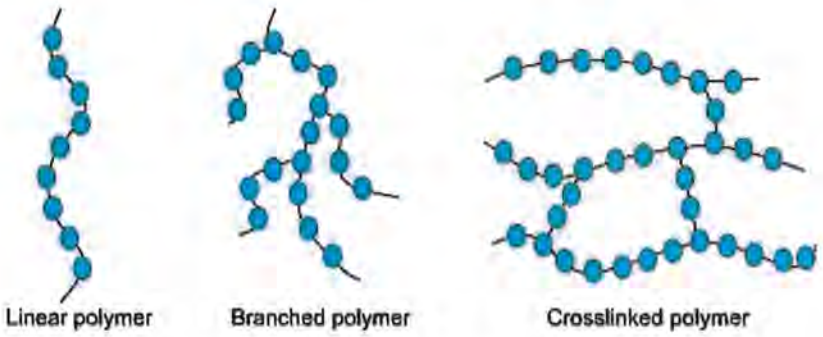

Fig 1.3: Structural representation of polymers

1.2.1.3 Classification based on molecular forces

Based on molecular forces, categorized into thermosetting and thermoplastic polymers.

a) Thermosetting polymers

Two or more components chemically react with each other results in the formation of three- a dimensional network. It typically exhibits high strength, rigidity, and thermal stability. They are lightweight, low cost, and easy to process making thermosets attractive for applications ranging from electronics packaging to the matrices of fiber composites.[19]

b) Thermoplastics polymers

The term was first introduced by General Electric Co. in the 1960's and they described it as a polymer alloy able to replace metals in many applications.[20] Due to availability in various colors and physical forms such as films, filaments, and powders that are widely employed in the dental industry.[21] The melting point ranges between 230 and 290 °C, and the technology demands mold casting.[22] One of the most well-known thermoplastics is polythene, well-known for its use in manufacturing and engineering circles for its adaptability as a packaging material.[23] Dynamic covalent network in thermoplastic and thermosetting polymers is shown in (Figure 1.4).

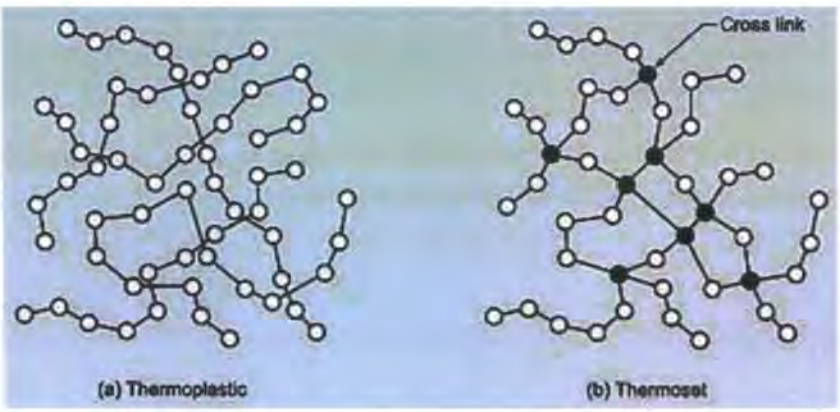

Fig 1.4: Dynamic covalent network in Thermosetting and thermoplastic polymers[24]

1.2.1.4 Classification based on polymerization mechanism

Based on the polymerization mechanism, categorized as addition polymers and condensation polymers.

a) Addition polymers

It is also termed group transfer polymers in which smaller unsaturated molecules react together through a rapid chain reaction initiated by a chemical catalyst.[25] It involves three distinct steps.[26]

1. Chain initiation—chain initiation refers to the initiation of the polymerization process by introducing a specific molecule or chemical, usually called as initiator that can initiate the formation of polymer chains. Based on the initiator it can be a radical (free radical polymerization), cation (cationic polymerization), anion (anionic polymerization), and organometallic complex (coordination polymerization).

2. Chain propagation—fundamental step, during which polymer chains continue to grow by adding monomer units one at a time, ultimately leading to the formation of long and interconnected polymer molecules. Chain propagation is responsible for the elongation of polymer chains.

3. Chain termination—the radical, cation, or anion is "neutralized" stopping the chain propagation

b) Condensation Polymers

Condensation polymers are formed when smaller molecules or monomers react with each other results in the formation of large structural units with the release of small molecules such as water, and methanol as byproduct.[27] Development of very first sticky

amber colored resin named Bakelite was made in 1907 by an American chemist Leo H. Baekeland.[28] The molecular weight of the polymer resulting from condensation polymerization increases quickly during the last stages of polymerization.[29]To exemplify this, formation of nylon 6,6 is shown in (Figure 1.5).

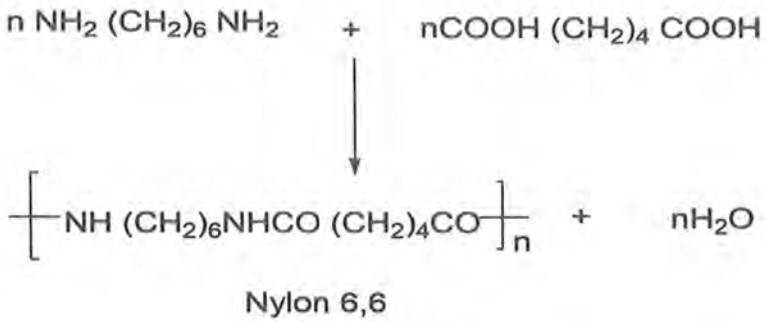

Fig 1.5: Structure of nylon 6,6[30]

1.3 Polyimides

Historical background, introduction, synthesis and applications of polyimides will be discussed in this section.

1.3.1 General aspects

Since the dawn of civilization, polymers have been essential to many fields. The Olmec, Maya, and Aztecs had been using the latex sap of "caoutchouc" trees (natural rubber) for many generations to produce balls and containers until it eventually found its way from South America to Europe in the 16th century.[31] The work on the modification of natural polymers by Braconnot, Parkes, Ludersdorf, Hayard and many others led to several significant advances in the field.[32] They made contributions that led to the discovery of materials including celluloid, rayon, vulcanized rubber, and ultimately Bakelite. In his seminal paper "Über Polymerization," which was published in 1920, Hermann Staudinger asserted that polymers were just long chains of atoms joined by covalent bonds. Long discussions ensured but finally his work was acknowledged by the scientific community.[33] Polyimide known as PI, is a class of high-temperature engineering polymers that contain imide groups. Sp^3 hybridized nitrogen bonded to two adjacent carbonyls formed when diamine was made to react with dianhydride in a polar aprotic solvent under an inert atmosphere. When diisocyanate reacts with dianhydride, it results in polymerization with the elimination of carbon

Dioxide.[34-35] The general structure of polyimide is shown in (Figure 1.6) where R groups might be alkyl or aryl.

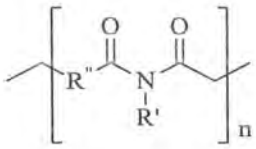

R'/R"=Alkyl/Aryl

Fig 1.6: General structure of polyimide

Different groups or functionalities can be introduced in diamine and dianhydride to study the impact of structural variation on flexibility, stiffness, solubility, stability, and other properties of polymer.[36-37]

The first discovery of polyimide was made in the 1950s at DuPont.[38] A typical polyimide called Kapton was created via a condensation process utilizing 4,4′-oxydianiline and pyromellitic dianhydride.[39] Bogart and Renshaw reported the discovery of the polyimide in 1908. They originally discovered 4-amino phthalic anhydride, which formed polyimide with a high molecular weight.[40] After that, Edward and Robinson used the fusion process to synthesize the semi-aliphatic polyimide employing diamines and tetra acid as the basic materials.[41] Examples of high-class polymers is shown in (Figure 1.7).

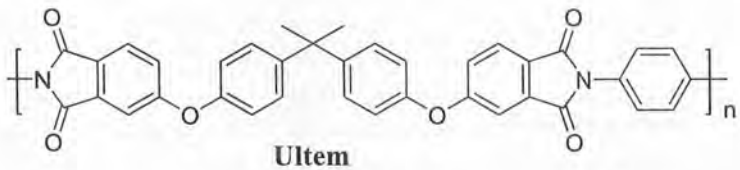

Ultem

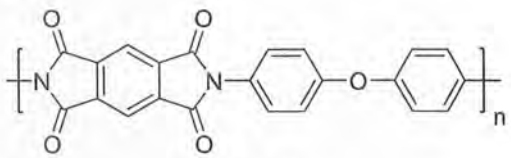

Kapton

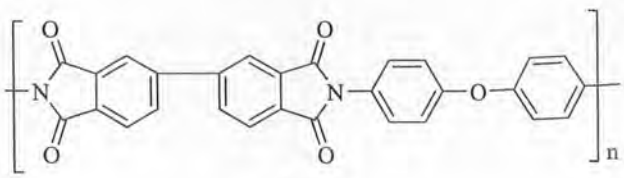

Upilex

Figure 1.7: Examples of commercial polyimides[42-44]

1.3.2 Classification of Polyimides

Based on the structure, polyimides are classified into three types;

a) Aromatic Polyimides

Aromatic polyimides are a class of high-performance polyimides synthesized from aromatic moieties which include diamine and dianhydride. They are renowned for their high levels of having excellent electrical insulating qualities, great mechanical toughness, low dielectric constants and dissipation factors, strong radiation and wear resistance, and high thermal stability. They are capable of being processed into a wide range of products, including films, fibers, carbon fiber composites, and engineering materials.[45-46] Aromatic polyimide films found applications in several high-tech industries including electric insulation[45-52], electronic packaging,[53-54]and aerospace[55-62] due to their utmost stability attributed to thermal, mechanical and electrical properties. Examples of commercially available aromatic polyimides is shown in (Figure 1.8).

Kapton

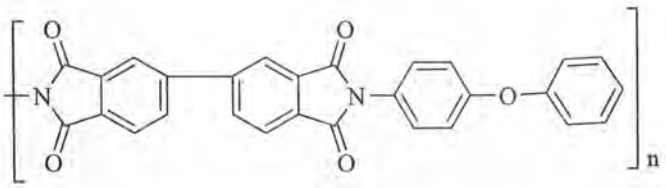

Upilex

Fig 1.8: Example of commercially available aromatic polyimides[63]

b) Semi-aromatic Polyimides

Semi-aromatic polyimides exhibit a combination of aromatic and aliphatic characteristics in their molecular structure. They exhibit a balance of properties between fully aromatic and aliphatic polyimides. Semi-aromatic polyimides prized for their exceptional combination of thermal, mechanical, and chemical properties, making them invaluable in numerous high-tech and demanding applications. Examples of synthesized colorless and optically transparent semi-aromatic polyimides is given below in (figure 1.9).

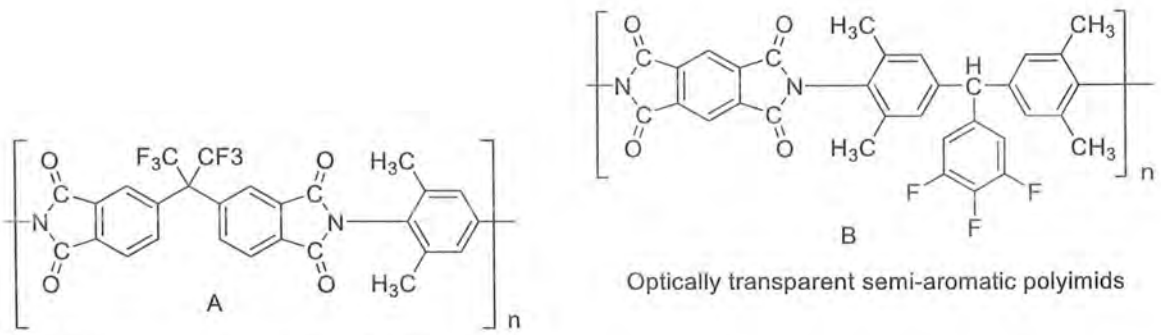

Fig 1.9: Examples of semi-aromatic polyimides A[64], B[65]

c) Aliphatic Polyimides

These polymers have a linear or branched aliphatic (non-aromatic) backbone structure. In addition to having a well-controlled molecular weight, a tolerable intrinsic viscosity, good transparency, increased solubility, low dielectric constants, a high glass transition temperature, and marginal thermal and mechanical stability, these polyimides also have good solubility.[66] To exemplify this, polyimides with rigid adamantyl or flexible aliphatic units is shown in (Figure 1.10).

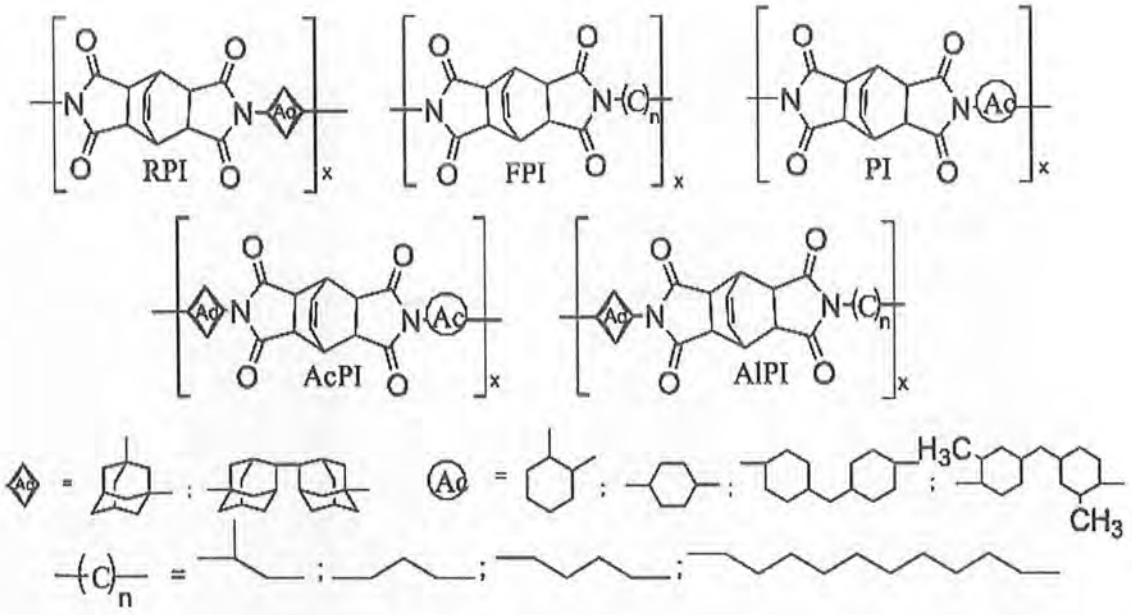

Figure 1.10: Aliphatic polyimides with rigid adamantly and flexible aliphatic units[66].

1.3.3 Synthesis of Polyimides

Polyimides can be synthesized using two approaches, one-step and common two-step polycondensation techniques as shown in (Figure 1.11). In one-step process, polyimide was formed by the direct polymerization of diamine and dianhydride in high boiling solvent. It involves keeping the polyimide in solution during the entire reaction.[67] While in the two-step polycondensation technique, first step involves the reaction of dianhydride and diamine in solvents such as NMP or DMAc under appropriate conditions to form poly(amic acid) precursors. This step involves the formation of amide linkages between the monomers. In the second step, polyamic acid is subjected to thermal imidization at high temperatures to get polyimides.[68-70]

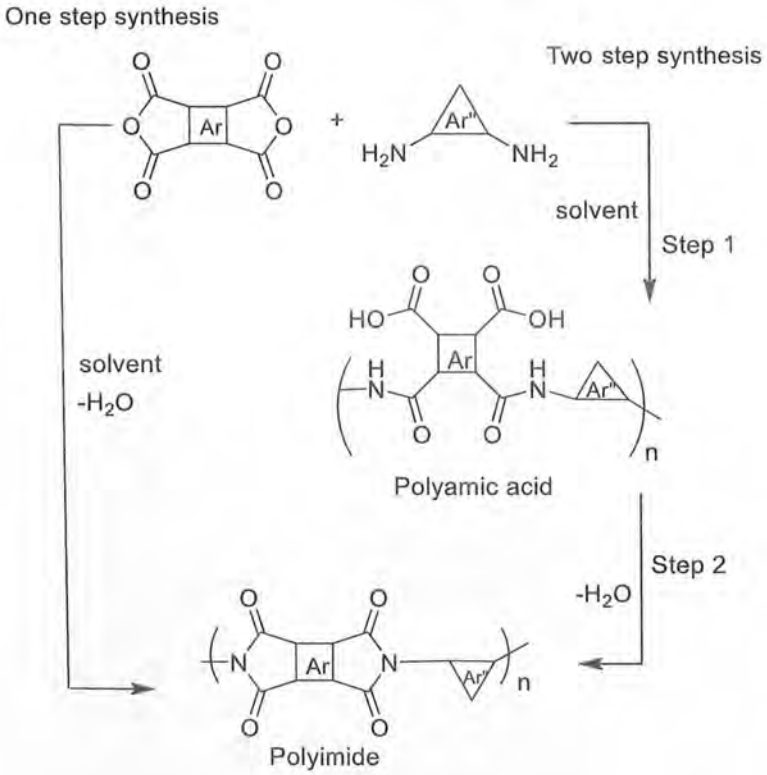

Figure 1.11: Two-way synthesis of polyimides

a) Thermal Imidization

Poly(amic acid) is converted into polyimide by the process of imidization, one of which is thermal imidization. When a polymer is needed in the form of coating, film, or fiber, thermal imidization is performed. Poly(amic acid) was poured onto a glass slide or petri dish and heated gradually between 50 and 300 °C.[71-72] During this heating process,

solvents evaporate, and the second step results in cyclodehydration and imidization. At 300 °C, imidization is completed with a 92-99% conversion rate to polyimide.[73]

b) Chemical Imidization

Chemical imidization is another process for turning poly(amic acid) into polyimide. This is possible at a temperature that is much lower than the temperature required for thermal imidization. This process includes cyclodehydration at a temperature between 20 and 80 °C utilizing a chemical dehydrating agent, often with a tertiary amine (base) as a catalyst. The most often used desiccants are ethanoic anhydride, benzoic anhydride, propionic anhydride, and n-butyric anhydride. Catalysts include triethyl amine, isoquinoline, lutidine, pyridine, and other amines.[73-74] Both soluble and insoluble polyimides may be employed at lower temperatures without compromising on their high molecular weights.[75] However, it provides a more complex and challenging procedure to be carried out.[76]

1.3.4 Applications of Polyimides

Polyimides have been renowned for their exceptional thermal stability, chemical resiliency, and mechanical toughness. Due to these characteristics, polyimides find applications in various industries and fields.

a) Electroluminescent polyimides

Polyimides with highly efficient chromophores can be used in a larger variety of optoelectronic devices. Polymers with good thermal and organo-soluble properties are being synthesized to make polymer chromophores for electroluminescent devices.[77] Electroluminescent devices are developed based on the solubility, thermal stability, and structural properties of the polyimides.[78] This kind of polyimide includes the EL polyimide Poly(2,5-dimethoxy-p-phenylene vinylene).

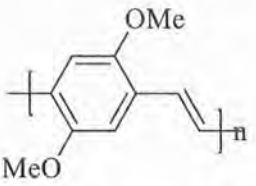

Poly(2,5-dimethoxy-p-phenylene vinylene)

b) **Polyimide Memory**

Polymer memory is significantly faster and less expensive than silicon memory.[79] Data is stored differently in polymer memory than it is in silicon memory. A polyimide memory stores data based on larger and smaller responses of conductivity to an applied voltage, as opposed to decoding "0" and "1" from the number of charges stored in the cell.[80] Polyimide memory devices may be able to store more information than traditional silicon memory systems. Each memory cell's polymer is sandwiched between electrodes to form a polymer memory device.[81-83] For instance, PEDOT poly(3,4-ethylenedioxythiophene) is a conducting polymer used in polymer memory.

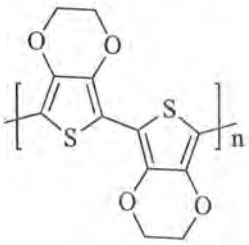

Poly(3,4-ethylenedioxythiophene)

c) **Electrochromic Polyimide**

Electrochromism is the process of altering a compound's color by applying potential at changing voltages using a battery. The only technological examples of this interesting property are chameleon polymers, large-scale electrochromic displays, and anti-glare glasses.[84] Electrochromic property depends upon the redox activity of polyimides.[85-86] When a voltage is supplied, an electrochromic polyimide called Poly(ethernaphthalimide) changes color going from being colorless (0.0 V) to red (1.1 V) then to dark blue (1.8 V).

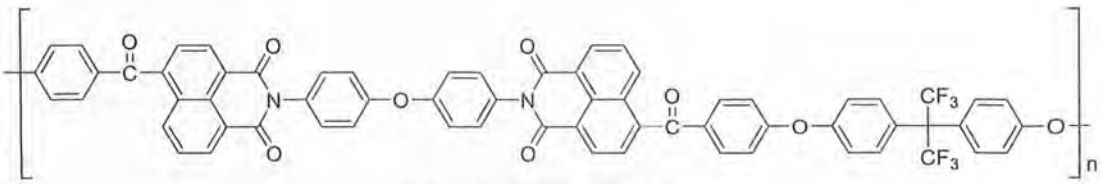

Poly(ethernaphthalimide)

1.4 Triphenylamine (TPA)

The chemical formula of triphenylamine is $(C_6H_5)_3N$. Triphenylamine is not basic, in contrast to most amines. It appears as a monoclinic, white crystalline solid at ambient temperature. It mixes well with diethyl ether and benzene, but it is essentially insoluble in water and very slightly soluble in ethanol. Charles J. Fox and Arthur L. Johnson discovered triphenylamine's three-dimensional propeller-shaped structure in 1966.[87] It is an ammonia derivative having three electron-rich aromatic rings with propeller geometry having a 120^0 dihedral angle between the phenyl rings, as well as an electroactive nitrogen core. All of the hydrogens have been replaced by aryl groups. The molecular geometry of TPA is a result of the interaction between two opposing forces. The first one is the stabilization of the electron systems by resonance, and secondly the steric repulsion between the protons of nearby phenyl rings. Steric repulsions are lessened by tilting the phenyl groups away from the plane, and the -electron systems of the phenyl groups are best conjugated in a planar shape (D3h symmetry). These two components combine to form a propeller-like structure (C3 symmetry).[88]

Conventionally, triarylamines are synthesized by Ullmann condensation of aryl iodides and diaryl amines with copper in the form of metal, alloy, Cu(I) or Cu(II) salt. The major limitation of this method is sensitivity to catalyst type and low to moderate yield of amines and elevated temperature.[89] Recently, milder Ullmann-type techniques for *N*-arylation of aniline employing copper-phenanthroline complexes as catalysts have been developed. These protocols are simple and mild and avoid the use of air sensitive and expensive phosphine ligands or additives.[90] Iron-catalyzed aromatic amination for synthesizing diarylamines and triarylamines has also been successfully developed.[88]

1.4.1 Structural properties and applications of triphenylamine

A molecule with a propeller-like shape and strong thermal and morphological stability can result in emerging optoelectronic features and potential applications. Importantly, the remarkable stability of the TPA corresponds to its strong oxidizability and intriguing electroactive and photoactive features.[91] Consequently, TPA derivatives or polymers are frequently utilized as photoconductors, light-emitting materials[92], electrochromics[93], and particularly materials that transmit holes, solar cells, organic field-effect transistors, organic light-emitting diodes, and photorefractive materials.[94-

[98] It is a very effective species for transporting holes due to the stability of its radical cation.[91] Due to its potential as hole transporting species, the family of adaptable redox-active chemicals known as triphenylamine (TPA) derivatives has drawn a lot of interest. [99-100] Recently, reports on TPA-based heterocyclic compounds, such as carbazoles and benzimidazoles, have been published.[101] The improved optical, photovoltaic, and phosphorescent characteristics of these compounds were evident that TPA molecules are distinguished by two features.

1. High oxidize ability due to their electron-rich nature
2. The development of a stable ammonium radical cation that aids in charge transfer.

   (Figure 1.12) illustrates the structure and some application of triphenylamine. Triphenylamine, for instance, is frequently utilized as a photoconductor in the Xerox® process in laser printers and photocopiers due to its efficiency as a hole conductor.[102]

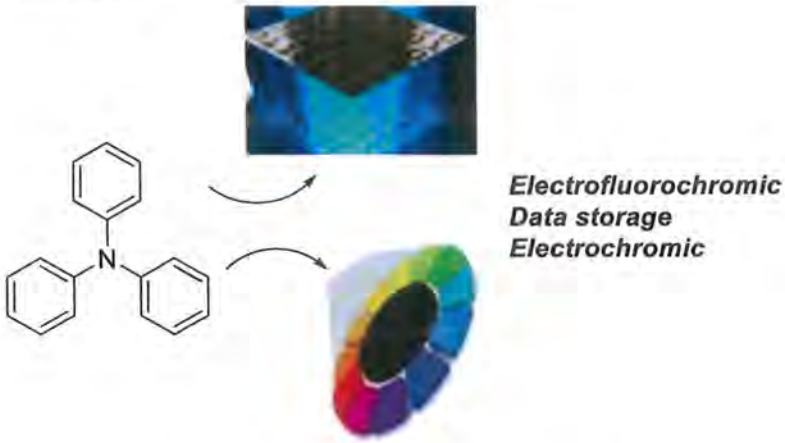

Fig 1.12: Structure of Triphenylamine[102]

Radical cations of parent triphenylamine unit are highly reactive and thus could not be isolated in pure form. Due to high reactivity can undergo dimerization and polymerization.[103] (Figure 1.13) and (Figure 1.14) depicts the structural representation of TPA-radical cation and dimerization respectively.

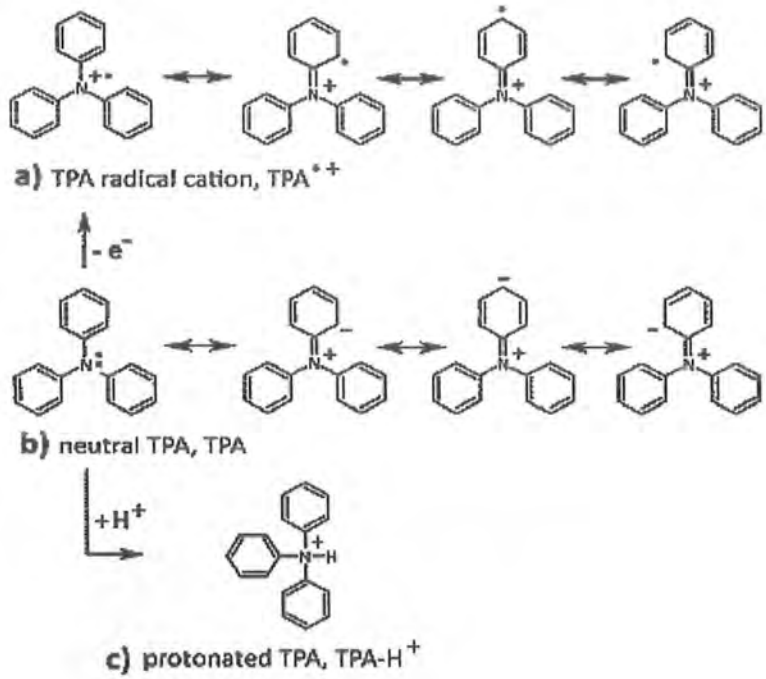

Fig 1.13: Structural representation of TPA radical cation upon oxidation

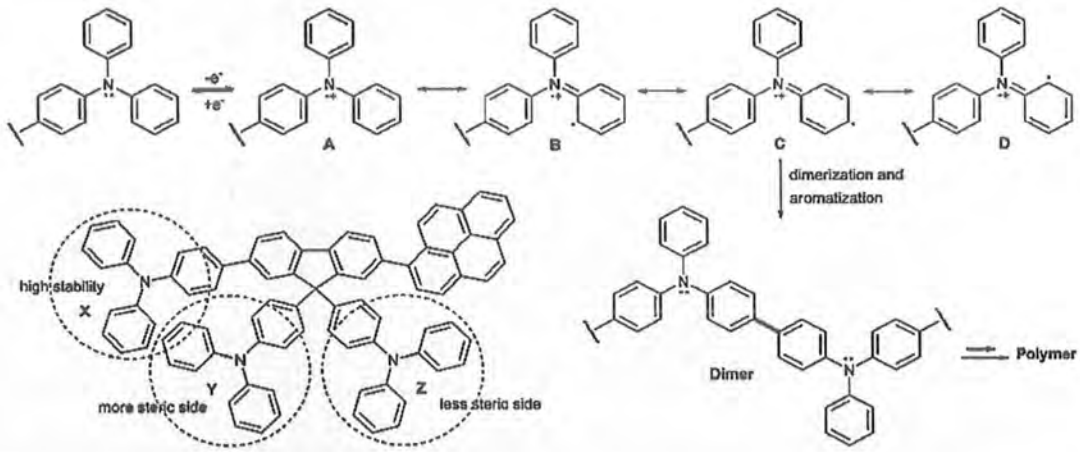

Fig 1.14: A proposed oxidation and electrochemical reaction of the triphenylamine moiety[104]

Researchers thought that TPA would be an active area of research that would encourage to create TPA based materials with multiple functionalities for various applications.[105]

1.5 Triphenylamine-based Polyimides

The class of polyimide polymers in which the polymer backbone incorporates triphenylamine moiety. They were reported for the first time in 1991 by the reaction of 4,4'-diamino TPA with various tetracarboxylic dianhydrides[106-108] shown in (figure

1.15). These polymers possess high thermal stability, excellent solubility in organic solvents, high glass transition temperature, and appreciable char yields.[109]

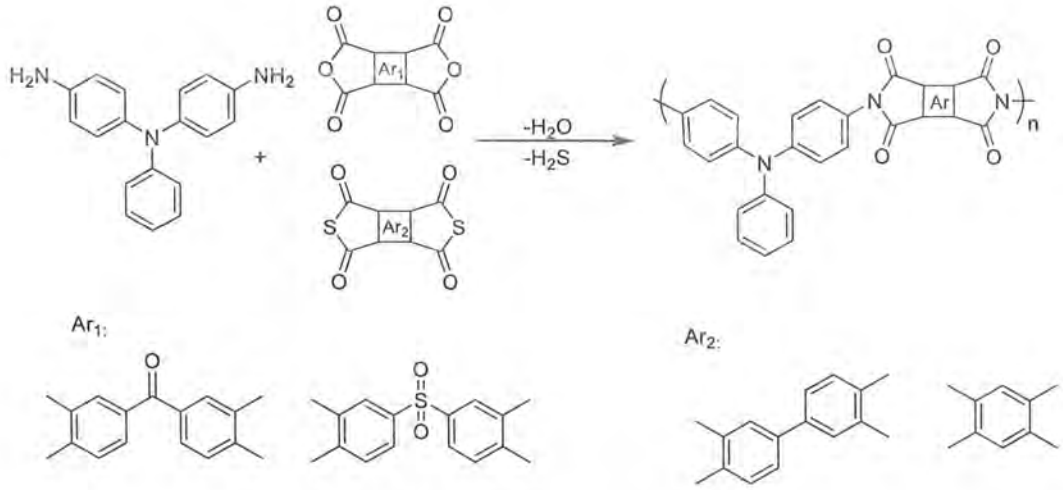

Fig 1.15: Synthesis of first TPA-based Polyimides[109]

After that a lot of work has been done to investigate the properties and applications of triphenylamine based polyimides. In 2005, EC properties of aromatic polyimides containing TPA groups from a newly synthesized diamine, *N*,*N*-bis(4-aminophenyl)-*N*',*N*'-diphenyl-1,4-phenylenediamine, and various tetracarboxylic dianhydrides by polycondensation reactions has been disclosed.[102] In 2006, Kang's group reported a linear PI (TP6F-PI), which contains TPA unit as the electron donor and phthalimide units as the electron acceptors, exhibited dynamic random access memory (DRAM) behavior. Since then, TPA and its derived structures were the most frequently used electron donors in preparation of resistive memory devices due to their outstanding charge transport ability and electrochemical stability.[151] Recent advances has been made in triphenylamine based electrochromic materials and polymers in 2019. They showed great potential for low energy-consumption displays, light-adapting mirrors in vehicles, and smart window applications.[130]

1.5.1 Significance of triphenylamine (TPA) unit in the polymer backbone

High-performance polyimides are a class of advanced polymers known for their exceptional combination of thermal stability, mechanical strength, chemical resistance, and electrical insulating properties.[110] High-performance polyimides gained much more attention as popular synthetic material of the 21st century. Over the past three decades, a large number of polymer chemists and physicists have focused a great deal of their

attention on the synthesis and development of HPPs. Under difficult operating conditions, HPPs often show exceptional chemical and dimension stability. By adding aromatic compounds to polymer chains, Hill and Walker first developed the HPPs, which significantly improved thermal stability.[111] As a result, HPPs, which typically contain aromatic backbone in their structure, have been in great demand to suit the demands of aerospace, military, electronic, and numerous industrial applications since the late 1950s. Thus, the aromatic polyimides are more appealing than other HPPs due to their exceptional properties which include inherent flame retardancy, high mechanical strength, oxidative and thermal stability along with good chemical and radiation resistance.[112-121]

However, the presence of a rigid backbone makes processability and fabrication of these high-performance polyimides difficult which were attributed to the strong intermolecular interaction which results in high glass transition and melting temperature along with low solubility in organic solvents.[122-124] As a result, the incorporation of bulky packing disruptive TPA facilitates overcoming these restrictions without compromising on thermal properties. Polyimides with triphenylamine backbone are mostly amorphous, along with good thermal stability, and film-forming ability which help in the fabrication of large area, thin film optoelectronic devices.[125-127]

1.5.2 Application of TPA-based Polyimides

Due to their distinctive characteristics, triphenylamine-based polyimides have gained interest in a variety of applications.

a) Electrochromic material

Due to mono-electron oxidation in arylamines, they form a radical cation along with the notable color change in organic solution. Triphenylamine has an electron-rich nitrogen center and can be easily oxidized to form radical cation which leads to outstanding color change.[128] They have remarkable applications in EC anti-glare car review mirrors, optical storage, sunglasses, military-grade protective camouflage eyewear, and smart windows for usage in buildings and automobiles.[129]

Fig 1.16: Electrochromic behavior of TPA derivtives[130]

b) Organic light-emitting diodes

Triphenylamine-based polyimides have been used as hole-transporting materials in OLED devices. [131] They facilitate the efficient injection and transport of holes (positive charge carriers) in OLEDs, transistors, and photorefractive materials leading to improved device performance and longer operational lifetimes.[132]

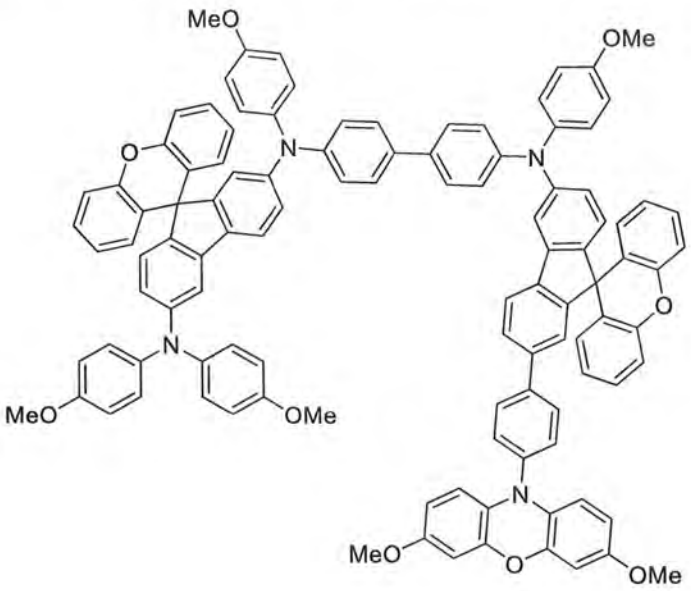

Fig 1.17: TPA- derivatives in High-efficiency solar cells[133]

c) Gas separation membranes

Some polyimides, including those containing triphenylamine moieties, are used in gas separation membranes. These membranes can be used for separating gases such as

carbon dioxide from flue gas or natural gas purification due to their high selectivity and permeability.[134] (Figure 1.18) depicts the structure of highly gas permeable polyimide.

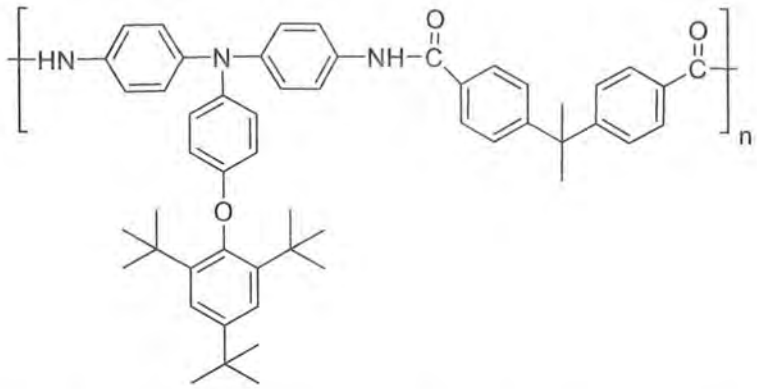

Fig 1.18: TPA based highly gas permeable polyimide[135]

d) Polymeric memory devices

Triphenylamine-based polyimides have gained attention in the development of polymeric memory devices due to their unique electronic and charge transport properties. These materials are considered promising candidates for organic memory applications, including organic resistive random-access memory (RRAM) and organic ferroelectric memory devices.[136] Ree and co-workers also propose a series of TPA-based PIs for memory characteristics.[137-138] AAPT-6FDA is a TPA based polyimide used in memory device applications.

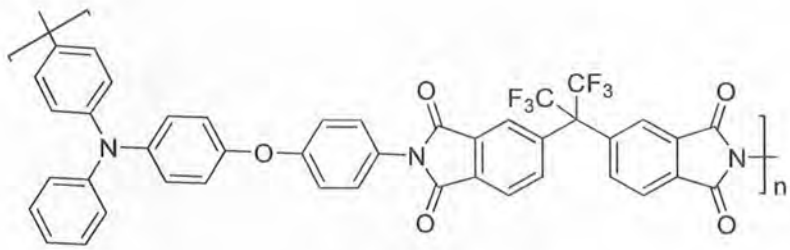

AAPT-6FDA[136]

e) Other applications[109]

Triphenylamine-based polyimides have found versatile applications across various industries due to their unique combination of properties. These polyimides exhibit excellent thermal stability, mechanical strength, and electrical insulating

characteristics. One notable application is in the field of organic electronics, where they serve as essential materials in the fabrication of organic light-emitting diodes (OLEDs) and organic photovoltaic (OPV) devices. Triphenylamine-based polyimides can function as hole-transporting materials in OLEDs, aiding the efficient movement of positive charge carriers, leading to improved device performance and longer operational lifetimes. Additionally, their chemical resistance and stability make them valuable candidates for protective coatings and insulating layers in the electronics and aerospace industries. Their versatility, combined with their excellent thermal and electrical properties, positions triphenylamine-based polyimides as promising materials for future innovations in advanced technologies and high-performance applications.

1.6 Objectives

This research work aims to synthesize TPA-based diamines with different *n*-alkoxy pendant groups, to develop semi-aromatic polyimides. Although, aromatic polyimides are known for their exceptional thermal, mechanical, and electrical properties but the main disadvantages of aromatic polyimides are their yellowish nature and low solubility which limits their applications. So, polyimides with optical transparency and increased solubility was planned to synthesize without sacrificing their qualities, such as their superior mechanical and high thermal stability with a wide range of applications in flexible electronic or micro-optical devices displays, memory, lighting, solar cells, sensors and waveguides.[139-145] The effect of the alkyl chain with different numbers of carbon atoms on the optical and electronic properties of polyimides will be investigated. It was intended to increase the solubility of polyimides without compromising their thermal stability by adding bulky pendant groups at the para position of TPA unit. Thus, the proposed synthetic scheme in this project will be designed to:

- Increase the electron density of TPA molecules in the main polymer chain so they can act as electron donors.
- Examine their electrical and optical properties.

1.7 Plan of work

To attain our objectives, this work was planned in following Parts:

Part A- Synthesis of aromatic diamines having *n*-alkoxy pendant group.

Part B-Synthesis of polyimides from synthesized diamine

Part C- Characterization of the synthesized monomers and polyimides

Aromatic diamines having *n*-alkoxy pendant groups will be synthesized following the general (scheme 1.1).

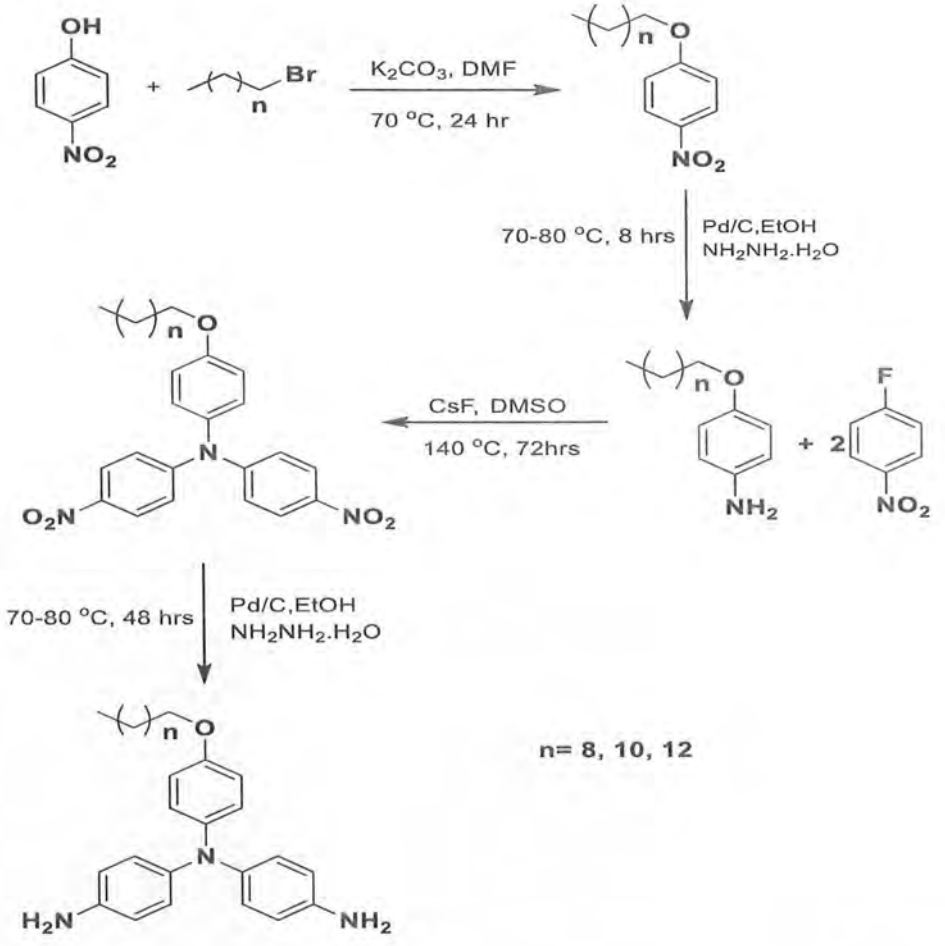

Scheme 1.1: General scheme for the synthesis of alkoxy substituted diamines

Different polyimides will be prepared by reaction of synthesized *n*-alkoxy diamines with different dianhydrides in polar aprotic solvent. The general (scheme 1.2) for the synthesis of polyimides is given below.

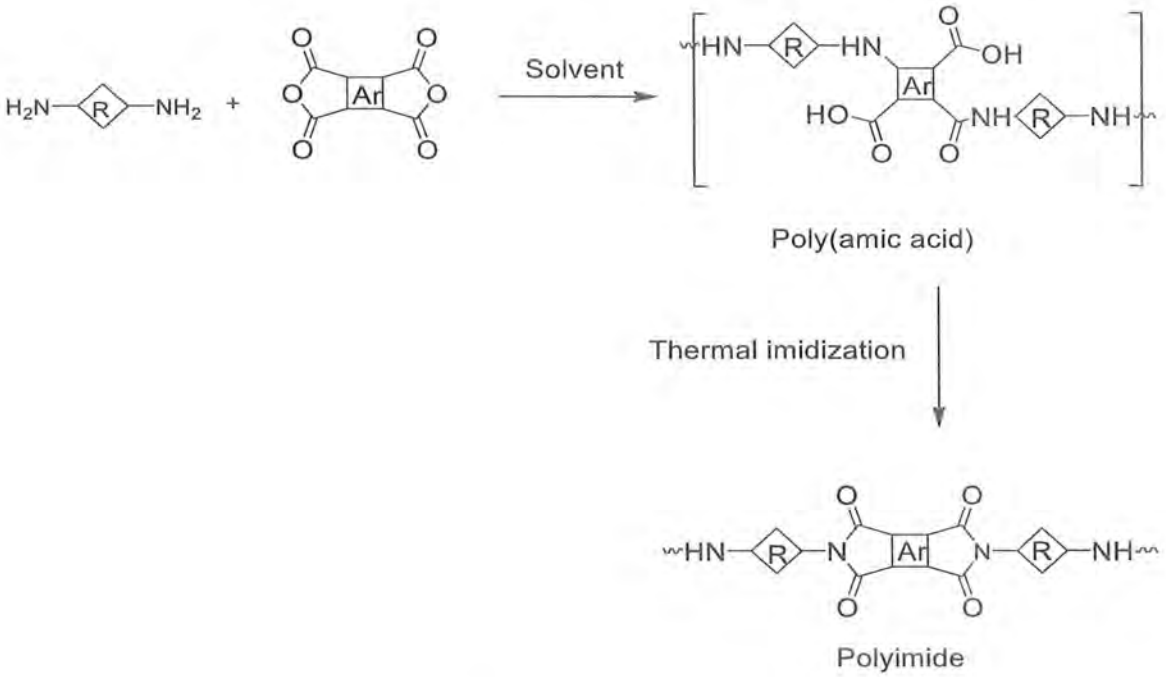

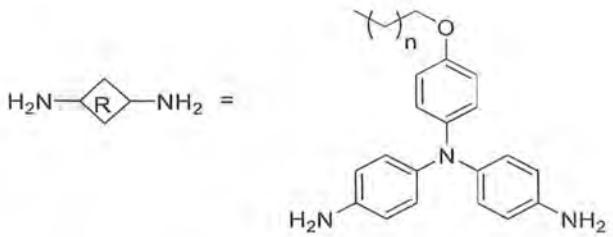

n= 8, 10

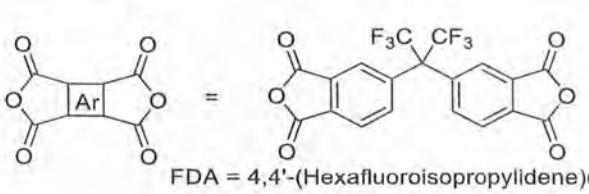

FDA = 4,4'-(Hexafluoroisopropylidene)dipthalic dianhydride

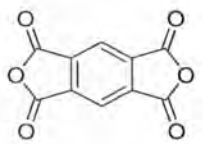

PMDA=Pyromellitic dianhydride

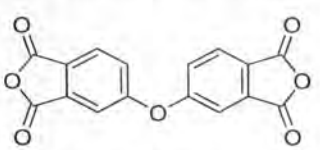

ODPA= 4,4'-Oxydipthalic dianhydride

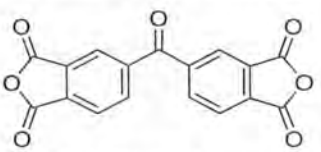

BTDA=Benzophenone tetracarboxylicacid dianhydride

Scheme 1.2: General scheme for the synthesis of triphenylamine-based polyimides

Chapter 2

EXPERIMENTAL

This section serves as a detailed account of materials used, characterization techniques, and procedure, offering a comprehensive view of the scientific rigor applied to our research.

2.1 Materials

All the reagents and chemicals that have been used were pure unless otherwise specified. A list of Chemicals with their suppliers is given below.

Chemicals	Manufacturer
4-nitrophenol (99%), 1-Fluoro-4-nitrobenzene (99%), Alkyl halides (99%) Anhydrous potassium carbonate (99.5%), Pd/C (10% on C), Cesium fluoride (99%) *N*-Methyl pyrrolidine (99%), Dimehthylsulfoxide (99%), *N, N'* -Dimethylacetamide (99%), *N, N'* -Dimethylformamide (99%),	Sigma- Aldrich
4,4'-(Hexafluoroisopropylidene)diphthalic anhydride (6FDA, 99%) 4,4' -Oxydipthalic anhydride (ODPA, 98%) 3,3',4,4'-benzophenone tetracarboxylic dianhydride (BTDA, 98%) Pyromellitic Dianyhydride (PMDA, 99%)	Tokyo Chemical Industry

2.2 Purification of solvents

High-purity solvents are crucial to obtain accurate and reliable results. Simple approaches were taken into consideration for purification purposes. A short rundown of the approaches used is provided below:

Ethanol (boiling point: 78 °C), ethanol was refluxed for three hours with CaO for drying, it was distilled and then preserved on molecular sieves.

***N, N'*-Dimethylformamide** (boiling point: 153 °C) was dried using CaH_2 as a drying agent, followed by vaccum distillation.

***N*-methyl pyrrolidone** (boiling point: 202°C) was used as received without further purification.

Ethyl acetate (boiling point: 77 °C) was agitated for a whole night with CaH_2 for drying purposes before being distilled and then preserved on molecular sieves.

***n*-Hexane** (boiling point: 69 °C) *n*-hexane was stirred overnight in the presence of CaH_2 for drying solvent, distilled, and saved using molecular sieve.

2.3 Characterization Techniques

Various characterization techniques have been used to evaluate the structure of synthesized compounds. This section will go through the instrumentation details and settings for the experiments.

2.3.1 Thin Layer Chromatography (TLC)

The completion of the reaction and purity of the product were inspected using the TLC. Ethyl acetate and *n*-hexane in various ratios were used as solvent systems. An alumina TLC plate with a layer thickness of 0.2 mm of precoated silica gel (H-F_{254}, E. Merk) was used and the developed chromatograms were exposed to UV light at λ_{max} = 254-366 nm.

A solvent system of different ratios was used:

n-Hex: EtOAc (3:7)

n-Hex: EtOAc (7:3)

n-Hex: EtOAc (9:1)

2.3.2 Melting Point

The melting points of all synthesized precursors were determined in an uncovered open-end capillary tube using the Stuart SMP30 instrument.

2.3.3 Infrared Spectroscopy using the Fourier transform (FTIR)

This approach was used to spot various functionalities in molecules. Using the attenuated total reflectance transform technique (ATR), an FTIR spectrometer (Bruker α-P model) records spectral data spanning from 4000 cm^{-1} to 500 cm^{-1} at ambient temperature.

2.3.4 X-Ray Diffraction Examination (XRD)

The crystallographic nature of polyimides was examined by XRD. It was performed using a PANalytical X-ray spectrophotometer with a Cu anode and K alpha radiation operating in the 2θ=20-80° range.

2.3.5 Cyclic Voltammetry

The Gammery cyclic voltammeter was used for CV having a three-electrode system consisting of platinum wire as an auxiliary, ITO as a working electrode, and a typical calomel electrode as a reference electrode. As a supporting electrolyte, dry acetonitrile containing 0.1 M $LiClO_4$ was used.

2.3.6 Ultraviolet-visible Absorption Spectroscopy

To study the impacts of auxochromes and chromophores, a double-beam Shimadzu UV/Vis spectrophotometer was used to record UV-visible spectra of all the synthesized monomers from 250 nm to 400 nm in NMP as solvent. The energy band gaps were calculated using the following equation.

$$E = hc/\lambda \quad \text{.....2.1}$$

2.3.7 Differential Scanning Calorimetry (DSC)

To determine the glass transition temperature (Tg), DSC was performed in an inert atmosphere from room temperature to 300 °C at a heating rate of 10 °C/min using the DSC 25 TA instruments.

2.4 Synthesis of precursor compounds

The following section provides a detailed procedure for the synthesis of precursor compounds.

2.4.1 General procedure for the synthesis of 1-alkoxy-4-nitrobenzene precursor (MN 1-3)

Mononitro precursors were synthesized via *O*-alkylation following a reported procedure.[152]

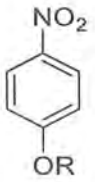

Synthesis was carried out by stirring 4-nitrophenol with base in DMF at 60 ^{0}C for half an hour in an inert atmosphere. After that, alkyl bromide was added dropwise and heated for 24 hours at 70 ^{0}C. TLC was performed to observe the progress of the reaction. On completion, off-white to light yellow precipitates appeared after pouring the reaction blend on crushed ice, which were collected, and then washed several times with water before recrystallization with DCM to get pure product.

2.4.1.1 Synthesis of 1-(decyloxy)-4-nitrobenzene (MN-1)

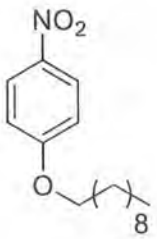

MN-1 was synthesized using (3.5 mmol, 0.5 g) of 4-nitrophenol, (4.5 mmol, 0.6 g) of anhydrous potassium carbonate, and (5.25 mmol, 1.16 g, 1.08 mL) of decyl bromide by following the aforementioned procedure. Off-white precipitates of MN-1 were obtained in good yield.

Yield: 87%. **Melting point**: 41-43 °C. R_f: 0.7*

* *n*-hex and EtOAc (7:3)

2.4.1.2 Synthesis of 1-(dodecyloxy)-4-nitrobenzene (MN-2)

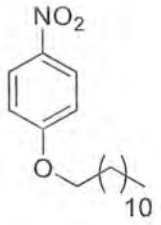

MN-2 was synthesized using (3.5 mmol, 0.5 g) of 4-nitrophenol, (7.5 mmol, 1.03 g) of anhydrous potassium, and (5.25 mmol, 1.36 g, 1.26 mL) of dodecyl bromide by following the aforementioned procedure. Light yellow precipitates of MN-2 were obtained in good yield.

Yield: 83%. **Melting point**: 50-52 °C (lit : 51-53 °C)[146] . $\mathbf{R}_f$: 0.8*

**n*-hex. and ethyl EtOAc (7:3)

2.4.1.3 Synthesis of 1-(tetradecyl)-4-nitrobenzene (MN-3)

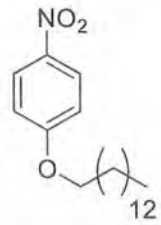

MN-3 was synthesized using (3.5 mmol mmol 0.5 g) of 4-nitrophenol, (10.7 mmol, 1.49 g) of anhydrous potassium, and (5.25 mmol, 1.45g, 1.39 mL) of tetradecyl bromide by following the aforementioned procedure. Off- white precipitates of MN-3 were obtained in good yield.

Yield: 83%. **Melting point**: 55-57 °C . $\mathbf{R}_f$: 0.8*

* *n*-hex. and EtOAc (7:3)

2.4.2 General procedure for the synthesis of *p*-alkoxyaniline (MA 1-3)

Three different monoamines were synthesized following the already mentioned procedure in the literature[152].

Reduction was carried out by treating 4-nitro-1- alkoxybenzene with palladium on activated charcoal (Pd/C) in dry distilled ethanol as a solvent. After an hour, hydrazine hydrate was added dropwise and the reaction was allowed to heat at 80℃ for 6 hours. After the reaction was completed, the surplus ethanol was removed under reduced pressure while hot filtration was done to remove palladium charcoal. White crystals of monoamines were obtained, which were filtered, rinsed with distilled water, and dried.

2.4.2.1 Synthesis of *p*-decyloxyaniline (MA-1)

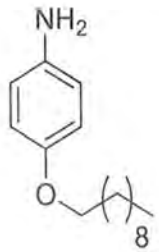

Reduction was performed by treating (1.7 mmol, 0.5 g) of 1-(decyloxy)-4-nitrobenzene with 0.05 g of 10 percent palladium charcoal (Pd/C). Following the aforementioned procedure, 80% hydrazine hydrate (8.5 mmol, 0.33 g, 0.31 mL) was added dropwise and refluxed at 80 °C for 6 hours. As a consequence, white crystals of MA-1 were obtained in good yield.

Yield: 70%. **Melting point**: 30-32 °C. R_f: 0.6*

*(*n*-Hex: EtOAc, 7:3)

FT-IR ($\tilde{\upsilon}$/cm^{-1}): (3308, 3280 -NH_2 stretch), (1596 C=C stretch, aromatic), (1238 C-N stretch), (1215, 1007 stretch, C-O-C), (832 CH_2 long chain).

2.4.2.2 Synthesis of *p*-dodecyloxyaniline (MA-2)

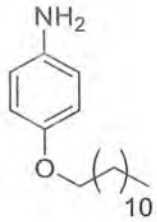

Reduction was performed out by treating (1.6 mmol 0.5 g) of 1-(dodecyloxy)-4-nitrobenzene, with 0.05 g of 10 percent palladium on activated charcoal (Pd/C). Following the aforementioned procedure, 80% hydrazine hydrate (8 mmol, 0.32 g, 0.31 mL) was added dropwise and refluxed at 80 °C for 6 hours. As a consequence, white crystals of MA-2 were obtained in good yield.

Yield: 78%. **Melting point**: 34-37 °C. R_f: 0.6*

*(*n*-Hex: EtOAc, 7:3)

FT-IR ($\tilde{\upsilon}$/cm^{-1}): (3308, 3280 -NH_2 stretch), (1596, C=C stretch), (1238, C-N stretch), (1215, 1007, C-O-C), (832 CH_2 long-chain).

2.4.2.3 Synthesis of *p*-tetradecyloxyaniline (MA-3)

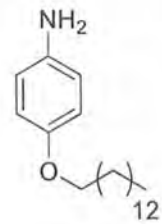

Reduction was performed out by treating (1.4 mmol, 0.5 g) of 1-(tetradecyloxy)-4-nitrobenzene with 0.05 g of 10 percent palladium on activated charcoal (Pd/C). Following the aforementioned procedure, 80% hydrazine hydrate (7 mmol, 0.28 g, 0.27 mL) was added dropwise and refluxed at 80°C for 6 hours. As a consequence, white crystals of MA-3 were obtained in good yield.

Yield: 70%. **Melting point**: 51-53 °C. R_f: 0.7*

*(*n*-Hex: EtOAc, 7:3)

FT-IR ($\bar{\upsilon}$/cm^{-1}): (3308, 3280 -NH_2 stretch), (1596, C=C stretch aromatic), (1238, C-N stretch), (1215, 1007 C-O-C), (832 CH_2 long-chain).

2.4.3 General procedure for the synthesis of triphenylamine-based dinitro precursor having *n*-alkoxy pendent groups (DN 1-3)

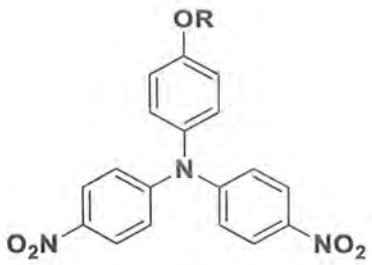

To a three-necked 250mL round-bottom flask equipped with a reflux condenser, 4-alkoxy aniline and cesium fluoride were agitated overnight in DMSO under an inert atmosphere. Afterward, the addition of 1-fluoro-4-nitrobenzene was carried out dropwise and heated at 140 °C for 72 hours. Afterward, the whole mixture was poured into 50 mL of methanol so that the byproduct was solubilized and precipitates of product formed on stirring which were collected and dried.

2.4.3.1 Synthesis of *N,N*-bis(4-nitrophenyl)decyloxy phenylamine (DN-1)

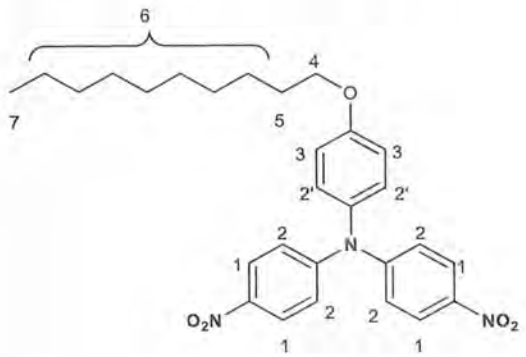

The aforementioned procedure was followed to carry out the synthesis of DN-1 by using 0.8mL (1.12 g) of 1-fluoro-4-nitrobenzene, 8 mmol (1.21 g) of CsF, and 4 mmol (1 g) of 4-decyloxyaniline. Orange precipitates of MN-1 were formed in moderate yield.

Yield: 68%. **Melting point:** 108-111 °C. **R_f:** 0.5 (*n*-Hex: EtOAc, 7:3)

FT-IR ($\bar{\upsilon}$/cm^{-1}): (3075 C_{sp2}-H), (2917, 2850, C_{sp3}-H stretch), (1312, C-N stretch), (1596, 1498 C=C stretch), (1578, 1337 NO_2 stretch), (1276, 1109 C-O-C), (847 CH_2 long-chain).

^{1}H-NMR (CDCl3), δ (ppm): 8.13 (4H, d, ^3J = 9 Hz, 1H), 7.2-7.09 (6H, m, 2H, 2'H), 6.96 (2H, d, ^3J = 8.7 Hz, 3H), 3.99 (2H, t, ^3J = 8.1 Hz, 4H), 1.87-1.78 (2H, m, 5H), 1.28- 1.51 (14H, m, 6H), 0.90 (3H, t, ^3J = 6.2 Hz, 7H)

^{13}C-NMR (CDCl3), δ (ppm): 158.30 (C-13), 151.94 (C-10), 142.35 (C-12), 137.02 (C-11), 128.91 (C-3), 125.49 (C-2), 121.65 (C-1), 116.26 (C-4), 68.42 (C-5), 31.9 (C-6), 29.50 (C-6'), 29.40 (C-6"), 29.34 (C-8, C-8'), 29.22 (C-9), 26.06 (C-7"), 22.71 (C-7'), 14.16(C-7),

2.4.3.2 Synthesis of *N,N*-bis(4-nitrophenyl)dodecyloxy phenylamine (DN-2)

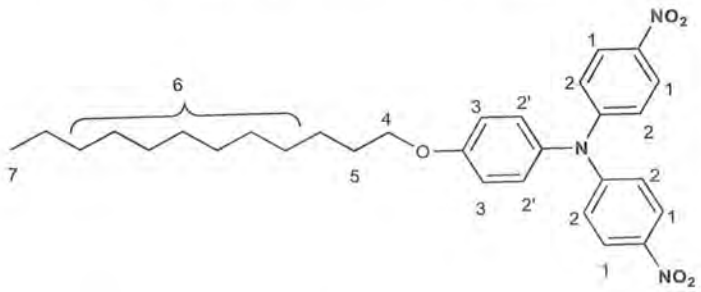

The aforementioned procedure was followed to carry out the synthesis of DN-2 by using 0.6mL (0.8 g) of 1-fluoro-4-nitrobenzene, 7.6 mmol (1.15 g) of CsF and 3.8 mmol (1 g) of 4-dodecyloxyaniline. Orange precipitates of DN-2 were obtained in good yield.

Yield: 78%. **Melting point:** 134-136 °C. **R_f:** 0.5 (*n*-Hex: EtOAc, 7:3)

FT-IR ($\bar{\upsilon}$/cm^{-1}): (3050 C_{sp2}-H), (2909,2829 C_{sp3}-H), (1235, C-N stretch), (1596, C=C stretch), (1550,1350 NO_2 stretch), (1215, 1007 C-O-C), (832 CH_2 long chain)

^{1}H-NMR (CDCl3), δ (ppm): 8.15 (4H, dd, ^3J = 6.9, 1H), 7.17-7.09 (6H, m, 2H, 2'H), 6.98 (2H, d, ^3J = 9.0 Hz, 3H), 3.99 (2H, t, ^3J = 6.6 Hz, 4H), 1.87-1.78 (2H, m, 5H), 1.28- 1.60 (18H, m, 6H), 0.90 (3H, t, ^3J = 6.9 Hz, 7H)

^{13}C-NMR (CDCl3), δ (ppm) : 158.30 (C-13), 151.94 (C-10), 142.34 (C-12), 137.02 (C-11), 128.93 (C-3), 125.50 (C-2), 121.65 (C-1), 116.25 (C-4), 68.29 (C-5), 31.94 (C-

6), 29.50 (C-6'), 29.40 (C-6"), 29.34 (C-8, C-8'), 29.22 (C-9), 29.18 (C-9'), 28.32 (C-9"), 26.06 (C-7"), 22.71 (C-7'), 14.41(C-7)

2.4.3.3 Synthesis of *N,N*-bis(4-nitrophenyl)tetradecyloxy phenylamine (DN-3)

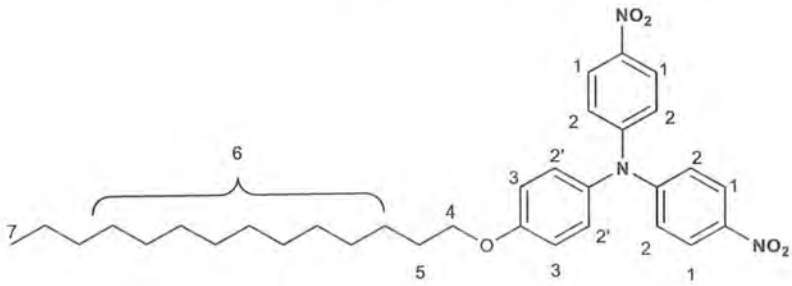

The aforementioned procedure was followed to carry out the synthesis of DN-3 by using 0.8mL (1.07 g) of 1-fluoro-4-nitrobenzene, 7.6 mmol (1.1 g) of CsF and 3.6 mmol (1 g) of 4-tetradecyloxyaniline. Orange precipitates of DN-2 were obtained in moderate yield.

Yield: 62%. **Melting point:** 118-120 °C. **R_f:** 0.5 (*n*-Hex: EtOAc, 7:3)

FT-IR ($\bar{\upsilon}$/cm^{-1}): (3310 C_{sp2}-H), (2916,2849 C_{sp3}-H), (1578,1341 NO_2 stretch), (1731,1596 C=C stretch), (1341 C-N stretch), (1241, 1106 C-O-C), (762 CH_2 long chain)

^{1}H-NMR (CDCl3), δ (ppm): 8.17 (4H, dd, ^3J = 12.3,1H), 7.20-7.09 (6H, m, 2H, 2'H), 6.96 (2H, d, ^3J = 8.7 Hz, 3H), 3.99 (2H, t, ^3J = 6.0 Hz, 4H), 1.87-1.78 (2H, m, 5H), 1.54- 1.27 (16H, m, 6H), 0.89 (3H, t, ^3J = 6.6 Hz, 7H)

^{13}C-NMR (CDCl3), δ (ppm): 158.29 (C-13), 151.94 (C-10), 142.32 (C-12), 137.01(C-11), 116.25 (C-4), 121.65 (C-1), 125.51 (C-2), 128.92 (C-3), 68.41 (C-5), 31.94 (C-6), 29.50 (C-6'), 29.40 (C-6"), 29.34 (C-8, C-8'), 29.22 (C-9), 29.18 (C-9'), 28.32 (C-9"), 28.16 (C-10'), 27.3 (C-10"), 26.06 (C-7"), 22.71 (C-7'), 14.41(C-7)

2.4.4 Synthesis of *N,N*-bis(4-aminophenyl)alkoxy phenylamine (DA 1-3)

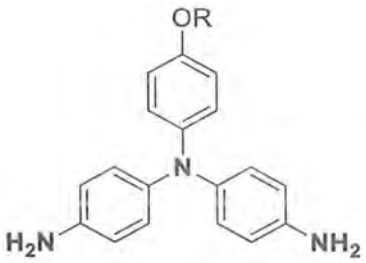

The reduction was carried out in ethanol by treating *N, N –bis* (4-nitrophenyl) alkoxy phenylamine with palladium charcoal (Pd/C) in a 250 mL round bottom flask equipped with a magnetic stirrer, condenser, and nitrogen gas inlet tube. The reaction was stirred at 80 °C until no existence of *N, N-bis* (4-nitrophenyl) alkoxy phenylamine was monitored by TLC. After the reaction was completed, the surplus ethanol was removed under reduced pressure while hot filtration was done to remove palladium charcoal. White crystals of diamines were obtained, which were filtered, rinsed with distilled water, and dried.

2.4.4.1 Synthesis of *N,N-bis*(4-aminophenyl)decyloxy phenylamine (DA-1)

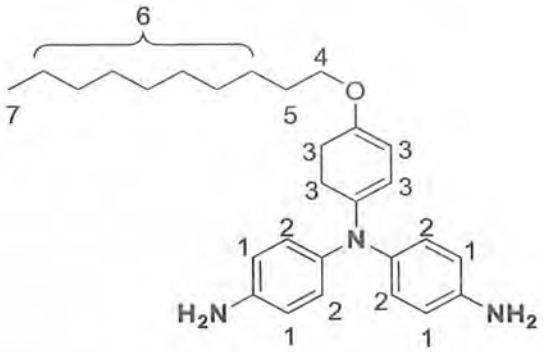

Reduction was performed by treating 4.07 mmol (0.2 g) of DN-1 with 0.02 g of 10 percent palladium on activated charcoal (Pd/C). Following the aforementioned procedure, 80% hydrazine hydrate (20.3 mmol, 0.81 g, 0.79 mL) was added dropwise and heated at 80 °C for 48 hours. As a consequence, white crystals of DA-1 were obtained in good yield.

Yield: 75%. **Melting point:** 65-67 °C.

R_f: 0.5 (*n*-Hex: EtOAc, 3:7)

FT-IR ($\bar{\upsilon}$/cm^{-1}): (3340, 3215 NH_2 stretch), (3100 C_{sp2}-H), (2915,2848 C_{sp3}-H), (1635 C=C stretch), (1502 N-H bend), (1391 C-N stretch), (1107,1231 C-O-C), (822 CH_2 long chain).

^{1}H-NMR (CDCl3), δ (ppm): 6.47 (4H, d, ^3J = 8.4 Hz, 1H), 6.63 (4H, d, ^3J = 7.8 Hz, 2H), 6.72 (4H, m, 3H, 3'H), 3.83 (2H, t, ^3J = 6.3 Hz, 4H), 4.86 (Amine H, s), 1.7-1.6 (2H, m, 5H), 1.24-1.39 (14H, m, 6H), 0.85 (3H, t, ^3J = 6 Hz, 7H)

^{13}CNMR δ (ppm): 152.6 (C-13), 144.8 (C-10), 143.3 (C-12), 137.8(C-11), 126.08 (C-3), 121.4 (C-2), 115.3.09 (C-1), 115.2 (C-4), 68.04 (C-5), 31.7 (C-6), 29.50 (C-6'), 29.40 (C-6"), 29.34 (C-8, C-8'), 29.17 (C-9), 26.02 (C-7"), 22.58 (C-7'), 14.44(C-7),

2.4.4.2 Synthesis of *N,N*-bis(4-aminophenyl)dodecyloxy phenylamine (DA-2)

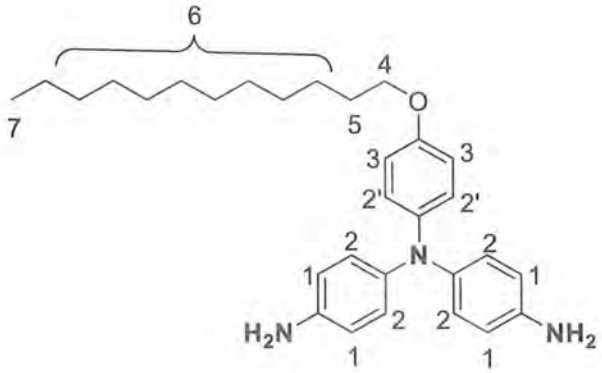

Reduction was performed by treating 3.9 mmol (0.2 g) of DN-2 with 0.02 g of 10 percent palladium on activated charcoal (Pd/C). Following the aforementioned procedure, 80% hydrazine hydrate (19.5 mmol, 0.78 g, 0.75 mL) was added dropwise and heated at 80 °C for 48 hours. As a consequence, white crystals of DA-2 were obtained in good yield.

Yield: 75%. **Melting point:** 88-90 °C.

R_f : 0.7 (*n*-Hex: EtOAc, 3:7)

FT-IR (ῡ/cm-1): (3347, 3274 NH_2 stretch), (3303 C_{sp2}-H), (2920, 2853 C_{sp3}-H), (1649,1500 C=C stretch), (1597 N-H bend), (1311 C-N stretch), (1228,1040 C-O-C), (813 CH_2 long chain)

^{1}H-NMR (CDCl3), δ (ppm): 6.94-6.86 (6H, m, 2H, 2'H), 6.76 (2H, d, ^3J = 9.0 Hz, 3H), 6.60 (4H, d, ^3J = 6.6 Hz, 1H), 3.93 (2H, t, ^3J = 6.6 Hz, 4H), 3.51 (Amine H, s), 1.81-1.79 (2H, m, 5H), 1.28-1.50 (18H, m, 6H), 0.90 (3H, t, ^3J = 6.9 Hz, 7H)

^{13}CNMR δ (ppm): 153.97 (C-13), 141.24 (C-10), 140.59 (C-12), 134.74 (C-11), 123.86 (C-2), 125.23 (C-3), 116.09 (C-1), 114.95 (C-4), 68.29 (C-5), 31.94 (C-6), 29.50 (C-6'), 29.40 (C-6"), 29.34 (C-8, C-8'), 29.22 (C-9), 29.18 (C-9'), 28.32 (C-9"), 26.06 (C-7"), 22.71 (C-7'), 14.41(C-7)

2.4.4.3 Synthesis of *N,N*-bis(4-aminophenyl)tetradecyloxy phenylamine (DA-3)

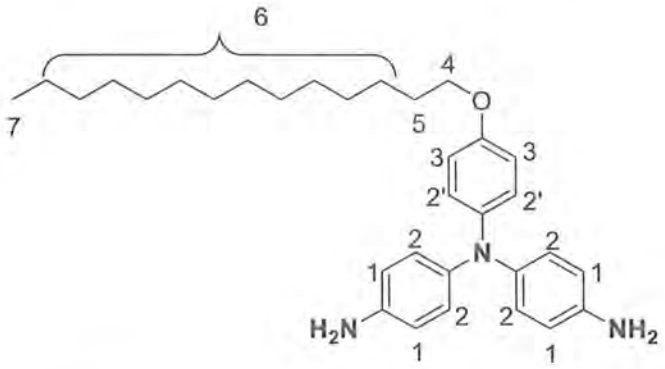

Reduction was performed by treating 3.6 mmol (0.2 g) of DN-3 with 0.02 g of 10 percent palladium on activated charcoal (Pd/C). Following the aforementioned procedure, 80% hydrazine hydrate (1.8 mmol, 0.72 g, 0.7 mL) was added dropwise and heated at 80 °C for 48 hours. As a consequence, white crystals of DA-3 were obtained in good yield.

Yield: 73%. **Melting point:** 89-92 °C.

R_f: 0.6 (*n*-Hex: EtOAc, 3:7)

FT-IR ($\bar{\upsilon}$/cm^{-1}): (3400, 3334 NH_2 stretch), (3035 C_{sp2}-H), (2918, 2849 C_{sp3}-H), (1499 N-H bend), (1624 C=C stretch), (1261 C-N stretch), (1227, 1023 C-O-C), (822 CH_2 long chain.

^{1}H-NMR (CDCl3), δ (ppm): 6.94-6.80 (6H, m, 2H, 2'H), 6.74 (2H, d, ^3J = 9.1 Hz, 3H), 6.62 (4H, d, ^3J = 8.5 Hz, 1H), 3.95 (2H, t, ^3J = 6.5 Hz, 4H), 3.43 (Amine H, s), 1.88-1.72 (2H, m, 5H), 1.20-1.52 (22H, m, 6H), 0.93 (3H, t, ^3J = 6.5 Hz, 7H)

^{13}CNMR δ (ppm): 153.71 (C-13), 144.56 (C-10), 140.62 (C-12), 136.53 (C-11), 124.32 (C-2), 121.71 (C-3), 115.64 (C-1), 114.99 (C-4), 68.34 (C-5), 31.65 (C-6), 29.43(C-6'), 29.41 (C-6"), 29.32 (C-8, C-8'), 29.22 (C-9), 29.18 (C-9'), 28.23 (C-9"), 28.16 (C-10'), 27.6 (C-10"), 26.01 (C-7"), 22.65 (C-7'), 14.34(C-7)

2.5 Synthesis of Polyimides

Different polyimides were synthesized from newly synthesized triphenylamine-based diamines having *n*-alkoxy pendant groups with various alkyl chains. Eight polyimides were successfully synthesized by treating DA-1 and DA-2 with four different commercially available dianhydrides.

2.5.1 General Procedure for Synthesis of Polyimides

A two-step polycondensation technique was followed to synthesize polyimides. Diamine and dianhydride were dissolved in DMAc and stirred for 24 hours under inert conditions. Polyamic acid was produced as an intermediate, which was indicated by the increase in the viscosity of the reaction mixture. Thermal imidization of polyamic acid was carried out in the second stage by heating PAA at a different temperature range from 60 °C to 300 °C (55 °C and 80 °C for 2 hours, 100 °C for 12 hours, 120°C, 150 °C, 180 °C, and 200 °C for 2 hours, 220 °C, 250°C, 280 °C for 1 hour each). Lower temperature allows solvent to evaporate and higher temperature involves the cyclization and removal of water molecules.

2.5.1.1 Synthesis of DA-1 (*N,N*-bis(4-aminophenyl)decyloxy phenylamine) based Polyimides

The following section will explain the stoichiometry and method followed to synthesize DA-1 based polyimides.

2.5.1.1.1 Synthesis of Polyimide DA1-F

Solution polymerization was carried out to synthesize DA1-F. 0.2 mmol (0.1g) of DA-1 and 0.2 mmol (0.15 g) of 6-FDA were solubilized in 1.7 mL of DMAc and stirred for 24 hours at room temperature. Thermal imidization of PAA to polyimide was achieved by following the aforestated procedure.

FTIR ($\bar{\upsilon}$ cm^{-1}): 1782 (C=O, imide $_{(asym)}$), 1717 (C=O, imide $_{(sym)}$), 1373 (C-N stretch), 1229 (C-O-C $_{(asym)}$), 820 (C-O-C $_{(sym)}$), 722 (C=O imide, bend).

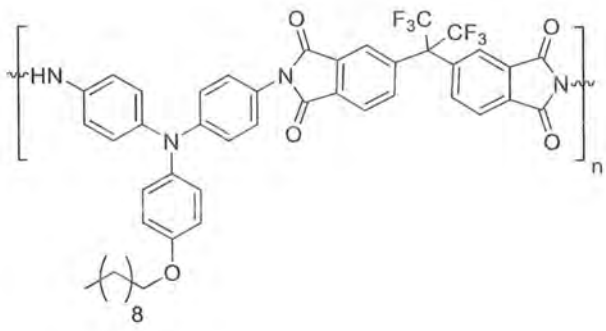

Fig 2.1: Structural representation of DA1-F

2.5.1.1.2 Synthesis of Polyimide DA1-O

Solution polymerization was carried out to synthesize DA1-O. 0.2 mmol (0.1 g) of DA-1 and 0.2 mmol (0.07g) of OPDA were solubilized in 1.5 mL of DMAc and stirred for 24 hours at room temperature. Thermal imidization of PAA to polyimide was achieved by following the aforestated procedure

FTIR ($\bar{\upsilon}$ cm^{-1}): 1777 (C=O, imide $_{(asym)}$), 1714 (C=O, imide $_{(sym)}$), 1361 (C-N stretch), 1224 (C-O-C $_{(asym)}$), 829 (C-O-C $_{(sym)}$), 739 (C=O imide, bend).

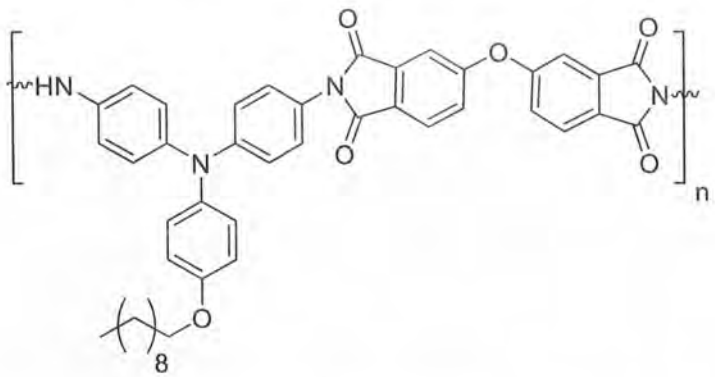

Fig 2.2: Structural representation of DA1-O

2.5.1.1.3 Synthesis of Polyimide DA1-B

Solution polymerization was carried out to synthesize DA1-B. 0.2 mmol (0.1 g) of DA-1 and 0.2 mmol (0.075 g) of BTDA were solubilized in 1.4 mL of DMAc and stirred for 24 hours at room temperature. Thermal imidization of PAA to polyimide was achieved by following the aforestated procedure.

FTIR ($\bar{\upsilon}$ cm^{-1}): 1776 (C=O, imide, $_{(asym)}$), 1715 (C=O, imide, $_{(sym)}$), 1369 (C-N stretch), 1207 (C-O-C $_{(asym)}$), 823 (C-O-C $_{(sym)}$), 718 (C=O imide, bend).

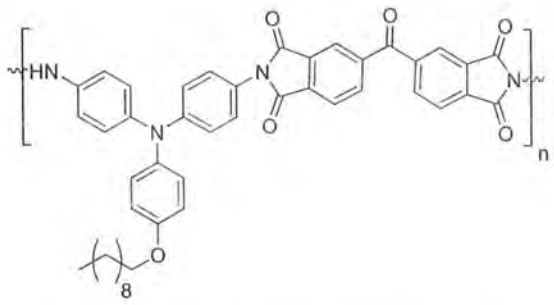

Fig 2.3: Structural representation of DA1-B

2.5.1.1.4 Synthesis of Polyimide DA1-P

Solution polymerization was carried out to synthesize DA1-P. 0.2 mmol (0.1 g) of DA-1 and 0.2 mmol (0.05 g) of PMDA were solubilized in 1.3 mL of DMAc and stirred for 24 hours at room temperature. Thermal imidization of PAA to polyimide was achieved by following the aforestated procedure.

FTIR ($\bar{\upsilon}$ cm^{-1}): 1775 (C=O, imide $_{(asym)}$), 1720 (C=O, imide $_{(sym)}$), 1359 (C-N stretch), 1221 (C-O-C $_{(asym)}$), 829 (C-O-C $_{(sym)}$), 721 (C=O imide, bend).

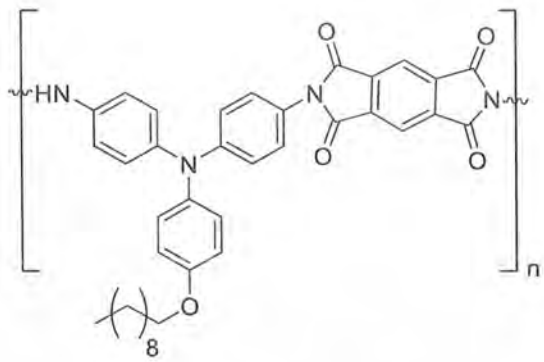

Fig 2.4: Structural representation of DA1-P

2.5.1.2 Synthesis of DA-2 (*N,N*-bis(4-nitrophenyl)dodecyloxy phenylamine) based Polyimides

The following section will explain the stoichiometry and method followed to synthesize DA-2 based polyimides.

2.5.1.2.1 Synthesis of Polyimide DA2-F

Solution polymerization was carried out to synthesize DA2-F. 0.2 mmol (0.1 g) of DA-2 and 0.2 mmol (0.09 g) of 6-FDA were solubilized in 1.6 mL of DMAc and stirred for

24 hours at room temperature. Thermal imidization of PAA to polyimide was achieved by following the aforestated procedure.

FTIR ($\bar{\upsilon}$ cm^{-1}): 1779 (C=O, imide $_{(asym)}$), 1720 (C=O, imide $_{(sym)}$), 1370 (C-N stretch), 1232 (C-O-C $_{(asym)}$), 824 (C-O-C $_{(sym)}$), 743 (C=O imide, bend).

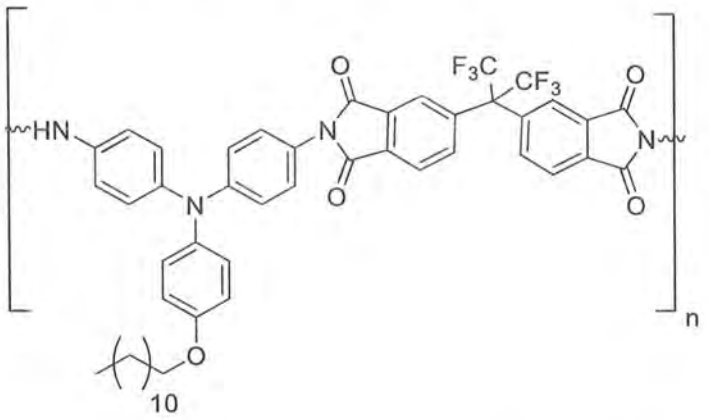

Fig 2.5: Structural representation of DA2-F

2.5.1.2.2 Synthesis of Polyimide DA2-O

Solution polymerization was carried out to synthesize DA2-F. 0.2 mmol (0.1 g) of DA-2 and 0.2 mmol (0.06 g) of OPDA were solubilized in 1.46 mL of DMAc and stirred for 24 hours at room temperature. Thermal imidization of PAA to polyimide was achieved by following the aforestated procedure.

FTIR ($\bar{\upsilon}$ cm^{-1}): 1775 (C=O, imide $_{(asym)}$), 1715 (C=O, imide $_{(sym)}$), 1370 (C-N stretch), 1262 (C-O-C $_{(asym)}$), 815 (C-O-C $_{(sym)}$), 743 (C=O imide, bend).

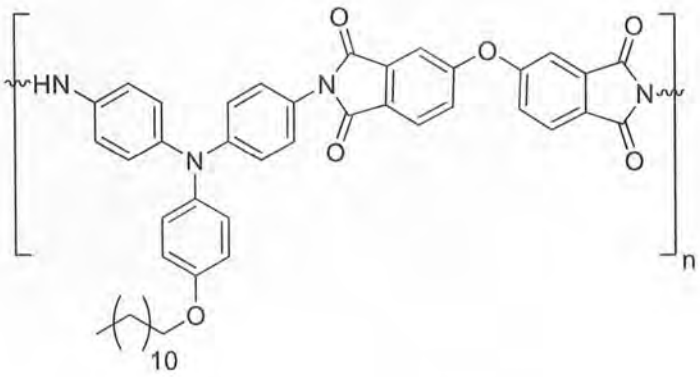

Fig 2.6: Structural representation of DA2-O

2.5.1.2.3 Synthesis of Polyimide DA2-B

Solution polymerization was employed to synthesize DA2-B. 0.2 mmol (0.1 g) of DA-2 and 0.2 mmol (0.06 g) of BTDA were solubilized in 1.46 mL of DMAc and stirred for 24 hours at room temperature. Thermal imidization of PAA to polyimide was achieved by following the aforestated procedure.

FTIR ($\bar{\upsilon}$ cm^{-1}): 1774 (C=O, imide $_{(asym)}$), 1710 (C=O, imide $_{(sym)}$), 1371 (C-N stretch), 1260 (C-O-C $_{(asym)}$), 810 (C-O-C $_{(sym)}$), 740 (C=O imide, bend).

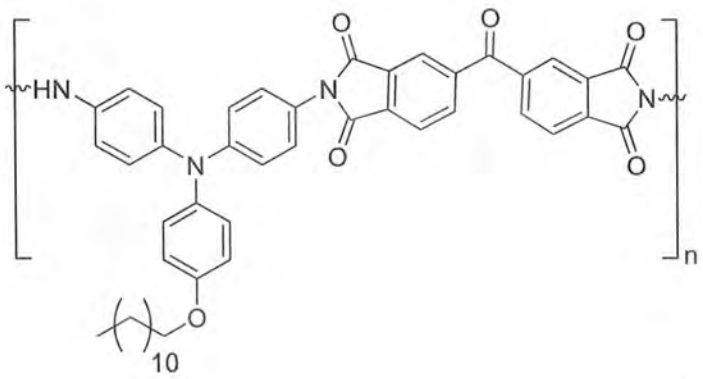

Fig 2.7: Structural representation of DA2-B

2.5.1.2.4 Synthesis of Polyimide DA2-M

Solution polymerization was employed to synthesize DA2-P. 0.2mmol (0.1 g) of DA-2 and 0.2mmol (0.14 g) of PMDA were solubilized in 2.1 mL of DMAc and stirred for 24 hours at room temperature. Thermal imidization of PAA to polyimide was achieved by following the aforestated procedure.

FTIR ($\bar{\upsilon}$ cm^{-1}): 1771 (C=O, imide $_{(asym)}$), 1712 (C=O, imide $_{(sym)}$), 1375 (C-N stretch), 1265 (C-O-C $_{(asym)}$), 810 (C-O-C $_{(sym)}$), 746 (C=O imide, bend).

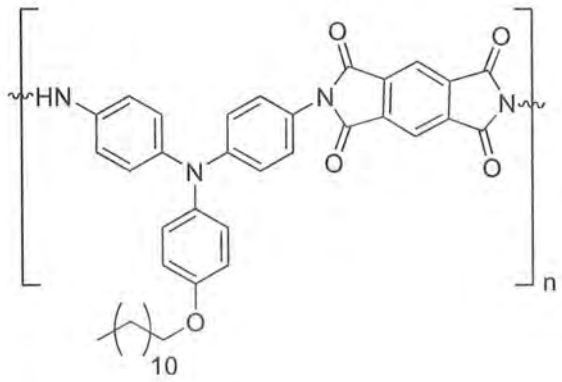

Fig 2.8: Structural representation of DA2-M

Chapter 3

RESULTS AND DISCUSSION

In this chapter, the culmination of rigorous research and analysis is unveiled, presenting a comprehensive exposition of the obtained results and their profound implications.

3.1 Synthesis of triphenylamine-based diamine having *n*-alkoxy pendant groups

Scheme 3.1 illustrates the synthetic plan followed to synthesize the triphenylamine (TPA) based diamines (DA 1-3) in four steps

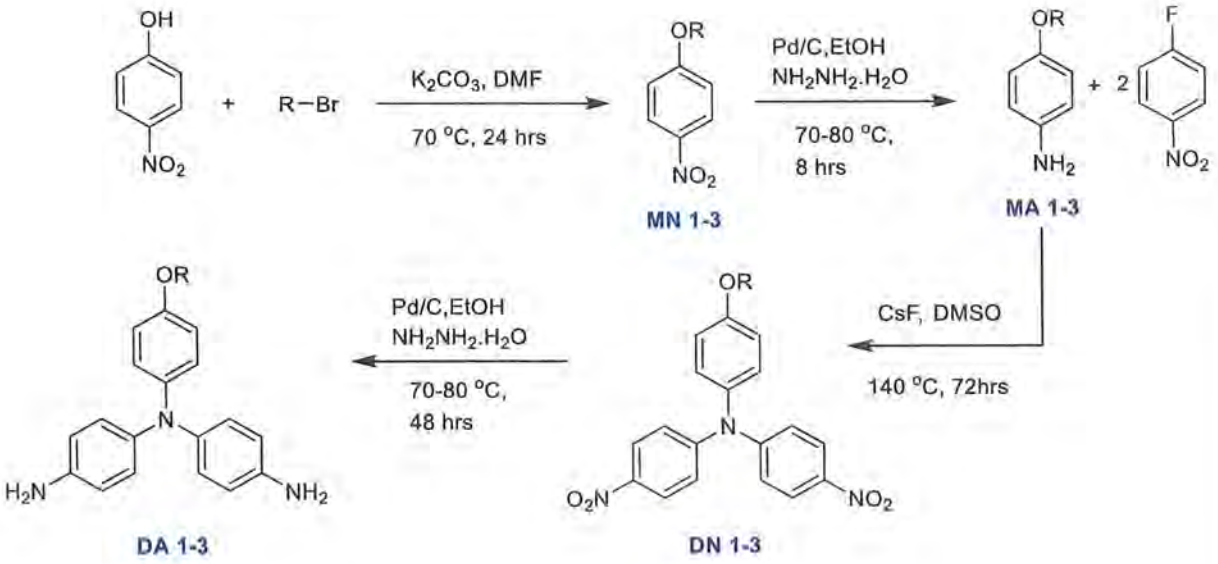

Scheme 3.1: Synthetic route for *n*-alkoxy substituted diamines

To get the alkoxy-substituted diamines, in the first step, alkoxy substitution was introduced by treating 4-nitrophenol with alkyl bromide of different chain lengths under anhydrous conditions to get 4-nitro-1-alkoxy benzene (MN 1-3). In the second step, 4-nitro-1- alkoxy benzene was reduced to its corresponding alkoxy aniline (MA 1-3) using Pd/C catalyst, hydrazine hydrate in ethanol under reflux for 6 hrs. In the third step, alkoxy anilines of different alkyl chain lengths were treated with 1-fluoro-4-nitobenzene using CsF as a base in DMSO at 140 °C for 60 hrs to get desired *N,N*-bis(4-nitrophenyl) alkoxy phenylamine (DN 1-3) followed by reduction into corresponding diamines (DA 1-3) in fourth step using Pd/C, hydrazine hydrate in ethanol under reflux for 24 hr.

The synthesized dinitro and diamine were obtained in good yield and exhibited orange and white color respectively. Physical data of synthesized mononitro (MN 1-3), monoamine (MA 1-3), dinitro (DN 1-3), and diamines (DA 1-3) are tabulated below.

Table 3.1: Physical data of 4-nitro-1-alkoxybenzene (Mononitro 1-3)

Compound	R	Physical state	Color	Yield (%)	m.p (°C)	R_f*
MN-1	*n*-$C_{10}H_{21}$	Powder	Off white	87	39-42	0.6
MN-2	*n*-$C_{12}H_{25}$	Powder	Light yellow	83	50-53	0.8
MN-3	*n*-$C_{14}H_{29}$	Powder	Off white	85	52-56	0.8

*Stationary phase= silica gel $60F_{254}$; mobile phase = *n*-Hexane : Ethyl acetate (7:3)

Table 3.2: Physical data of Alkoxy aniline (Monoamine 1-3)

Compound	R	Physical state	Color	Yield (%)	m.p (°C)	R_f*
MA-1	*n*-$C_{10}H_{21}$	Crystalline	white	87	30-32	0.6
MA-2	*n*-$C_{12}H_{25}$	Crystalline	White	83	34-37	0.6
MA-3	*n*-$C_{14}H_{29}$	Crystalline	White	85	51-53	0.7

*Stationary phase= silica gel $60F_{254}$; mobile phase = *n*-Hexane : Ethyl acetate (7:3)

Table 3.3: Physical data of *N,N*-bis(4-nitrophenyl)alkoxyaniline (Dinitro 1-3)

Compound	R	Physical state	Color	Yield (%)	m.p (°C)	R_f*
DN-1	*n*-$C_{10}H_{21}$	Powder	Orange	68	108-111	0.5
DN-2	*n*-$C_{12}H_{25}$	Powder	Orange	78	134-136	0.5
DN-3	*n*-$C_{14}H_{29}$	Powder	Orange	62	118-120	0.5

*Stationary phase= silica gel $60F_{254}$; mobile phase = *n*-Hexane : Ethyl acetate (7:3)

Table 3.4: Physical data of *N,N*-bis(4-aminophenyl)alkoxyaniline (Diamine 1-3)

Compound	R	Physical state	Color	Yield (%)	m.p (°C)	R_f*
DA-1	*n*-$C_{10}H_{21}$	Crystalline	white	75	65-67	0.5
DA-2	*n*-$C_{12}H_{25}$	Crystalline	white	75	88-90	0.7
DA-3	*n*-$C_{14}H_{29}$	Crystalline	white	73	89-92	0.6

*Stationary phase= silica gel $60F_{254}$; mobile phase = *n*-Hexane : Ethyl acetate (3:7)

3.1.1: Fourier Transform Infrared Spectroscopy (FTIR) of dinitro (DN-1) and diamine (DA-1)

The two bands that appeared at 1560 (cm^{-1}) and 1337 (cm^{-1}) were attributed to the characteristic stretching bands of -N-O in the NO_2 group, which confirms the formation of dinitro (DN-1). A moderately intense peak at 3076 (cm^{-1}) was assigned to the C_{sp2}-H stretching of the aromatic ring and two sharp peaks at 2915 (cm^{-1}) and 2850 (cm^{-1}) were attributed to the C_{sp3}-H stretching of the alkyl chain. Bands at 1596 (cm^{-1}) and 1633 (cm^{-1}) correspond to the C=C (aromatic) stretching of triphenylamine unit in dinitro and diamine respectively.

The N-H bending in diamine appeared at 1495 (cm^{-1}). Reduction of dinitro (DN-1) to a monomer diamine (DA-1) was confirmed by the appearance of characteristic stretching absorption bands of N-H of primary amine at 3427 (cm^{-1}) and 3322 (cm^{-1}) along with the disappearance of NO_2 stretching band from its respected region. All other peaks were observed at similar positions as there was no other structural change occurred and tabulated in (Table 3.9).

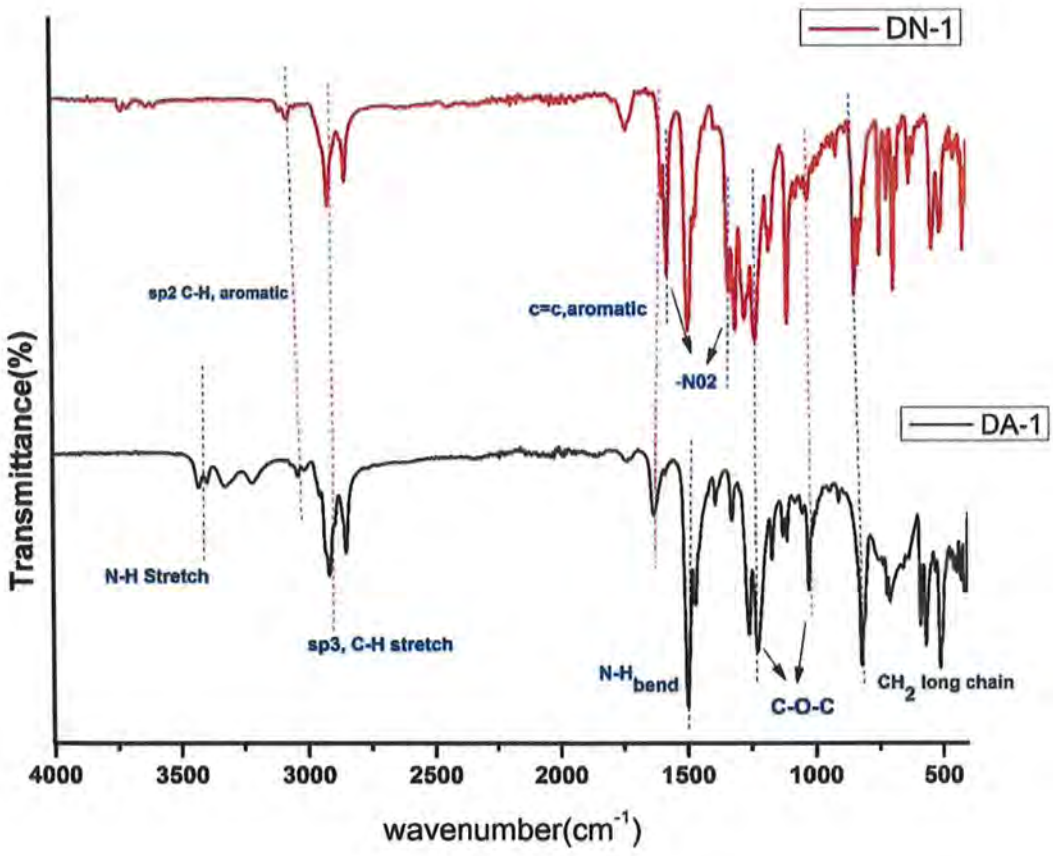

Fig 3.1: FTIR spectra of dinitro (DN-1) and diamine (DA-1)

Table 3.5: FTIR spectral data of dinitro (DN-1) and diamine (DA-1)

Band assignment	wavenumber $\bar{\upsilon}$ (cm^{-1}) (DN-1)	wavenumber $\bar{\upsilon}$ (cm^{-1}) (DA-1)
C_{sp}^2 -H (stretch)	3076	3067
C_{sp}^3 -H (stretch)	2917, 2850.3	2915, 2850
C=C (aromatic)	1596	1633
N-H (bend)	-	1496
N-H (stretch)	-	3427,3322
N-O (Nitro)	1560,1337	-
C-O-C (asym)	1229	1223
C-O-C (sym)	1025	1023
$-CH_2$ long chain	849	821

3.1.2: NMR Spectroscopy of Dinitro (DN-1)

The structure of dinitro (DN-1) was confirmed by ^{1}H-NMR and ^{13}C-NMR spectroscopy. (Figure 3.2) depicts the ^{1}H NMR spectrum of dinitro (DN-1), with data listed in (Table 3.6).

A triplet at 0.9 ppm for three protons is attributed to the terminal methyl (7) of the alkoxy chain. A multiplet at 1.8 ppm corresponds to the two methylene protons (5) of the aliphatic chain. Another triplet at 3.9 ppm is assigned to the two methylene protons (4) next to oxygen. A doublet at 6.9 ppm is ascribed to the two aromatic protons (3) of TPA ortho to the alkoxy chain. Another multiplet at 7.1 ppm corresponds to the six aromatic protons (2) ortho to nitrogen of the TPA unit. Another downfield doublet at 8.1 ppm belongs to the four aromatic protons (1) of TPA meta to nitrogen.

A multiplet at 1.4 ppm for fourteen protons (6) corresponds to the methylene envelope of the alkoxy chain

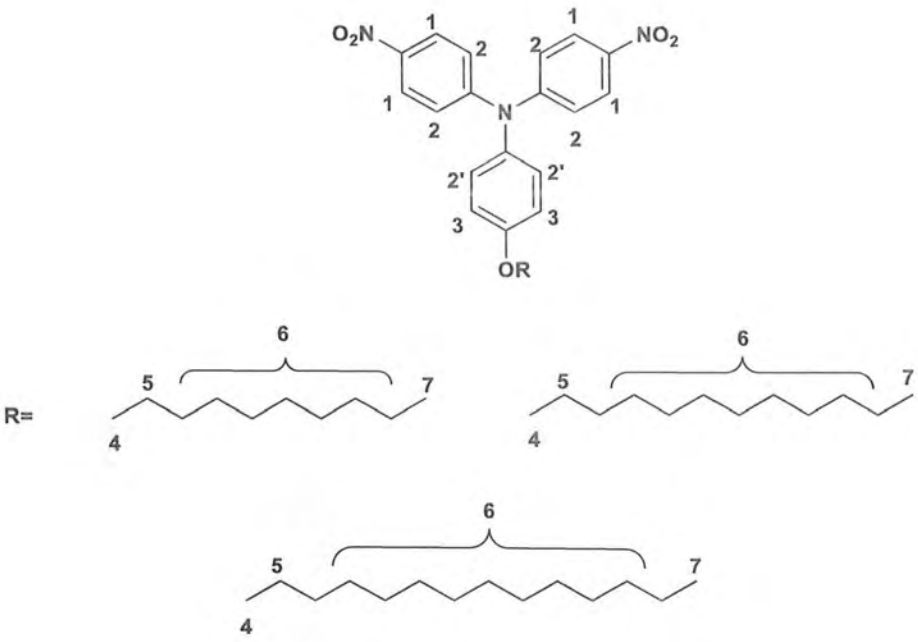

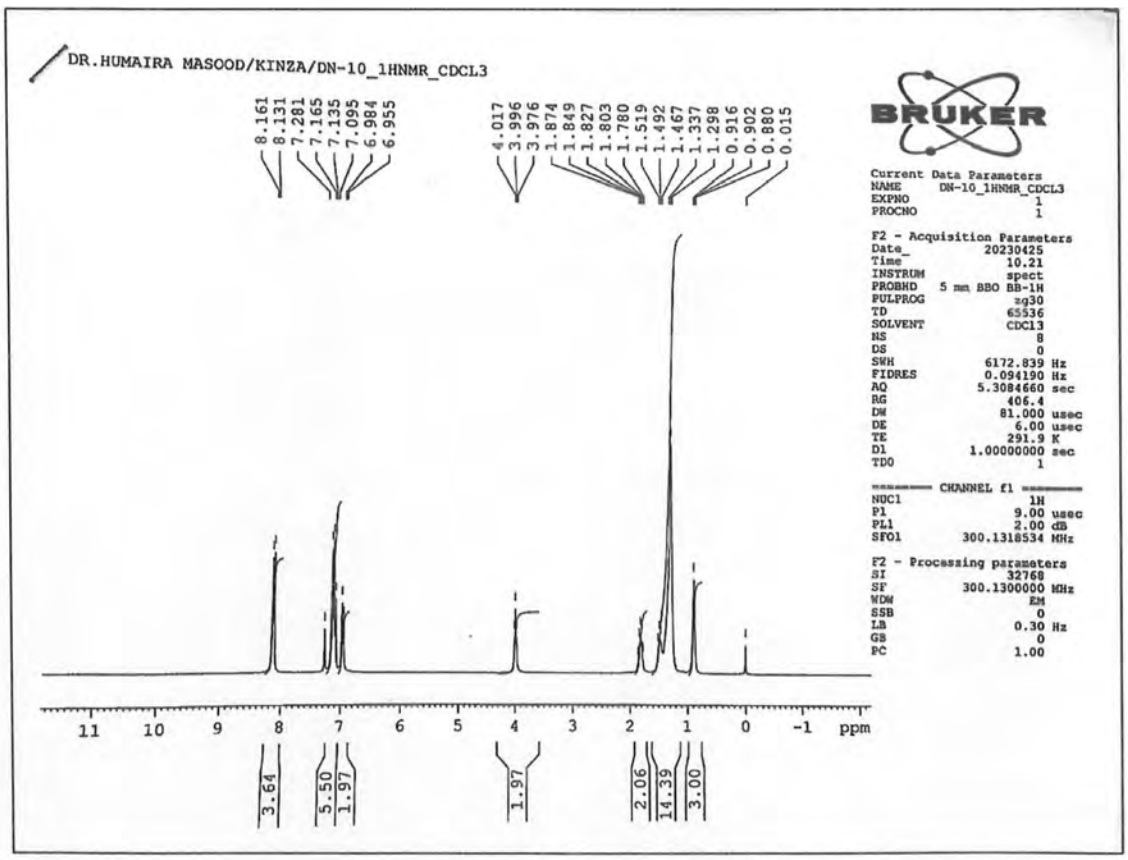

Fig 3.2: ^{1}H NMR spectrum of dinitro (DN-1)

Table 3.6: ^{1}H NMR data of dinitro (DN 1-3)

Compound	Protons	Chemical shift δ(ppm)	Multiplicity	Integration	*J* (Hz)
DN-1	1	8.16-8.13	d	4	$^{3}J = 9.1$
	2,2'	7.16	m	6	-
	3	6.96	d	2	$^{3}J = 8.7$
	4	3.9	t	2	$^{3}J = 8.1$
	5	1.8	m	2	-
	6	1.5-1.29	m	14	-
	7	0.9	t	3	$^{3}J = 6.2$
DN-2	1	8.15	d	4	$^{3}J = 7.2$
	2,2'	7.17-7.09	m	6	-
	3	6.98	d	2	$^{3}J = 9$
	4	3.99	t	2	$^{3}J = 6.6$
	5	1.87-1.78	m	2	-
	6	1.60-1.28	m	18	-
	7	0.9	t	3	$^{3}J = 6.9$
DN-3	1	8.17	d	4	$^{3}J = 12.3$
	2,2'	7.20-7.09	m	6	-
	3	6.96	d	2	$^{3}J = 8.7$
	4	3.99	t	2	$^{3}J = 6.0$
	5	1.87-1.78	m	2	-
	6	1.54-1.27	m	22	-
	7	0.89	t	3	$^{3}J = 6.6$

The structure elucidation of dinitro (DN-1) was further established by ^{13}C-NMR as shown in (Figure 3.3). An upfield signal at 14.1 ppm belongs to the methyl carbon (7) of the alkoxy chain. A signal at 68.4 ppm corresponds to the methylene carbon (5) next to oxygen. Another signal at 31.9 is attributed to the methylene carbon (6). A downfield signal at 158.8 ppm corresponds to deshielded carbon (13) ipso to the alkoxy chain. Another signal at 151.9 ppm belongs to the quaternary carbon (10) ipso to the nitro

group. While the signal at 142.3 ppm is attributed to the quaternary carbon (12) para to alkoxy chain. Another signal at 137.02 ppm corresponds to the carbon (11) ipso to the nitrogen of the TPA unit. While the rest of the signals in the aromatic region belong to their respective aromatic carbons. An upfield signal at 20-25 ppm corresponds to the methylene carbons (8) of the alkoxy chain.

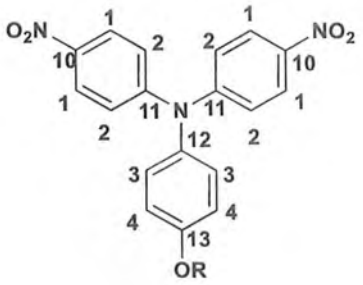

R=

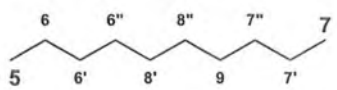

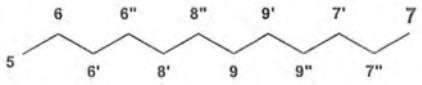

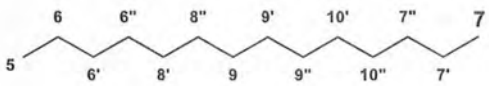

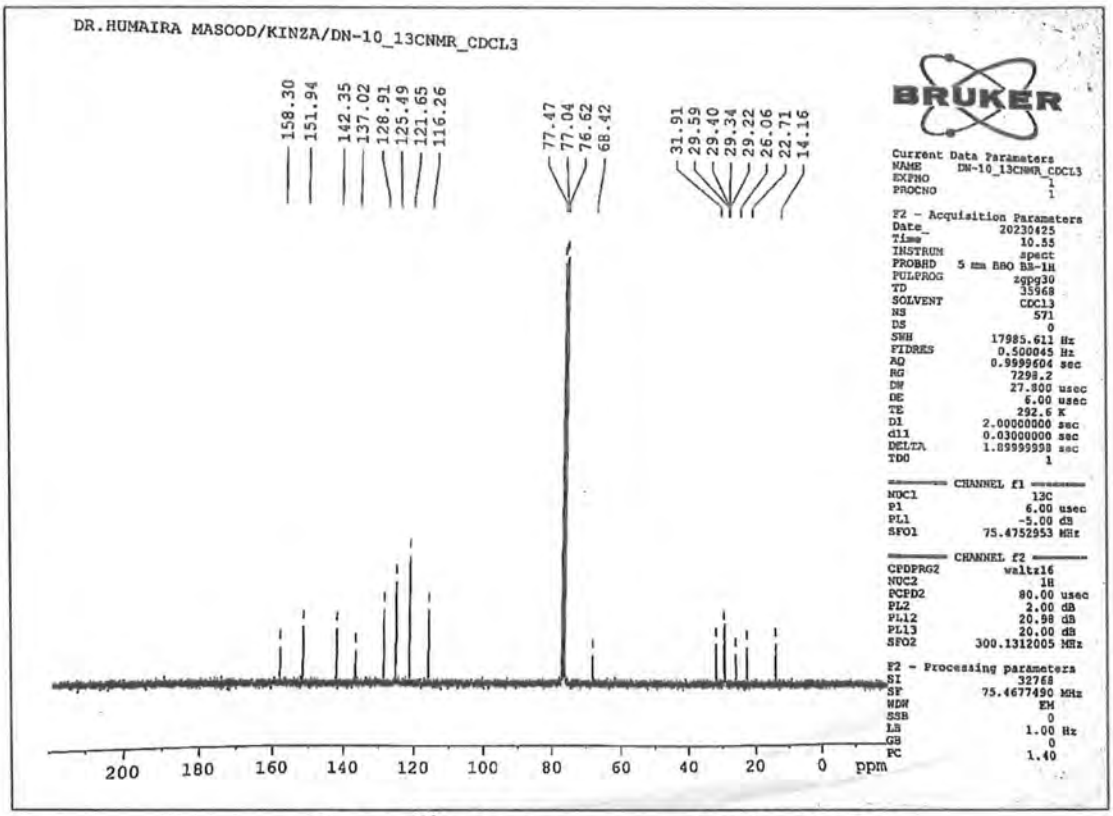

Fig 3.3: ^{13}C NMR spectrum of dinitro (DN-1)

Table 3.7: ^{13}C NMR data of dinitro (DN 1-3)

Carbons	Chemical shifts δ (ppm)		
	DN-1	DN-2	DN-3
13	158.30	158.30	158.29
10	151.94	151.94	151.94
12	142.35	142.34	142.32
11	137.02	137.02	137.01
3	128.91	128.91	128.92
2	125.49	125.50	125.51
1	121.65	121.65	121.65
4	116.26	116.25	116.25
5	68.42	68.29	68.41
6	31.9	31.96	31.97
6'	29.50	29.50	29.50
6"	29.40	29.40	29.40

8, 8'	29.34	29.34	29.34
9	29.22	29.22	29.22
9'	-	29.18	29.18
9"	-	28.32	28.32
10'	-	-	28.16
10"	-	-	27.3
7"	26.06	26.06	26.06
7'	22.71	22.71	22.71
7	14.16	14.41	14.41

3.1.3: NMR Spectroscopy of Diamine (DA-1)

The structure of diamine (DA-1) was confirmed by ^{1}H-NMR and ^{13}C-NMR spectroscopy. (Figure 3.4) depicts the ^{1}H NMR spectrum of diamine (DA-1), with data listed in (Table 3.8).

A triplet at 0.8 ppm for three protons is attributed to the terminal methyl (7) of the alkoxy chain. A multiplet at 1.6 ppm is assigned to the two methylene protons (5) of the aliphatic chain. Another triplet at 3.8 ppm corresponds to the two methylene protons (4) next to oxygen. A sharp singlet at 4.8 ppm is attributed to the four N-H protons of the amino group. An upfield doublet at 6.4 ppm ascribes to the four aromatic protons (1) of TPA ortho to the amino group. Another signal at 6.6 ppm corresponds to the four aromatic protons (2) of TPA unit meta to the amino group. A downfield signal at 6.7 ppm belongs to the four aromatic protons (3) of the phenoxy ring. A multiplet at 1.3 ppm is assigned to the remaining methylene protons (6) of the alkoxy chain.

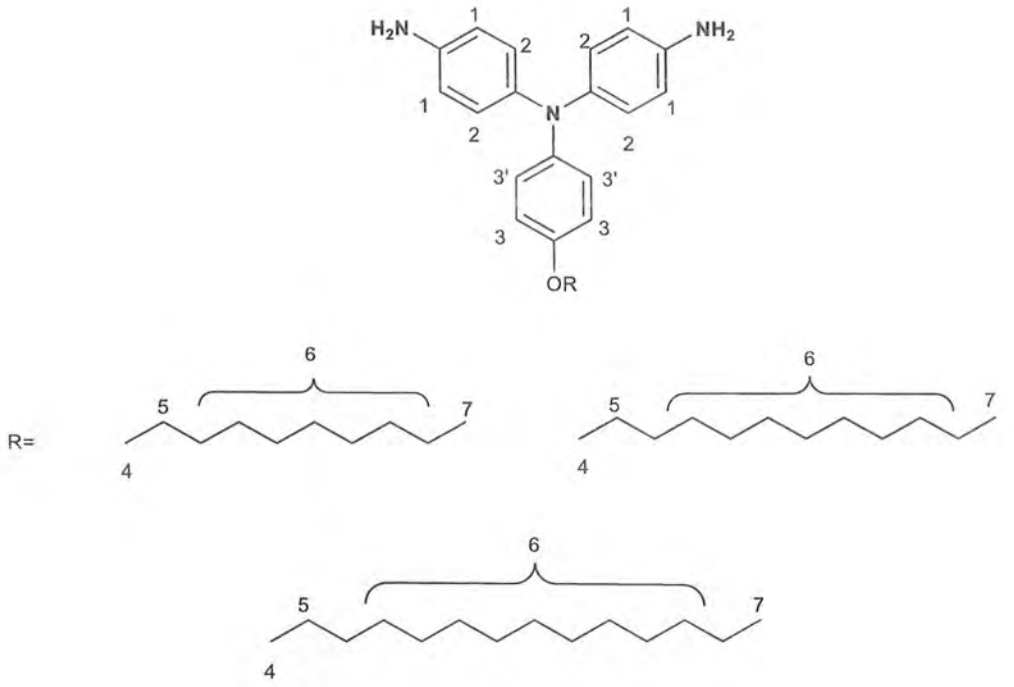

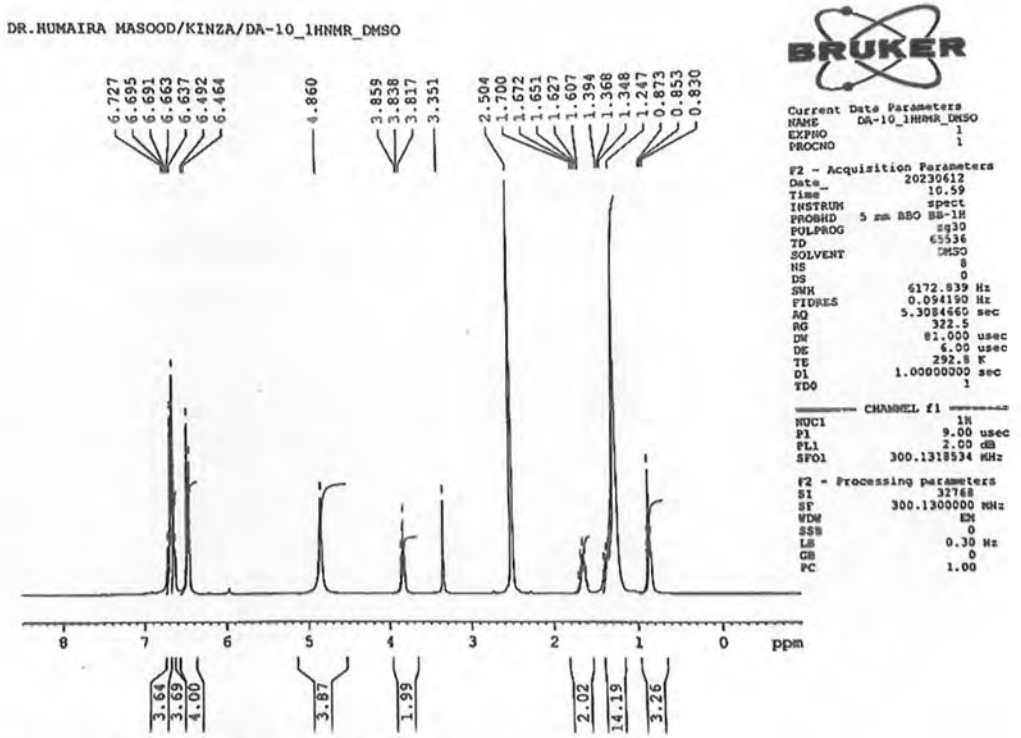

Fig 3.4: ^{1}H-NMR spectrum of diamine (DA-1)

Table 3.8: ^{1}H NMR data of diamine (DA 1-3)

Compound	Protons	Chemical shift δ(ppm)	Multiplicity	Integration	*J* (Hz)
DA-1	3,3'	6.72	m	4	-
	2	6.63	d	4	^{3}J=7.8
	1	6.47	d	4	^{3}J= 8.4
	4	3.83	t	4	^{3}J= 6.3
	5	1.7	m	2	-
	6	1.39-1.24	m	14	-
	7	0.85	t	3	^{3}J= 6.0
	Amine	4.86	s	4	-
DA-2	2,3'	6.94-6.86	m	6	-
	3	6.76	d	2	^{3}J= 9.0
	1	6.60	d	4	^{3}J= 8.7
	4	3.93	t	2	^{3}J= 6.6
	5	1.81-1.72	m	2	-
	6	1.50-1.28	m	18	-
	7	0.90	t	3	^{3}J= 6.9
	Amine	3.51	s	4	
DA-3	2,3'	6.94-6.80	m	6	-
	3	6.74	d	2	^{3}J= 9.1
	1	6.62	d	4	^{3}J= 8.5
	4	3.95	t	2	^{3}J= 6.5
	5	1.88-1.72	m	2	-
	6	1.52-1.20	m	22	-
	7	0.93	t	3	^{3}J= 6.5
	Amine	3.43	s	4	-

The structure elucidation of diamine (DA-1) was further established by ^{13}C-NMR as shown in (Figure 3.5). An upfield signal at 14.4 ppm corresponds to the terminal methyl carbon (7) of the alkoxy chain. Another signal at 31.7 ppm is assigned to the methylene carbon (6) of the aliphatic chain. While the signal at 68.4 ppm belongs to the methylene carbon (5) next to oxygen. A downfield signal at 152.6 ppm ascribes to the quaternary (13) ipso carbon of the phenoxy ring and the signal at 144.8 ppm corresponds to the quaternary ipso carbon (10) of the amino group. The signal at 143.3 ppm is assigned to the quaternary carbon (12) para to the alkoxy chain. While the rest of the signals in the aromatic region correspond to their respective aromatic carbons. An upfield signal at 22-29 ppm ascribes to the methylene carbon (8) of the alkoxy chain.

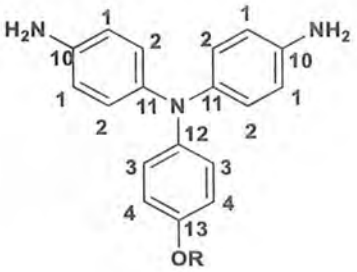

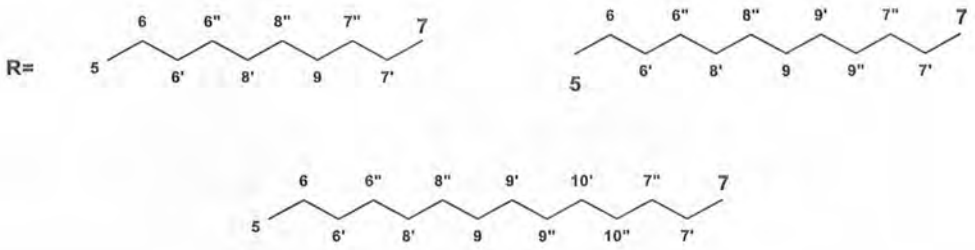

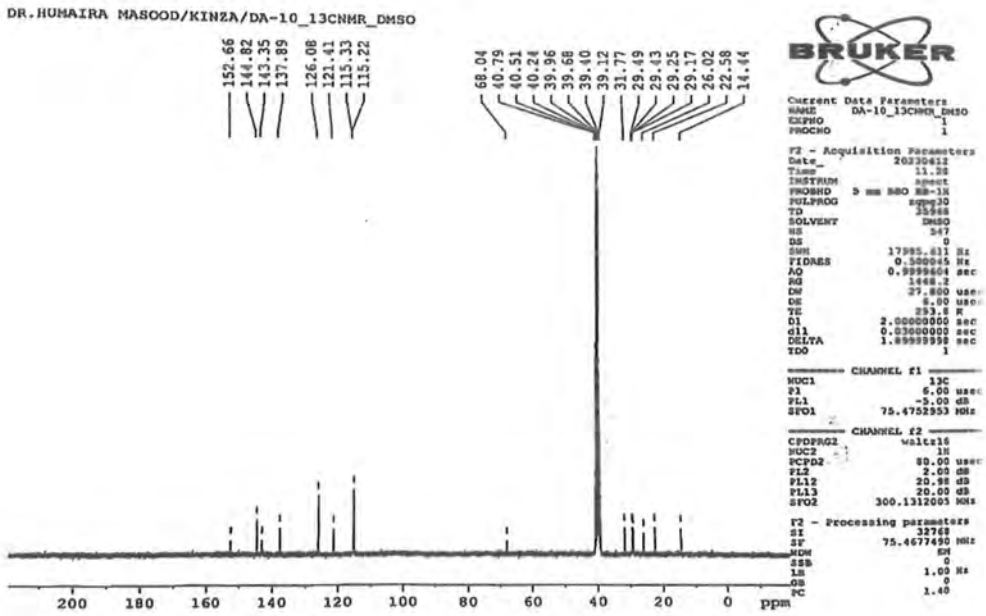

Fig 3.5: ^{13}C-NMR spectrum of diamine (DA-1)

Table 3.9: ^{13}C NMR data of diamine (DA 1-3)

Carbons	Chemical shifts δ (ppm)		
	DA-1	DA-2	DA-3
13	152.66	153.97	153.71
10	144.82	141.24	144.56
12	143.35	140.59	140.62
11	137.89	134.74	136.53
3	126.08	125.23	124.32
2	121.41	123.86	121.71
1	115.33	116.09	115.64
4	115.22	114.95	114.99
5	68.04	68.29	68.34
6	31.7	31.94	31.65
6'	29.50	29.50	29.43
6"	29.40	29.46	29.41
8,8'	29.34	29.31	29.32
9	29.17	29.22	29.22
9'	-	29.18	29.18
9"	-	28.32	28.23

10'	-	-	28.16
10"	-	-	27.6
7"	26.02	26.06	26.01
7'	22.58	22.71	22.65
7	14.44	14.41	14.34

3.2 Synthesis and characterization of Polyimides from synthesized diamines having *n*-alkoxy pendant groups DA-1, DA-2

The polyimides were synthesized using a two-step polycondensation technique. In-first step, synthesized diamines were reacted with different dianhydride in the presence of DMAc as solvent. Ring-opening of dianhydride took place due to the nucleophilic attack of amine nitrogen. Polyamic acid was formed as an intermediate which was indicated by the increase in the viscosity of the reaction mixture. Thermal imidization of polyamic acid to polyimides was carried out in the second step, with the loss of water by the condensation process. (Scheme 3.2) represents the synthesis of polyimides.

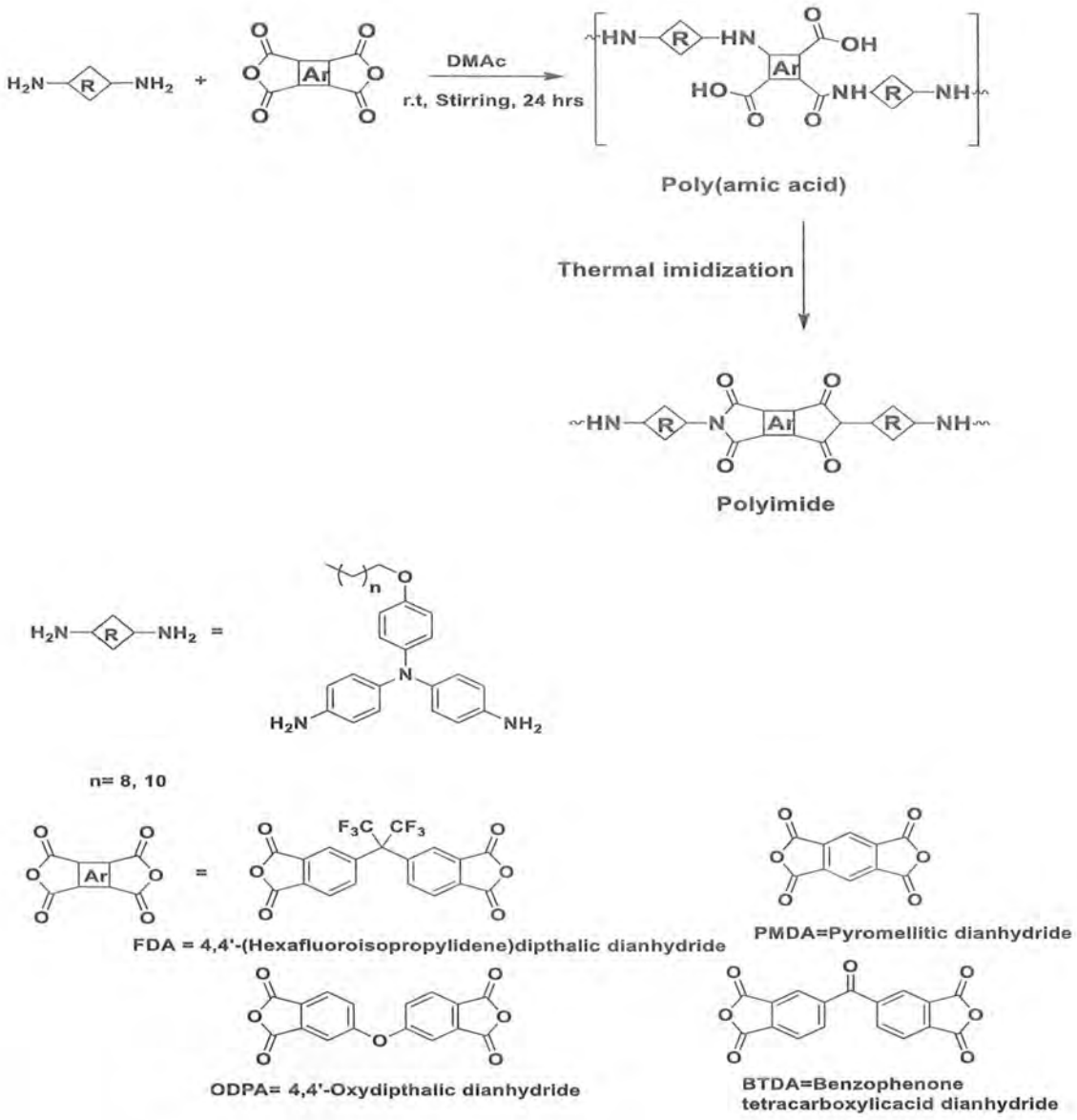

Scheme 3.2: Synthetic route for polyimides having *n*-alkoxy pendant group

Table 3.10: Structure and codes of polyimides synthesized from diamines

S.NO.	Reactants	Structure of Polyimides	Code
1	DA-1, 6-FDA	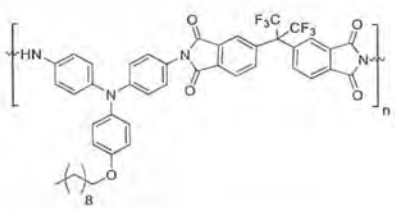	DA1-F

2	DA-1, BTDA	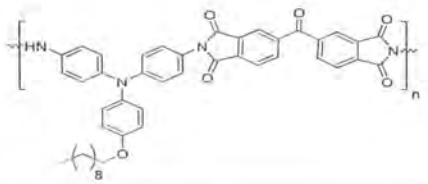	DA1-B
3	DA-1, OPDA	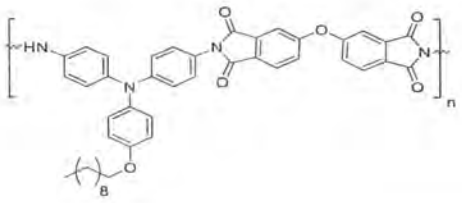	DA1-O
4	DA-1, PMDA	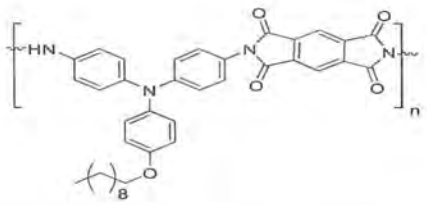	DA1-P
5	DA-2, 6-FDA	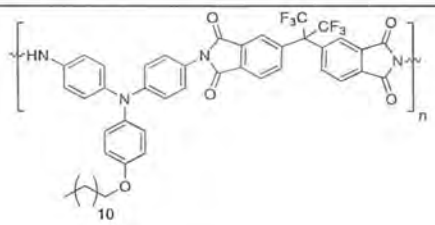	DA2-F
6	DA-2, BTDA	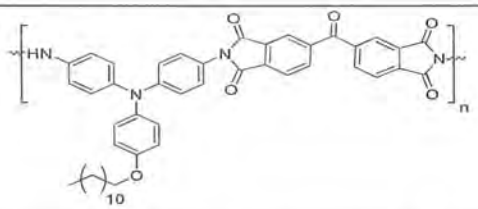	DA2-B
7	DA-2, OPDA	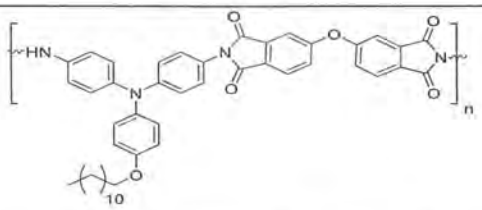	DA2-O
8	DA-2, PMDA	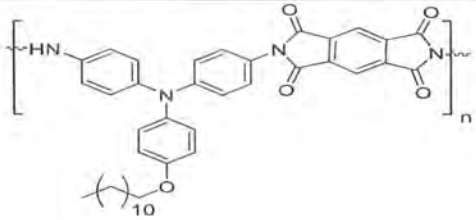	DA2-M

3.2.1 Characterization of DA-1 (*N,N*-bis(4-aminophenyl)decyloxyaniline) based polyimides

Different spectroscopic techniques, cyclic voltammetry, and XRD analysis were carried out to characterize polyimides.

3.2.1.1 FTIR spectral analysis of polyamic acid and polyimides (PAA-O, & DA1-O)

FTIR spectral analysis was carried out to confirm the formation of polyimide films. The bands at various wavenumbers (cm^{-1}) were observed and assigned to their respective functional groups. (Figure 3.6) shows the FTIR spectra of Polyamic acid and polyimides PAA-O and DA1-O.

A broad band of O-H around 3415-3200 ($cm^{-1)}$ in PAA-O and at 1618 ($cm^{-1)}$ for amide C=O stretching, are the primary indications of the polyamic acid characteristics bands. Disappearance of broad O-H band in the IR spectrum of polyimide (DA1-O) after thermal curing and appearance of peaks at 1776 (cm^{-1}) for carbonyl asymmetric stretching and 1720 (cm^{-1}) for carbonyl symmetric stretching, 1366 (cm^{-1}) for C-N stretching, and at 742 (cm^{-1}) assigns to carbonyl bending, that is the primary indication of polyimide absorption bands, indicated that PAA was successfully converted to PI.

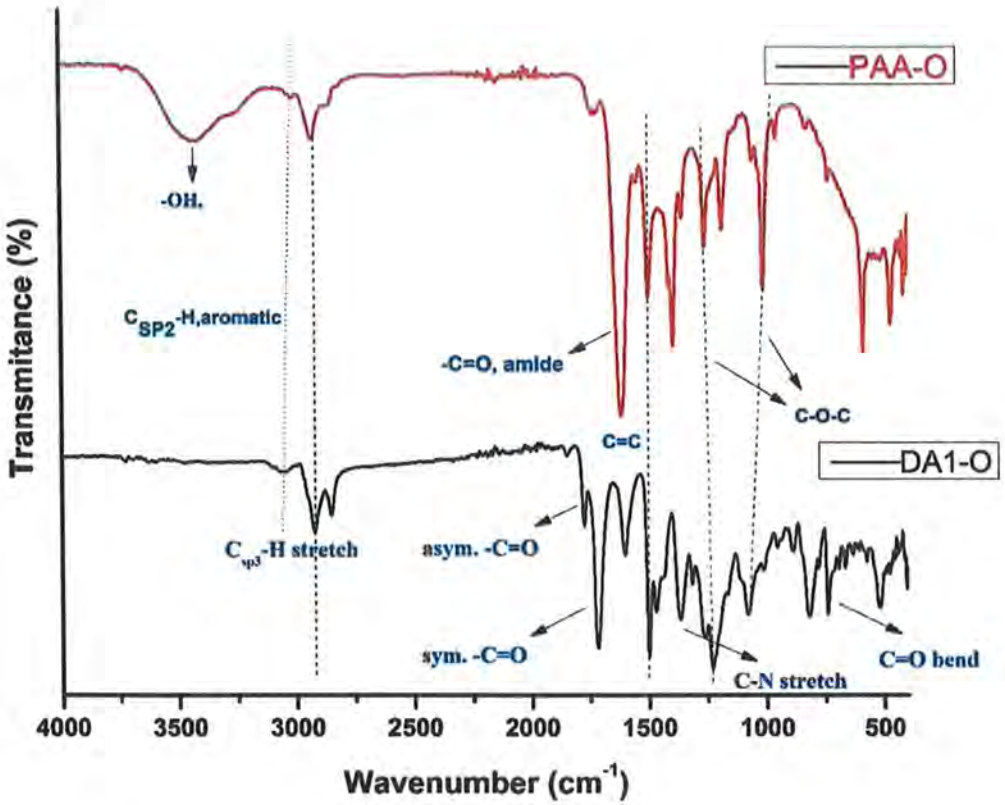

Fig 3.6: FTIR spectra of polyamic acid (PAA-O) and polyimide (DA1-O)

. **Table 3.11:** FTIR spectral data of polyamic acid (PAA-O) and polyimide (DA1--O)

	$\bar{\upsilon}$ (cm^{-1})					
Functional Groups	**OH, amic acid**	**C=O, str. imide**	**C-N, imide**	**C=C, aromatic**	**C-O-C, ether**	**Imide ring def.**
PAA-O	3415-3200	-	-	1507	1259,1011	-
DA1-O	-	1776,1720	1366	1496	1227,1071	742

3.2.1.2 FTIR spectral analysis of polyimides synthesized from DA-1

FTIR spectra of polyimides were obtained to confirm the formation of polyimide films. Signals at various wavenumbers (cm^{-1}) were observed and assigned to their respective

functional groups. (Figure 3.7) shows the FTIR spectra of polyimides DA1-B, DA1-0 & DA1-F.

Table 3.12 represents the spectral data of DA1-O, DA1-B & DA1-F. The asymmetric and symmetric stretching bands for imide carbonyl in DA1-O were observed at 1776 (cm^{-1}) and 1720 (cm^{-1}) respectively. But in the case of DA1-F, these characteristic peaks were observed at 1780 (cm^{-1}) and (1721cm^{-1}). All other functional groups were observed at their respective stretching frequency as indicated by their spectrum.

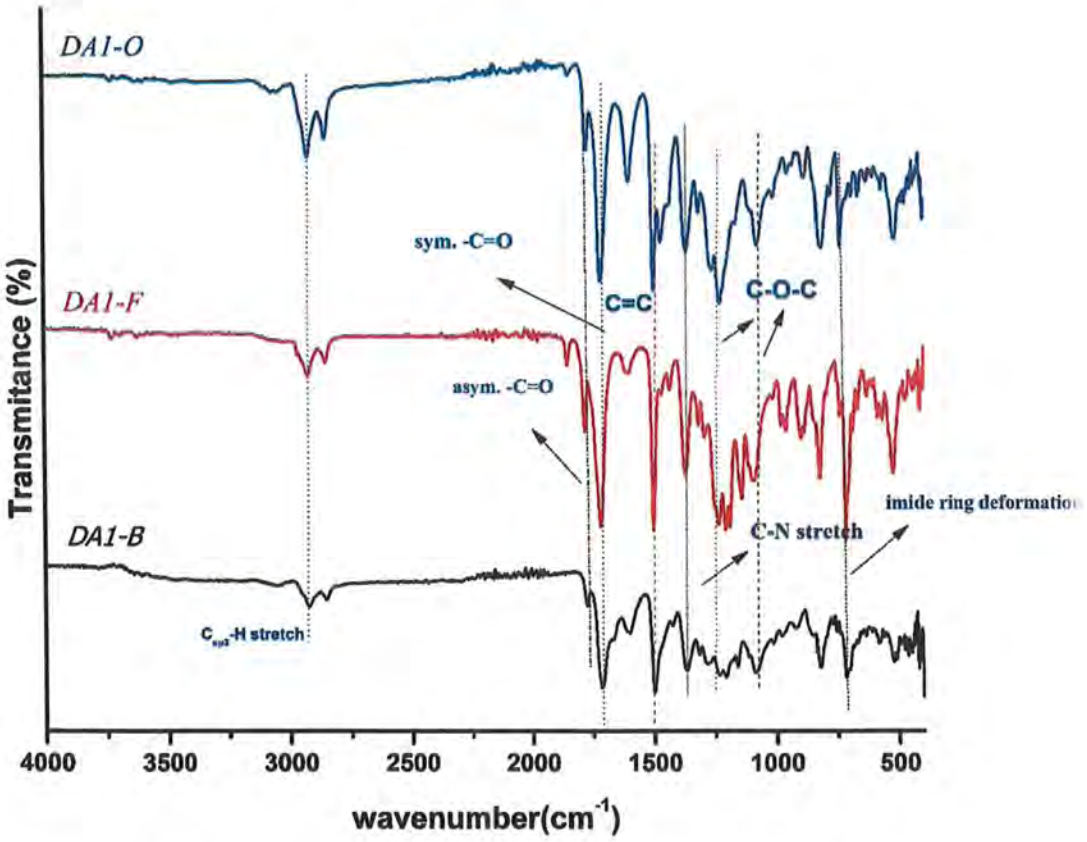

Fig 3.7: FTIR spectra of polyimides synthesized from DA-1

Table 3.12: FTIR spectral data of polyimides synthesized from DA-1

Band assignment :	**$\bar{\upsilon}$ (cm^{-1}) DA1-O**	**$\bar{\upsilon}$ (cm^{-1}) DA1-B**	**$\bar{\upsilon}$ (cm^{-1}) DA1-F**
C_{sp}^3-H (str.)	2932, 2848	2934, 2847	2939, 2846
C=O (imide)	1781(asym), 1711(sym)	1782(asym), 1706(sym)	1788(asym), 1714(sym)
C=C(aromatic)	1497	1495	1500
C-N (imide)	1361	1374	1355
C-O-C (asym)	1238	1245	1231
C-O-C (sym)	1075	1078	1083
Imide ring Deformation	737	723	716

3.2.1.3 XRD analysis of Polyimides (DA1-F, DA1-O, DA1-B, DA1-P) synthesized from DA-1

The XRD diffractogram of polyimides is shown in (Fig 3.8). The amorphous nature of polyimides was disclosed by XRD examination in the 2 θ = 10-80° range, as a highly diffused pattern was observed except in DA1-O which shows semi-crystalline behavior. There is no crystallinity in the polymeric matrix except in the case of DA1-O which were attributed to ether (O) linkages in their backbone, which can influence chain packaging and create ordered domains. Although C-CO-C in BTDA has a larger valance angle than C-O-C in ODPA but due to the greater polarity of CO it interacts strongly and forms a strong network. Based on these two variables, ODPA-based polyimide emerged as the chain with the greatest flexibility. And the polyimide-based on BTDA showed greater stiffness.[147]

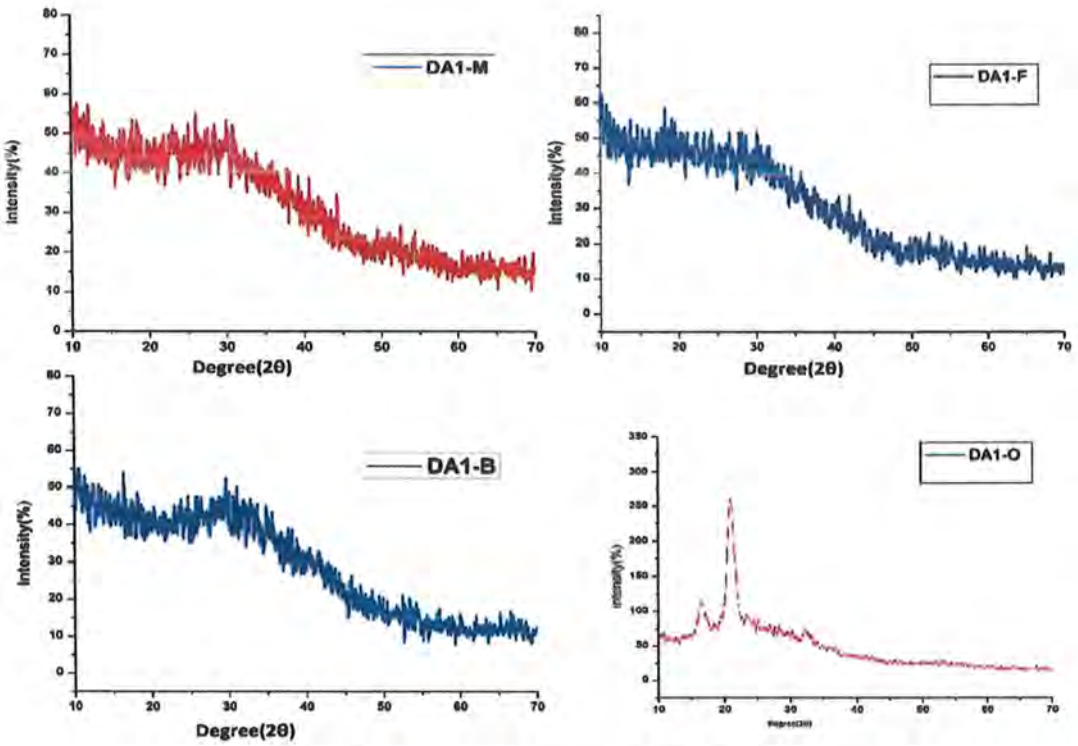

Fig 3.8: XRD pattern of DA-1 based polyimides

3.2.1.4 Organosolubility of polyimides synthesized from DA-1

The solubility of polyimides was checked in various solvents. For this purpose, 10 mg of the polyimide films were dissolved in 1 mL of different organic solvents. It was observed that polyimide films were insoluble in the majority of the organic solvents at ambient temperature but partially or completely soluble upon heating. The solubility of semi-aromatic PI films might be attributed to their alicyclic feature and aggregated structures. The bulky alkyl pendant effectively increased the distance and free volume between molecular chains, and further hindered stacking density of chains.[65] (Table 3.13) illustrates the Solubilization data of polyimide films.

Table 3.13: Solubilization data of DA-1 based polyimides

Codes	DMAc	DMSO	NMP	DMF	THF	m-cresol
DA1-F	++	--	++	--	--	+-
DA1-B	++	--	++	--	--	+-
DA1-O	++	--	++	--	--	+-
DA1-M	++	--	++	--	--	+-

(++) = soluble upon heating, (+-) = partially soluble upon heating, (--) = insoluble on heating

3.2.1.5 Photophysical Properties Polyimides

Photophysical analysis of polyimides was conducted using the ultraviolet-visible (UV-vis) technique. UV-visible absorption spectra of polyimides were measured by making a 10 μM solution in NMP. (Figure 3.9) depicts UV-visible spectra of DA-1 based polyimides, and (Table 3.14) summarizes UV-visible absorption data. Plank's equation was used to calculate energy band gaps.

Strong absorption bands at 310–330 nm were detected which were ascribed to π-π^* transitions of the aromatic ring. A shoulder appeared 320-360 nm was attributed to the n-π^* transition belonging to the non-bonding electron of the ether linkages. Eg values were found in the range of 2.7 to 3.1. The inter- and intra-molecular CT interactions could significantly suppressed due to the introduction of alicyclic moieties, and steric hindrance. The weaker CT interactions can lead to lower absorption intensities, and reduce the likelihood of non-radiative recombination processes, such as exciton quenching, which can be advantageous in reducing heat generation and improving the stability of optoelectronic devices like OLEDs and making them more stable for use in optoelectronic devices.[65]

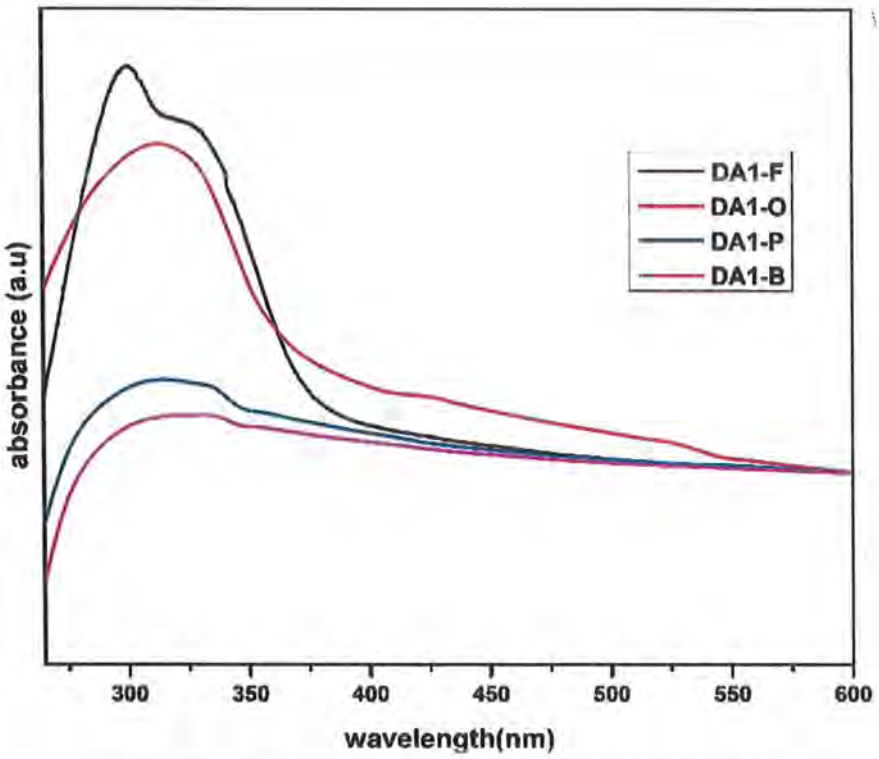

Fig 3.9: UV-vis spectra of DA-1 based polyimides

Table 3.14: UV-vis data DA-1 based polyimides

Sr.No.	Codes	$\lambda_{max, abs}$ (nm)	λ_{onset} (nm)	E_g (nm)
1.	DA1-F	327	390	3.1
2.	DA1-O	316	425	2.9
3.	DA1-P	326	450	2.7
4.	DA1-B	312	400	3.1

3.2.1.6: Electrochemical behavior of DA-1 based polyimides

The electrochemical stability of the synthesized polyimides was studied by measuring the oxidation onset value. The electrolyte used to support the ions was Lithium perchlorate in dry acetonitrile, and 0.1 mM solutions were prepared in NMP solvent. Studies were carried out at room temperature under a nitrogen environment. Polyimides show irreversible electrochemical oxidation behavior. The lack of reduction of

polyimide should be a result of the reduced electron affinity due to the alicyclic structure. The reduction of polyimides can be kinetically slower than their oxidation. This means that even if the reduction is thermodynamically possible, it may not occur readily on the timescale of a typical cyclic voltammetry experiment.[148] To better understand the electronic nature of polymers, the HOMO, LUMO energy gaps (Eg) were calculated using equations 3.1 and 3.2. Figure 3.10 depicts cyclic voltammograms, and the results are mentioned in (Table 3.15). The E_{onset} oxidation potentials of polyimides were found to be in the range of 0.9-1.15 V. The values for HOMO energy levels varied from -5.3 to -5.55. The low E_{onset} oxidation and such high-lying HOMO indicated that these polyimides may be the potential candidates for optoelectronics.

$$E_{HOMO} = -e[E_{onset} + 4.4]v \quad \text{Eq (3.1)}$$

$$E_{LUMO} = E_g - E_{HOMO} \quad \text{Eq (3.2)}$$

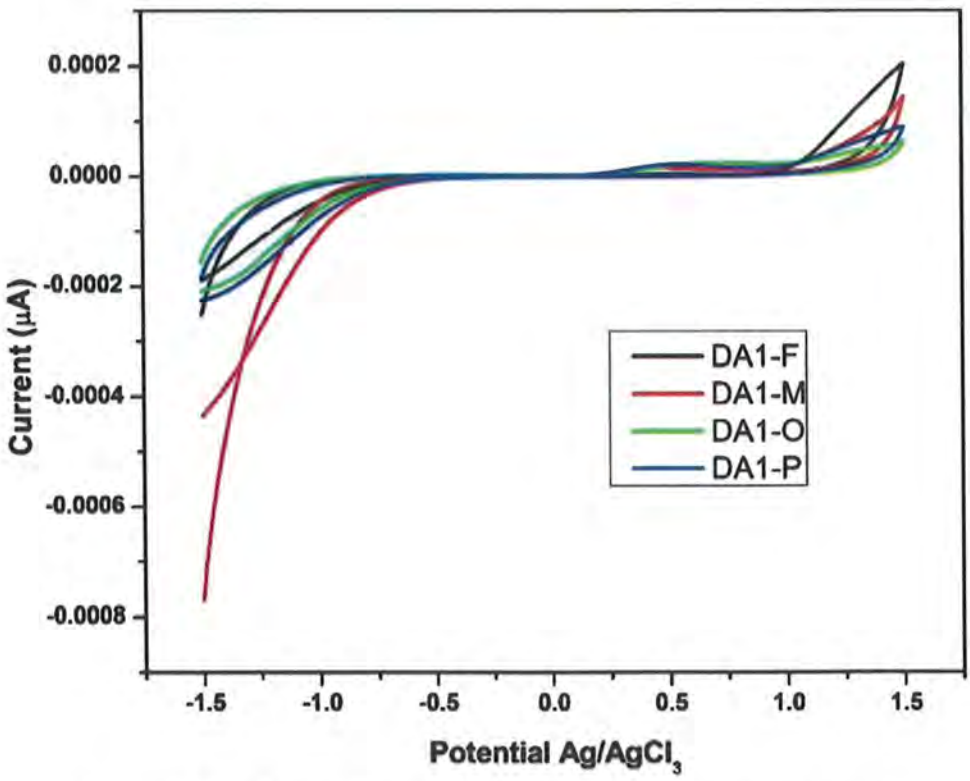

Figure 3.10: Cyclic voltammogram of DA-1 based polyimides

Table 3.15: Electrochemical data of DA-1 based polyimides

Sr.No.	Codes	$E_{onset\ oxi.}$ (V)	E_{HOMO} (eV)	E_{LUMO} (eV)	E_g (eV)
1.	DA1-F	1.06	-5.46	-2.36	3.1
2.	DA1-B	0.9	-5.3	- 2.2	3.1
3.	DA1-O	1.01	-5.41	- 2.51	2.9
4.	DA1-M	1.15	-5.55	-2.65	2.9

3.2.1.7: Differential scanning calorimetry (DSC):

DSC technique was employed to evaluate the glass transition temperature of the prepared polyimides. The glass transition temperature (Tg) of the synthesized linear polyimides was investigated using differential scanning calorimetry in an inert atmosphere. The polyimides not show transition temperature (Tg) in the range of 25-300. DSC analysis showed a high thermal stability up to 300 °C as these compounds had no glass transition temperature due to electroactive sites, i.e triphenylamine units, in their structure.

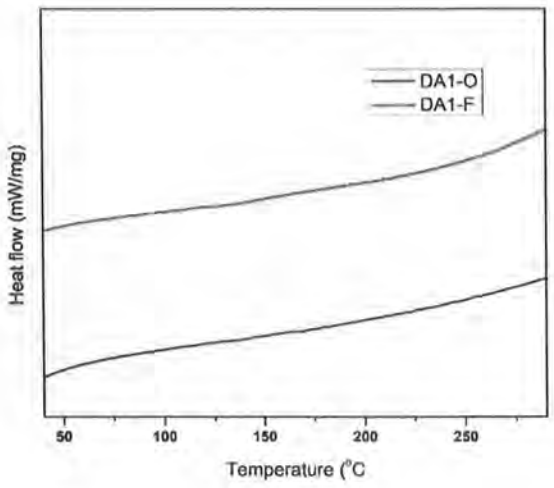

Figure 3.20: DSC of DA-1 based polyimides

3.2.2 Characterization of DA-2 (*N,N*-bis(4-aminophenyl)dodecyloxyaniline) based polyimides

Different spectroscopic techniques, cyclic voltammetry, and XRD analysis were employed to characterize polyimides.

3.2.2.1 FTIR spectral analysis of polyamic acid and polyimides (PAA2-O, & DA2-O)

FTIR spectral analysis was carried out to confirm the formation of polyimide films. The bands at various wavenumbers (cm^{-1}) were observed and assigned to their respective functional groups. Figure 3.11 shows the FTIR spectra of polyamic acid and polyimides PAA2-O & DA2-O respectively.

A broad band of O-H around 3414-3198 (cm^{-1}) in PAA-O and at 1610 (cm^{-1}) for amide C=O, stretching, are the primary indications of the polyamic acid characteristics bands. The disappearance of broad O-H band in the IR spectrum of polyimide (DA1-O) after thermal curing and appearance of bands at 1771 (cm^{-1}) for carbonyl asymmetric stretching and 1707 (cm^{-1}) for carbonyl symmetric stretching, 1363 (cm^{-1}) for C-N stretching, and at 740 (cm^{-1}) assigns to carbonyl bending, which is the primary indication of polyimide absorption bands, indicated that PAA was successfully converted to polyimide.

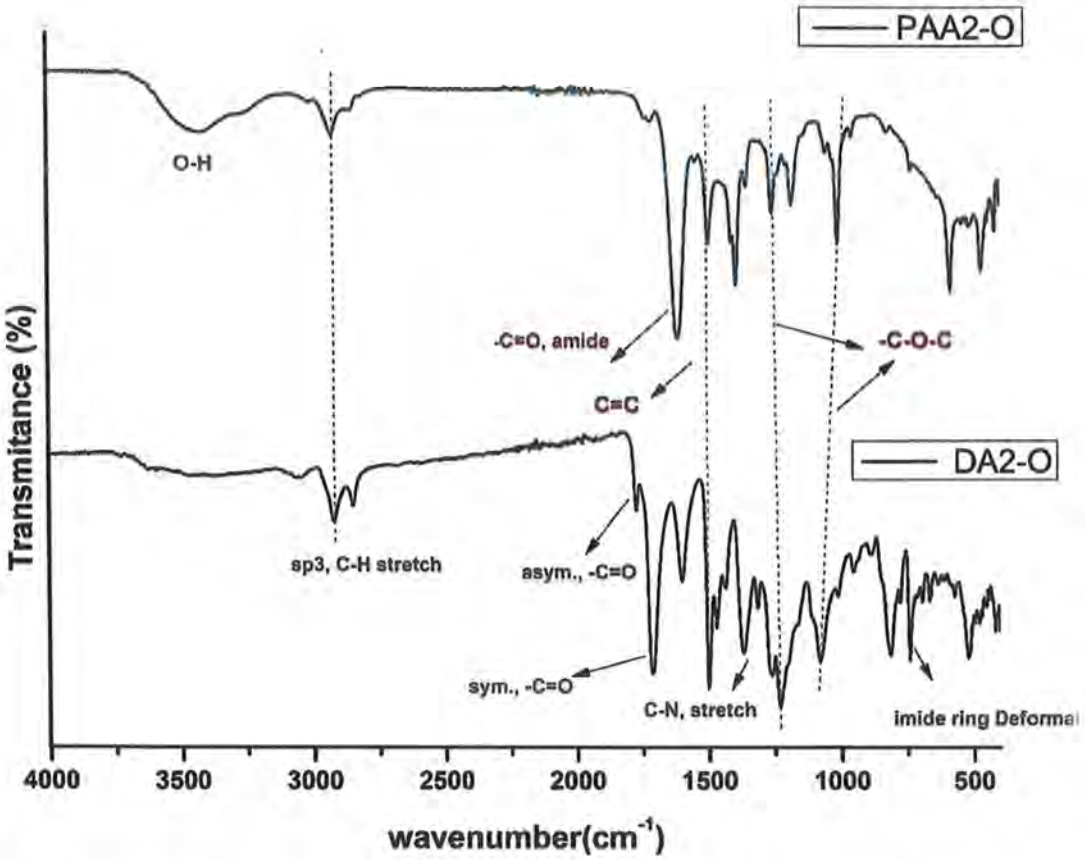

Fig 3.11: FTIR spectra of polyamic acid (PAA2-O) and polyimide (DA2-O)

Table 3.16: FTIR spectral data of polyamic acid (PAA2-O) and polyimide (DA2-O)

	$\bar{\upsilon}$ (cm^{-1})					
Functional Groups	**OH, amic acid**	**C=O, str. Imide**	**C-N, imide**	**C=C, aromatic**	**C-O-C, ether**	**Imide ring def.**
PAA-O	3414-3198	-	-	1507	1257,1017	-
DA1-O	-	1771,1707	1363	1497	1225,1071	740

3.2.2.2 FTIR spectral analysis of polyimides synthesized from DA-2

FTIR spectra analysis was carried out to confirm the formation of polyimide films. Signals at various wavenumbers (cm^{-1}) were observed and assigned to their respective functional groups as depicted in (Figure 3.12). Table 3.17 represents the spectral data of DA1-O, DA1-B & DA1-F. The asymmetric and symmetric stretching bands for imide carbonyl in DA2-O were observed at 1771 (cm-1) and 1713 (cm^{-1}) respectively. But in the case of DA2-F, these characteristic peaks were observed at 1785 (cm^{-1}) and

1717 (cm^{-1}). All other functional groups were observed at their respective stretching frequency as indicated by their spectrum.

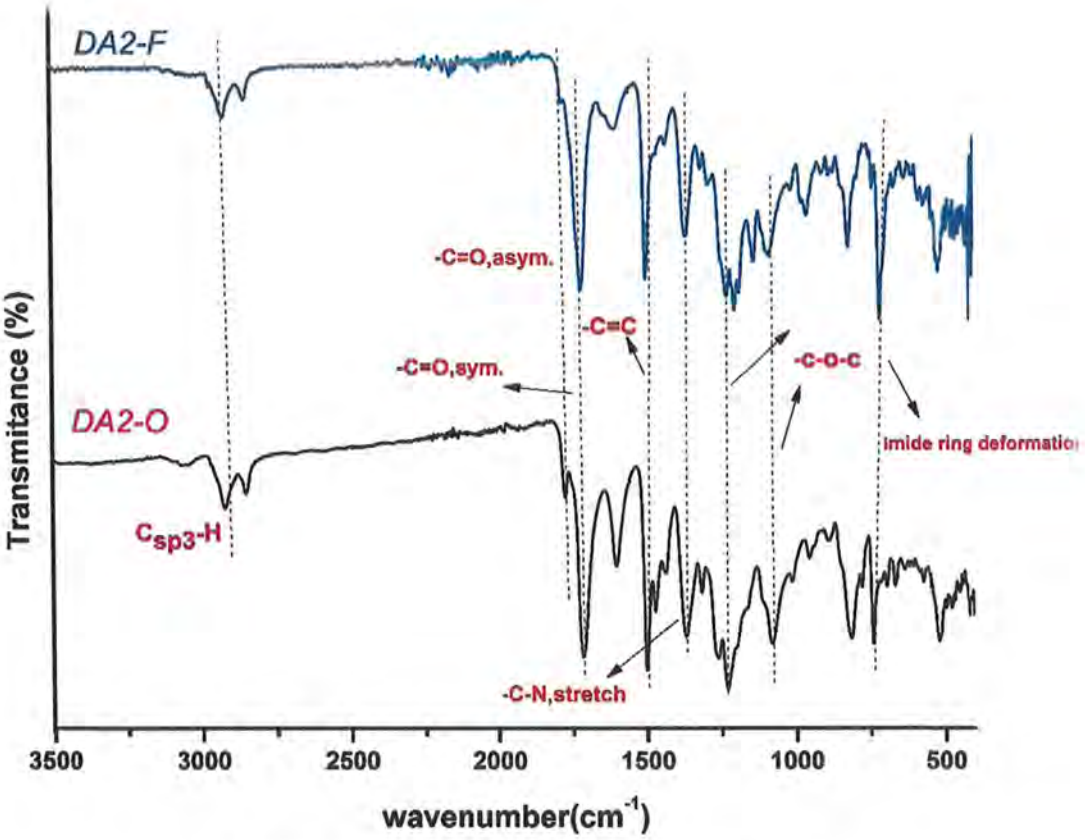

Fig 3.12: FTIR spectra of DA-2 based polyimides

Table 3.17: FTIR spectral data of DA-2 based polyimides

Band assignment :	**$\bar{\upsilon}$ (cm^{-1}) DA2-O**	**$\bar{\upsilon}$ (cm^{-1}) DA2-F**
Csp3-H (stret.)	2933, 2855	2932, 2858
C=O (imide)	1771 (asym), 1713 (sym)	1785 (asym), 1717 (sym)
C=C	1497	1499
C-N (imide)	1364	1362
C-O-C (asym)	1236	1238
C-O-C (sym)	1081	1086
Imide ring Deformation	741	720

3.2.2.3 Organosolubility of DA-2 based polyimides

The solubility of polyimides was checked in various solvents. For this purpose, 10 mg of the polyimide films was dissolved in 1 mL of different organic solvents. It was observed that polyimide films were insoluble in the majority of the organic solvents at ambient temperature but partially or completely soluble upon heating. Table 3.18 illustrates the Solubilization data of polyimide films.

Table 3.18: Solubilization data of DA-2 based polyimides

Codes	DMAc	DMSO	NMP	DMF	THF	m-cresol
DA2-F	++	--	++	--	--	+-
DA2-B	++	--	++	--	--	+-
DA2-O	++	--	++	--	--	+-
DA2-M	++	--	++	--	--	+-

(++) = soluble upon heating, (+-) = partially soluble upon heating, (--) = insoluble on heating

3.2.2.4 Photophysical properties of DA-2 based Polyimides

Photophysical analysis of polyimides was conducted using the ultraviolet-visible (UV-vis) technique. UV-visible absorption spectra of polyimides were measured by making a 10 μM solution in NMP. Figure 3.13 depicts UV-visible spectra of DA-2 based polyimide and (Table 3.19) summarizes UV-visible absorption data. Eg is the molecular orbitals energy gap and can be calculated by (Planck's Equation). Eg values were calculated using equation 2.1.

Strong UV-vis absorption bands at 310–330 nm were detected which were ascribed to π-π^* transitions of aromatic rings. A shoulder appeared 320-360 nm was attributed to the n-π^* transition belonging to the non-bonding electron of the ether linkage. Eg values were found in the range of 2.6 to 2.9. These values are significant for absorbing solar radiation and are expected to have excellent optoelectronic properties.

As given in the literature, the activating groups will increase the energy of HOMO and LUMO which are two primary frontier orbitals. It usually interacts through electron-rich non-bonding orbital and is energetically laying near to HOMO than LUMO, generating a stronger effect on the former particularly, in organic substances. [149-150] So, it is inferred that the presence of the alkoxy side chain increases the electron-donating ability of the triphenylamine unit, resulting in decreasing electrochemical band gap as the chain length increases.

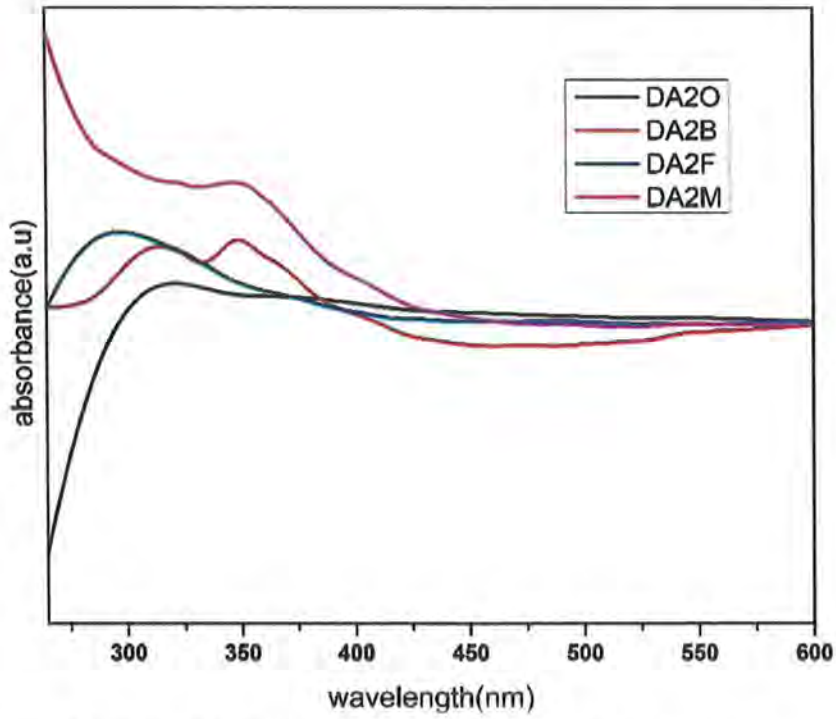

Fig 3.13: UV-vis spectra of DA-2 based polyimides

Table 3.19: UV-vis data of DA-2 based polyimides

Sr.No.	Codes	$\lambda_{max, abs}$ (nm)	λ_{onset} (nm)	E_g (nm)
1.	DA2-F	320	425	2.9
2.	DA2-O	321	495	2.5
3.	DA2-M	319	450	2.7
4.	DA2-B	326	475	2.6

3.2.2.5 Electrochemical behavior of DA-2 based Polyimides

The electrochemical stability of the synthesized polyimides was studied by measuring the oxidation onset value. The electrolyte used to support the ions was Lithium perchlorate in dry acetonitrile, and 0.1 mM solutions were prepared in NMP solvent.

Studies were carried out at room temperature under a nitrogen environment. Polyimides show irreversible electrochemical behavior. The lack of imide reduction of polyimide should be a result of the reduced electron affinity due to the alicyclic structure. The reduction of polyimides can be kinetically slower than their oxidation. This means that even if the reduction is thermodynamically possible, it may not occur readily on the timescale of a typical cyclic voltammetry experiment[148].

To better understand the electronic nature of polymers, the HOMO, LUMO energy gaps (Eg) were calculated using equations 3.1 and 3.2. Figure 3.14 depicts cyclic voltammograms, and the results are mentioned in (Table 3.20). The Eonset oxidation potentials of polyimides were found to be in the range of 1.06-1.12 V. The values for HOMO energy levels varied from -5.46 to -5.52. The low E_{onset} oxidation and such high-lying HOMO indicated that these composites may be potential candidates for optoelectronics.

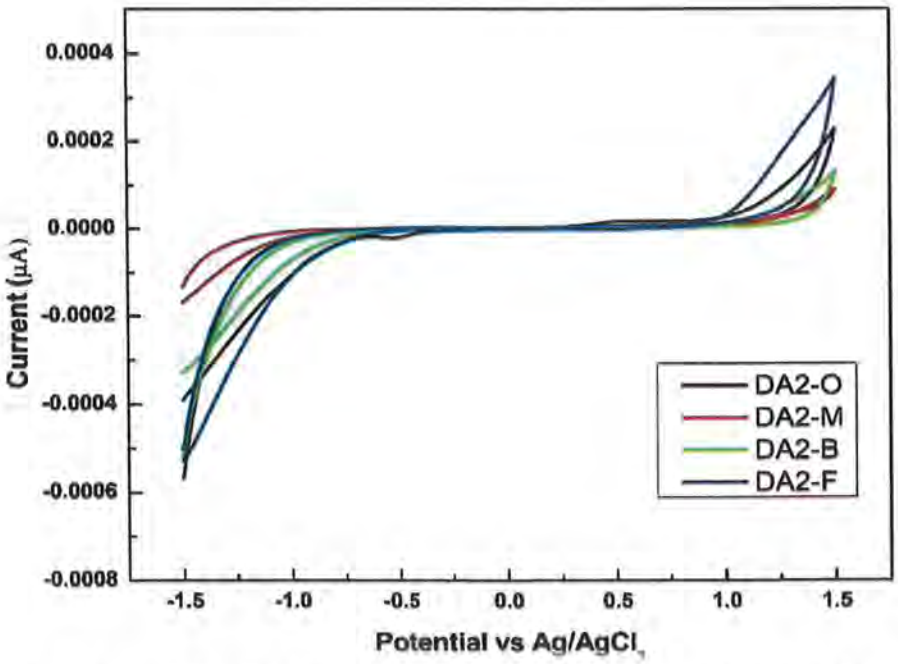

Figure 3.14: Cyclic voltammogram of DA-2 based polyimides

Table 3.20: Electrochemical data of DA-2 based polyimides

Sr.No.	Codes	$E_{onset\ oxi.}$ (V)	E_{HOMO} (eV)	E_{LUMO} (eV)	E_g (eV)
1.	DA2-F	1.08	-5.48	-2.58	2.9
2.	DA2-B	1.09	-5.46	- 2.88	2.6
3.	DA2-O	1.06	-5.46	- 2.96	2.5
4.	DA2-M	1.12	-5.52	-2.82	2.7

Conclusion:

Three triphenylamine-based diamines having alkoxy groups of different chain lengths were successfully synthesized with a relatively good yield. Each of the synthesized diamines was successfully polymerized with four different commercially available dianhydrides, resulting in the formation of eight different polyimides. Synthesized monomers and polyimides were characterized by FTIR, ^{1}H NMR, and ^{13}C NMR spectral analysis, UV-visible, and electrochemical analysis including cyclic voltammetry.

The structural features of synthesized diamines and polyimides were confirmed by ^{1}H NMR, ^{13}C NMR, and FTIR. Completion of thermal curing was confirmed by the disappearance of a broad band around 3415- 3200 (cm^{-1}) and the appearance of characteristic imide carbonyl asymmetric and symmetric stretching at 1770—1785 (cm^{-1}) and 1705-1720 (cm^{-1}) respectively.

XRD analysis demonstrated that all the synthesized polyimides are amorphous except DA1-O which is semi-crystalline. This could be attributed to ether (O) linkages in both the diamine and anhydride backbone, which can influence chain packaging and create ordered domains in resulting polyimide.

The organosolubility data revealed that polyimides showed good organosolubility in dipolar aprotic solvents which include NMP, m-cresol, and DMAc due to the presence of packing disruptive TPA and methylene spacer.

The band gaps calculated by cyclic voltammetry were in the range of 2.6-3.1 eV. Due to the low onset oxidation potential and high laying HOMO – (5.00-6.00) eV, these polyimides can be used in the optoelectronics.

UV-vis data depicted that Eg values were in the range of 2.7-3.1 for DA-1 based polyimides but for DA-2 based polyimides Eg values were found in the range of 2.5-2.9. This effect was due to activating groups usually interacting through electron-rich nonbonding orbital and being energetically laying near to HOMO than LUMO, generating a stronger effect on the former. So, it is inferred that the presence of the alkoxy side chain increases the electron- donating ability of the triphenylamine unit, resulting in decreasing electrochemical band gap as the chain length increases.

So, all these findings lead to the conclusion that:

- The introduction of the *n*-alkoxy pendant group in conjunction with triphenylamine moiety have impact on material morphology and self-assembly behavior.
- Alkoxy groups with different chain lengths in the backbone of polyimides lead to changes in optical and electronic properties.
- The solubility of synthesized polyimides in Organic solvents will facilitate their processing and fabrication.

Future Plans:

- Further characterization of remaining compounds.
- Synthesis of new polyimides with different alkoxy chain lengths to study the structural effect on transition mechanism.
- TGA analysis of the synthesized polyimides to investigate the thermal stability of the polyimides.
- Exploration of polyimides with tailored pendant groups for further optoelectronic applications.

References:

1. Jensen, W. B. The origin of the polymer concept. *J. Chem. Educ.* **2008**, 85 (5), 624.

2. Young, R, J.; & Lovell, P. A. Introduction to polymers. *CRC Press.* **2011,** 15-16.

3. Gaylord, N. G.; & Eirich, F. R. Allyl Polymerization. II. Decomposition of benzoyl peroxide in allyl esters. *J. Am. Chem. Soc.* **1952,** 74 (2), 334-337.

4. Noor, R. M.; Ahmad, Z.; Don, M. M.; & Uzir, M. H. Modelling and control of different types of polymerization processes using neural networks technique. *A Review. J. Chem. Eng.* **2010**, 88 (6), 1065-1084.

5. Chemical & Engineering News. "Facts & figures for the chemical industry." Vol. 70, No. **1992**.26, June 29, 62-63.

6. Belgacem, M. N.; & Gandini, A. Monomers, polymers and composites from renewable resources. *Elsevier.* **2011.**

7. Saldívar, E.; & Vivaldo, E. Introduction to polymers and polymer types: Handbook of polymer synthesis, characterization, and processing. *John Wiley & Sons.* **2013**, 1-14.

8. Satturwar, P.M.; Fulzele, S.V.; & Dorle A.K. Biodegradation and in vivo biocompatibility of rosin: A natural film-forming polymer. *AAPS Pharm. Sci. Tech.* **2003**, 4: 1-6.

9. Nishiyama, Y.; Langan, P.; & Chanzy, H. Crystal structure and hydrogen- bonding system in cellulose Iβ from synchrotron x-ray and neutron fiber diffraction. *J. Am, Chem. Soc.* **2002**, 124(31), 9074–9082.

10. Kulkarni Vishakha, S.; Butte Kishor, D.; Rathod Sudha, S. Natural polymers–A comprehensive review. *Int. J. Res. Pharm. Biomed. Sci.* **2012**, *3*(4), 1597-1613.

11. Fisher, H. L. Vulcanization of rubber vulcanization of rubber. *Ind. Eng. Chem. Res.* **1993,** *31*(11), 1381-1389.

12. *Bijker, Wiebe, E. "The Fourth Kingdom: The social construction of bakelite". cambridge, MIT Press.* ***1997****, 101–198.*

13. Lendlein, A.; Rehahn, M.; Buchmeiser, M. R.; & Haag, R. Polymers in biomedicine and electronics. *Macromol. Rapid. Commun.* **2010,** 31(17), 1487-91.

14. Maitz, M. F. Applications of synthetic polymers in clinical medicine. *Biosurface Biotribology*, **2015,** 1(3), 161-176.

15. Liu, F.; & Wang, X. Synthetic polymers for organ 3D printing *polymers*. **2020**, 12(8), 1765.

16. Fuller, C. S. The investigation of synthetic linear polymers by x-rays. *Chem. Rev.* **1940**, *26*(2), 143-167.

17. Gaborieau, M.; & Castignolles, P. Size-exclusion chromatography (SEC) of branched polymers and polysaccharides. *Anal. Bioanal. Chem.* **2011,** Vol. 399, 1413-1423.

18. Nielsen, L. E. Cross-linking–effect on physical properties of polymers. *J. Macromol. Sci.* **1969**, 3(1), 69-103.

19. Li, C.; & Strachan, A. Molecular scale simulations on thermoset polymers: A review. *J. Polym. Sci., part B: Poly. Phys.* **2015**, 53(2), 103-122.

20. Freitag, D.; Fengler, G.; & Morbitzer, L. Routes to new aromatic polycarbonates with special material properties. *Angew. Chem., Int. Ed. Engl.* **1991**, 30(12), 1598-1610.

21. Björkner, B. Plastic materials. *Textbook of contact dermatitis*. **1995**, 539-572.

22. Tsao, C. W.; & DeVoe, D. L. Bonding of thermoplastic polymer microfluidics. *Microfluid. Nanofluidics.* **2009**, 6(1), 1-16.

23. Mohanty, A. K.; Misra, M.; & Drzal, L. T. Natural fibers, biopolymers, and biocomposites. *CRC press*. **2005**, pp 347.

24. Bobo, E. Development of a controllable polymer system using interpenetrating networks, Mechanical (and Materials). *Engineering–Dissertations, Theses, and Student Research*. **2013,** pp 53.

25. Webster, O. W.; Hertler, W. R.; Sogah, D. Y.; Farnham, W. B.; & RajanBabu, T. V. Group-transfer polymerization. A new concept for addition polymerization with organosilicon initiators. *J. Am. Chem. Soc.* **1983**, 105(17), 5706-5708.

26. Warden, R. B.; & Amundson, N. R. Stability and control of addition polymerization reactions: A theoretical study. *Chem. Eng. Sci.* **1962**, 17(10), 725-734.

27. Flory, P. J. Fundamental principles of condensation polymerization. *Chem. Rev.* **1946**, 39(1), 137-197.

28. Baekleland, L.H. The synthesis, constitution, and uses of Bakelite. *J. Ind. Eng. Chem.* **1909**, 1(3), 149-161.

29. Secor, R. M. The kinetics of condensation polymerization. *AIChE J.* **1969**, *15*(6), 861-865.

30. Chavarria, F., & Paul, D. R., Comparison of nanocomposites based on nylon 6 and nylon 66. *Polymer.* **2004**, 45(25), 8501-8515

31. Hurley, P. E. History of natural rubber. *J. Macromol. Sci.* **1981**, 15(7), 1279-1287.

32. Feldman, D. Polymer history. *Des. Monomers Polym.* **2008**, 11(1), 1-15.

33. Frey, H.; & Johann, T. Celebrating 100 years of "polymer science": Hermann Staudinger's 1920 manifesto. *Polym. Chem.* **2020**, 11(1), 8-14.

34. Sroog, C. E. Polyimides. *Prog. Polym. Sci.* **1991**, 16(4), 561-694.

35. Bryant, R. G. Polyimides. *Ency. polym. Sci. technol.* **2002**, 640-645.

36. Ghosh, A.; Sen, S. K.; Banerjee, S. Solubility improvements in aromatic polyimides by macromolecular engineering. *RSC Adv.* **2012**, 2(14), 5900-5926.

37. Hergenrother, P. M. The use, design, synthesis, and properties of high performance high temperature polymers: An overview: *High Perform. Polym.* **2003**, 15(1), 3-45.

38. Xu, Z.; Croft, Z. L.; Guo, D.; & Cao, K. Recent development of polyimides: synthesis, processing, and application in gas separation. *J. Polym. Sci.* **2021**, 59(11), 943-962.

39. Jamshidian M.; Tehrany EA.; & Imran M. Poly-lactic acid: Production, applications nanocomposites, and release studies. *Compr. Rev. Food Sci. Food Saf.* **2010**, Vol. 9, 552-571.

40. Lopez-Rubio A.; Gavara R.; & Lagaron J. M. Bioactive packaging: Turning foods into healthier foods throughbiomaterials. *Trends Food Sci. Technol.* **2006**, 17: 567-575.

41. .Alfei S.; Schito, AM.; & Zuccari, G. Biodegradable and compostable shopping bags under investigation by FTIR spectroscopy. *Appl. Sci.* **2021**, 11: 621.

42. Xia, J.; Liu, S.; Pallathadka, P. K.; Chng, M. L.; & Chung, T. S. Structural determination of extem and its gas permeability comparison with polysulfone and ultem via molecular simulation. *Ind. Eng. Chem. Res.* **2010**, 49(23), 12014-12021.

43. Yung, K. C.; & Zeng, D. W. Laser ablation of upilex-S polyimide: influence of laser wavelength on chemical structure and composition in both ablated area and halo. *Surf. Coat.Technol.* **2001**, 145(1-3), 186-193.

44 .Su, J.; & Lua, A. C. Effects of carbonisation atmosphere on the structural characteristics and transport properties of carbon membranes prepared from Kapton polyimide. *J. Membr. Sci.* **2007,** 305(1-2), 263-270.

45. Ohya, H.; Kudryavtsev, V.V.; & Semenova, S.I. Polyimide membranes, applications, fabrications, and properties. *Kodansha Ltd: Tokyo, Japan.* **1996,** 232-267.

46. Ruan, K.; Guo, Y.; & Gu, J. Liquid crystalline polyimide films with high intrinsic thermal conductivities and robust toughness. *Macromolecules*. **2021**, 54, 4934–4944.

47. Zhou, Y.; Zhang, S.Y.; Zheng, F.; & Lu, Q.H. Intrinsically black polyimide with retained insulation and thermal properties. *Macromolecules.* **2021**, 54, 9307–9318.

48. Zhao, H.; Yin, J.H.; Liu, X.X.; & Feng, Y. Polyimide-based composite film synergistically modulated via a nano-micro multidimensional filler system toward insulation flexible device applications. *Macromol. Chem. Phys.* **2021**, 222(4), 2000376.

49. Zhang, X.D.; Dong, J.W.; Pan, D.; & Yang, G. Constructing dual thermal conductive networks in electrospun polyimide membranes with highly thermally conductivity but electrical insulation properties. *Adv. Compos. Hybrid Mater.* **2021**, *4, 1102–1112.*

50. Sun, X.; Chi, M.H.; Weng, L.; & Shi, J.H. Excellent electrical performance and thermal properties insulation paper based on polyimide porous fiber membrane modified by nano-SiO_2. *J. Mater. Sci. Mater. Electron.* **2021**, *32*, 26548–26554.

51. Schander, A.; Gancz, J. M.; Tintelott, M.; & Lang, W. Long-term stable polyimide-based flexible electrical insulation for chronically implanted neural electrodes. *Micromachines.* **2021**, *12*, 1279.

52. Hui, H. L.; Li, Y. P.; Feng, Y.; & Li, J. L. Low-content metal-organic framework enhanced interface effect to improve the insulation properties of polyimide-based composite films. *Polym. Adv. Technol.* **2022**, 1–10.

53. Li, C.; Wang, Y.; Yin, Y.; & Li, Y. A comprehensive study of pyrazine-contained and low-temperature curable polyimide. *Polymer.* **2021**, 228, 1239-63.

54. Sui, Y.; Li, J.; Wang, T.; & Sun, D. Low temperature curing polyimides with covalent-boned 5-aminobenzimidazole. *Polymer.* **2021**, 218, 123-514.

55. Gouzman, I.; Grossman, E.; Verker, R.; & Atar, N. Advances in polyimide-based materials for space applications. *Adv. Mater.* **2019**, 31, 1807-738.

56. Zhang, Y.; Wu, B. H.; Wang, H. L.; & Wu, H. Preparation and characterization of transparent polyimide nanocomposite films with potential applications as spacecraft antenna substrates with low dielectric features and good sustainability in atomic-oxygen environments. *Nanomaterials.* **2021**, 11, 1886.

57. Zhang, K.; Zheng, L.G.; Pei, R.; & Chen, L. Light-weight, high-gain antenna with broad temperature adaptability based on multifunctional 3D woven spacer Kevlar/polyimide composites. *Compos. Commun.* **2022**, 30, 1010-61.

58 .Wang, Y.Y.; Sun, W.J.; Yan, D.X.; & Dai, K. Ultralight carbon nanotube/graphene/polyimide foam with heterogeneous interfaces for efficient electromagnetic interference shielding and electromagnetic wave absorption. *Carbon.* **2021**, 176, 118–125.

59. Wang, C.; Ma, S.; Li, D.; & Zhao, J. 3D Printing of lightweight polyimide honeycombs with the high specific strength and temperature resistance. *ACS Appl. Mater. Interfaces.* **2021**, 13, 15690–15700.

60. Pan, X. F.; Wu, B.; Gao, H. L.; & Chen, S. M. Double-layer nacre-inspired polyimide-mica nanocomposite films with excellent mechanical stability for LEO environmental conditions. *Adv. Mater.* **2022**, 34, e2105299.

61. Kim, J.; Kim, G.; Kim, S.Y.; & Lee, S. Fabrication of highly flexible electromagnetic interference shielding polyimide carbon black composite using hot-pressing method. *Compos. Part B Eng.* **2021**, 221, 109010.

62. Cheng, Y.; Zhang, X.; Qin, Y.; & Dong, P. Super-elasticity at 4 K of covalently crosslinked polyimide aerogels with negative Poisson's ratio. *Nat. Commun.* **2021**, 12, 4092.

63. Inagaki, M.; Ohta, N.; & Hishiyama, Y. Aromatic polyimides as carbon precursors. *Carbon,* **2013**, 61, 1-21.

64. Boroglu, M. S.; & Yumru, A. B. Gas separation performance of 6FDA-DAM-ZIF-11 mixed-matrix membranes for H2/CH4 and CO2/CH4 separation. *Sep. Purif. Technol.* **2017**, 173, 269-279.

65. Liu, H.; Zhai, L.; Bai, L.; He, M.; Wang, C.; Mo, S.; & Fan, L. Synthesis and characterization of optically transparent semi-aromatic polyimide films with low fluorine content. *Polymer*. **2019**,163, 106-114.

66. Mathews, A. S.; Kim, I.; & Ha, C. S. Fully aliphatic polyimides from adamantane-based diamines for enhanced thermal stability, solubility, transparency, and low dielectric constant. *J. Appl. Poly.Sci.* **2006,** 102(4), 3316-3326.

67. Hasanain, F.; & Wang, Z. Y. New one-step synthesis of polyimides in salicylic acid. *Polymer*. **2008,** 49(4), 831-835.

68. Chisca, S.; Musteata, V. E.; Sava, I.; & Bruma, M. Dielectric behavior of some aromatic polyimide films. *Eur. Polym. J.* **2011**, 47(5), 1186-1197.

69. Bruma, M.; Damaceanu, M. D.; Constantin, C. P.; & Belomoina, N. M. Study of fluorinated polyimides containing fused aromatic rings. *Rev. Roum. Chim.* **2013,** 58, 121-127.

70. Zhang, S.; Li, Y.; Wang, X.; Zhao, X.; Shao, Y.; & Yang, S. Synthesis and properties of novel polyimides derived from 2, 6-bis (4-aminophenoxy-4′-benzoyl) pyridine with some of dianhydride monomers. *Polymer*, **2005**, 46(25), 11986-11993.

71. Wu, F.; Zhou, X.; & Yu, X. Synthesis and characterization of novel star-branched polyimides derived from 2,2-bis[4-(2,4-diaminophenoxy)phenyl] hexafluoropropane. *RSC adv.* **2017**, 7(57), 35786-35794.

72. Sroog, C. E. History of the invention and development of the polyimides: In Polyimides. *CRC Press.* **2018**, 1-6.

73. Brandom, D. K.; & Wilkes, G. L. Study of the multiple melting behaviour of the aromatic polyimide LaRC CPI-2. *Polymer*, **1994**, 35(26), 5672-5677.

74. Bell, V. L.; Stump, B. L.; & Gager, H. Polyimide structure–property relationships. II. Polymers from isomeric diamines. *J. Polym. Sci.: Polym. Chem. Ed.* **1976**, 14(9), 2275-2291.

75. Lau, K. S. High-performance polyimides and high temperature resistant polymers. *Handbook of thermoset plastics*, **2014**, 15(7), 297-424.

76. Brekner, M. J.; & Feger, C. Curing studies of a polyimide precursor. *J.Polym. Sci. Part A: Polym. Chem.* **1987**, 25(7), 2005-2020.

77. Lavrov, S. V.; Talankina, O. B.; Vorob'yev, V. D.; Izyumnikov, A. L.; & Kardash, I. Y. Kinetics of ring formation of aromatic polyamido-acids with different structure of the dianhydride component. *Polym. Sci. USSR.* **1980**, 22(8), 2069-2074.

78. Zhuang, Y.; Seong, J. G.; Lee, Y. M. Polyimides containing aliphatic/alicyclic segments in the main chains. *Prog. Polym. Sci.* **2019**, 92, 35-88.

79. Vinogradova, S. V.; Vygodskii, Y. S.; Vorob'ev, V. D.; Churochkina, N. A.; Chudina, L. I.; Spirina, T. N.; & Korshak, V. V. Chemical cyclization of poly (amido-acids) in solution. *Polym. Sci. USSR.* **1974**, 16(3), 584-589.

80. Mal'tsev, E. I.; Brusentseva, M. A.; Lypenko, D. A.; Berendyaev, V. I.; Kolesnikov, V. A.; Kotov, B. V.; & Vannikov, A. V. Electroluminescent properties of anthracene-containing polyimides. *Polym. Adv. Technol.* **2000**, 11(7), 325-329.

81. Wang, J., & Lee, P. S. Progress and prospects in stretchable electroluminescent devices. *Nanophotonics*, **2017**, 6(2), 435-451.

82. Sroog, C. E. Polyimides. *Prog. Polym. Sci.* **1991**, 16(4), 561-694.

83. Kurosawa, T.; Higashihara, T.; & Ueda, M. Polyimide memory: a pithy guideline for future applications. *Polym. Chem.* **2013**, 4(1), 16-30.

84. Kaya, İ.; & Kamacı, M. Synthesis, optical, and thermal properties of polyimides containing flexible ether linkage. *J. Appl. Polym. Sci.* **2018**, 135(31), 46573.

85. Rai, V.; Lee, K. P.; Safanama, D.; Adams, S.; & Blackwood, D. J. Oxygen reduction and evolution reaction (ORR and OER) bifunctional electrocatalyst operating in a wide pH range for cathodic application in Li–air batteries. *ACS Appl. Energy Mater.* **2020**, 3(9), 9417-9427.

86. Rosseinsky, D. R.; & Mortimer, R. J. Electrochromic systems and the prospects for devices. *Adv. Mater.* **2001**, 13(11), 783-793.

87. Ruff, A.; Heyer, E.; Roland, T.; Haacke, S.; & Ziessel, R. Electrochemical and optical properties of molecular triads based on triphenylamine, diketopyrrolopyrrole and boron-dipyrromethene. *Electrochim. Acta.* **2015,** *173*, 847-859.

88. Blanchard, P.; Malacrida, C.; Cabanetos, C.; Roncali, J.; & Ludwigs, S. Triphenylamine and some of its derivatives as versatile building blocks for organic electronic applications. *Polym. Int.* **2019**, 68(4), 589-606.

89. Patil, N. M.; Kelkar, A. A.; & Chaudhari, R. V. Synthesis of triarylamines by copper-catalyzed amination of aryl halides. *J. Mol. Catal. A: Chem.* **2004,** 223(1-2), 45-50.

90. Gujadhur, R. K.; Bates, C. G.; & Venkataraman, D.Formation of aryl− nitrogen, aryl− oxygen, and aryl− carbon bonds using well-defined copper (I)-based catalysts. *Org. let.* **2001,** 3(26), 4315-4317.

91. Lambert, C.; & Nöll G. Intervalence charge-transfer bands in triphenylamine-based polymers. *Synth Met.* **2003**, 139, 57–62.

92. Fang Z.; Chellappan V.; Webster R.D.; Ke L.; Zhang T.; & Liu B. Bridged-triarylamine starburst oligomers as hole transporting materials for electroluminescent devices. *J. Mater. Chem.* **2012**, 22: 15397–404.

93. Chou MY.; Mk Leung.; Su YO.; Chiang CL.; Lin CC.; & Liu J. H. Electropolymerization of starburst triarylamines and their application to electrochromism and electroluminescence. *Chem. Mater.* **2004**, 16:654–61.

94. Yuan, K.; Xiang, T.; Hong, J.; Lin, H..; Liou, S.; & Cheng, S. H. Novel trends of electrochemical oxidation of amino-substituted triphenylamine derivatives. *J. Electroanal. Chem.* **2005**, 575:95–101.

95. Natera, J.; Otero, L.; Sereno, L.; Fungo, F.; & Wang, N. S. A novel electrochromic polymer synthesized through electropolymerization of a new donor−Acceptor bipolar system. *Macromol.* **2007**, 40:4456–63.

96. Hsiao, S. H.; Wang, H. M.; & Liao, S. H. Redox-stable and visible/near-infrared electrochromic aramids with main-chain triphenylamine and pendent 3,6-di-tert-butylcarbazole units. *Polym. Chem.* **2014**, 5:2473–83.

97. Quinton, C.; Alain-Rizzo, V.; & Dumas-Verdes, C. Redox-controlled fluorescence modulation (electrofluorochromism) in triphenylamine derivatives. *RSC Adv.* **2014**, 4:34332–42.

98. Sek, D.; Jarzabek, B.; Grabiec, E.; & Kaczmarczyk, B. A study of thermal, optical and electrical properties of new branched triphenylamine-based polyazomethines. *Synth. Met.* **2010**, 160:2065–76.

99. Shirota, Y. Organic materials for electronic and optoelectronic devices Basis of a presentation given at Materials Chemistry Discussion No. 2, 13–15 September 1999, University of Nottingham, UK. *J. Mater. Chem.* **2000,** 10(1), 1-25.

100. Degli, A.; Fattori, V.; Sabatini, C.; Casalbore-Miceli, G.; & Marconi, G. The electron transfer rate of large TPA based compounds: a joint theoretical and electrochemical approach. *Phys. Chem. Chem. Phys.* **2005**, 7(21), 3738-3743.

101. Zhou, L.; Jia, C.; Wan, Z.; Li, Z.; Bai, J.; Zhang, L.; & Zhang, J. Triphenylamine based organic dyes containing benzimidazole derivatives for dye sensitized solar cells. *Dyes Pigm.* **2012**, 95, 743-750.

102. Yen, H. J.; & Liou, G. S. Design and preparation of triphenylamine-based polymeric materials towards emergent optoelectronic applications. *Prog. Polym. Sci.* **2019**, 89, 250-287.

103. Mao, L.; Zhou, M.; Shi, X.; & Yang, H. B. Triphenylamine (TPA) radical cations and related macrocycles. *Chin. Chem. Lett.* **2021**, 32(11), 3331-3341.

104. Thangthong, A. M.; Prachumrak, N.; Tarsang, R.; Keawin, T.; & Jungsuttiwong, S. Blue light-emitting and hole-transporting materials based on 9,9-bis (4-diphenylaminophenyl) fluorenes for efficient electroluminescent devices. *J. Mater. Chem.* **2012**, 22(14), 6869-6877.

105. Lian, X.; Zhao, Z.; & Cheng, D. Recent progress on triphenylamine materials: synthesis, properties, and applications. *Mol. Cryst. Liq.* **21017**, 648(1), 223-235.

106. Oishi, Y.; Ishida, M.; Kakimoto, MA.; Imai, Y.; & Kurosaki T. Preparation and properties of novel soluble aromatic polyimides from 4,4'-diaminotriphenylamine and aromatic tetracarboxylic dianhydrides. *J. Polym. Sci. Part A: Polym. Chem.* **1992**, 30:1027–35.

107. Okamoto.; Tanaka, K.; Kita, H.; Ishida, M.; & Imai, Y. Gas permeability and permselectivity of polyimides prepared from 4,4'-Diaminotriphenylamine. *Polym. J.* **1992**, 24, 451–7.

108. Vasilenko, N. A.; Akhmet'eva, Y. I.; Sviridov, Y. B.; Berendyayev, V. I.; Rogozhkina, Y. D.; & Alkayeva, OF. Soluble polyimides based on 4,4'-diaminotriphenylamine. Synthesis, molecular mass characteristics and solution properties. *Polym. Sci. USSR.* **1991**, 33, 1439–50.

109. Yen, H. J.; & Liou, G. S. Design and preparation of triphenylamine-based polymeric materials towards emergent optoelectronic applications. *Prog. Polym. Sci.* **2019**, 89, 250-287.

110. Huang, C.; Qian, X.; & Li, Y. High-performance aromatic polyimides. *Prog. Polym.* Sci. **2012**, 37(12), 1530-1551.

111. Hill, R. & Walker, E. Polymer constitution and fiber properties. *J. Polym. Sci.* **1948**, 3:609–30.

112. Bell, V. L.; Stump, B. L.; & Gager, H. Polyimide structure–property relationships. II. Polymers from isomeric diamines. *J. Polym. Sci. Part A: Polym. Chem.* **1976**, 14, 2275–91.

113. Cassidy, P. E. Thermally stable polymers: synthesis and propertie. *New York: Marcel Dekker*. **1980**, 393.

114. Clair, T. L. S.; & Yamaki, D. A. U.S. Patent No. 4,398,021. *Washington, DC: U.S. Patent and Trademark Office*.**1983.**

115. Clair, T. L. S.; & Yamaki, D. A. US 4489027 Process for preparing solvent resistant, thermoplastic aromatic poly(imidesulfone). **1984.**

116. Hergenrother, P. M. High performance thermoplastics. *Angew. Macromol. Chem.* **1986**, 145, 323–41.

117. Wilson, D.; & Stenzenberger, H. D.; Hergenrother, P. M. Polyimides. *New York: Springer Netherlands.* **1990**, 297.

118. Yang, H. Kevlar aramid fiber. *New York: John Wiley & Sons.* **1993,** 210.

119. Ghosh, M. K.; & Mittal, K. L. Polyimides: fundamentals and applications. New York: Marcel Dekker; **1996**, 912.

120. Abajo, J.; & Campa, J. G. Processable aromatic polyimides., *Progress in polyimide chemistry I. Heidelberg: Springer.* **1999,** 23–59.

121. Mittal, K. L. Polyimides: synthesis, characterization, and applications. *New York: Plenum.* **1984,** 614.

122. Yang, H.H. Aromatic high-strength fibers. New York: John Wiley & Sons, Inc.; 1989. p. 873. [21] Abadie MJM, Polyimides Mittal B. Other high temperature polymers. *Amsterdam: Elsevier,* **1991,** 320.

123. Yang, H.H. Aromatic high-strength fibers. *New York: John Wiley & Sons, Inc.* **1989**, 873.

124. Abadie, M. J. M. Polyimides Mittal B. Other high temperature polymers. *Amsterdam: Elsevier.* **1991**, 320.

125. Liou, G. S.; Hsiao, S. H.; Ishida, M.; Kakimoto, M.; & Imai, Y. Synthesis and characterization of novel soluble triphenylamine-containing aromatic polyamides based on *N,N'*-bis(4-aminophenyl)-*N,N'*-diphenyl-1,4-phenylenediamine. *J. Polym. Sci. Part A: Polym. Chem.* **2002**, 40, 2810–8.

126. Liou, G.S.; & Hsiao, S. H. Synthesis and properties of new soluble triphenylamine-based aromatic poly(amine amide)s derived from *N,N'*-bis(4-carboxyphenyl)-*N,N'*-diphenyl-1,4-phenylenediamine. *J. Polym. Sci. Part A: Polym. Chem.* **2003**, 41,94–105.

127. Hsiao, S. H.; Chen, C. W.; & Liou, G. S. Novel aromatic polyamides bearing pendent diphenylamino or carbazolyl groups. *J Polym Sci Part A: Polym. Chem.* **2004**, 42:3302–13.

128. Yen, H. J.; & Liou, G. S. Recent advances in triphenylamine-based electrochromic derivatives and polymers. *Polym. Chem.* **2018**, 9:3001–18.

129. Monk, P.; Mortimer, R.; & Rosseinsky, D. Introduction to electrochromism. In: Rosseinsky D, Monk P, Mortimer R, editors. *Electrochromism and electrochromic devices. Cambridge: Cambridge University Press.* **2007**, 1–24.

130. Yen, H. J.; & Liou, G. S. Recent advances in triphenylamine-based electrochromic derivatives and polymers. *Polym. Chem.* **2018**, 9(22), 3001-3018.

131. Lambert, C.; & Nöll, G. Intervalence charge-transfer bands in triphenylamine-based polymers. *Synth. Met.* **2003**, 139:57–62.

132. Fang, Z.; Chellappan, V.; Webster, R. D.; & Zhang, T. Bridged-triarylamine starburst oligomers as hole transporting materials for electroluminescent devices. *J. Mater. Chem.* **2012**, 22:15397–404.

133. Siddique, S. A.; Siddique, M. B. A. ; Hussain, R.; Liu, X.; Mehboob, M. Y.; Irshad, Z.; & Adnan, M. Efficient tuning of triphenylamine-based donor materials for high-efficiency organic solar cells. *Comput. Theor. Chem.* **2020**, 1191, 113045.

134. Yen, H. J.; Guo, S. M.; Yeh, J. M.; & Liou, G. S. Triphenylamine-based polyimides with trimethyl substituents for gas separation membrane and electrochromic applications. *J. Polym. Sci. Part A: Polym. Chem.* **2011**, 49(16), 3637-3646.

135. Bera, D.; Padmanabhan, V.; & Banerjee, S. Highly gas permeable polyamides based on substituted triphenylamine. *Macromolecules*, **2015**, 48(13), 4541-4554.

136. Kuorosawa, T.; Chueh, C. C.; Liu, C. L.; Higashihara, T.; Ueda, M.; & Chen, W. C. High performance volatile polymeric memory devices based on novel triphenylamine-based polyimides containing mono-or dual-mediated phenoxy linkages. *Macromolecules*. **2010**, 43(3), 1236-1244.

137. Lee, T. J.; Chang, C. W.; Hahm, S. G.; Kim, K.; Park, S.; Kim, D. M; & Ree, M. Programmable digital memory devices based on nanoscale thin films of a thermally dimensionally stable polyimide. *Nanotechnology*. **2009**, *20*(13), 135204.

138. Kim, K.; Park, S.; Hahm, S. G.; Lee, T. J.; Kim, D. M.; Kim, J. C.; & Ree, M. Nonvolatile unipolar and bipolar bistable memory characteristics of a high temperature polyimide bearing diphenylaminobenzylidenylimine moieties. *J. Phys. Chem. B.* **2009**, 113(27), 9143-9150.

139. Zhang, W.; Xu, H. J.; Yin, J.; Guo, X. X.; Ye, Y. F.; & Wang, Z. G. Preparation and properties of organosoluble, colorless, and high-pretilt-angle polyimides based on an alicyclic dianhydride and long-main-chain alkyl-group-containing diamines. *J. Appl. Polym. Sci.* **2001**, 81(11), 2814-2820.

140. Lim, H.; Cho, W. J.; Ha, C. S.; Ando, S.; Kim, Y. K.; & Lee, K. Flexible organic electroluminescent devices based on fluorine-containing colorless polyimide substrates. *Adv. Mater.* **2002**, 14(18), 1275-1279.

141. Li, T. L.; & Hsu, S. L. C. Preparation and properties of a high temperature, flexible and colorless ITO coated polyimide substrate. *Eur. Polym. J.* **2007**, 43(8), 3368-3373.

142. Choi, M. C.; Hwang, J. C.; Kim, C.; & Ha, C. S. New colorless substrates based on polynorbornene-chlorinated polyimide copolymers and their application for flexible displays. *J. Polym. Sci. Part A: Polym. Chem.* **2010**, 48(8), 1806-1814.

143. Li, T. L.; & Hsu, S. L. C. Preparation and properties of transparent conductive indium-tin-oxide/polyimide substrates via a sol-gel process. *Thin Solid Films.* **2010**, 518(23), 6761-6766.

144. Liu, J. M.; Lee, T. M.; Wen, C. H.; & Leu, C. M. High-performance organic-inorganic hybrid plastic substrate for flexible displays and electronics. *J. Soc. Inf. Disp.* **2011**, 19(1), 63-69.

145. Mizoguchi, K.; Shibasaki, Y.; & Ueda, M. Development of negative-type photosensitive semi-alicyclic polyimide using a photobase generator. *J. Photopolym. Sci. Technol.* **2007**, 20(2), 181-186.

146. Gui, Y. 1-Dodecyloxy-4-nitrobenzene. *Acta Cryst.* **2009**, 65(12), o3034.

147. Chao, M. Synthesis and characterization of semicrystalline polyimides containing bridged linkages. *Int. J. of Polym. Sci. **2018.***

148. Hsiao, S. H.; Yeh, S. J.; Wang, H. M.; Guo, W.; & Kung, Y. R. Synthesis and optoelectronic properties of polyimides with naphthyldiphenylamine chromophores. *J. Polym. Res.* **2014**, 21, 1-12.

149. Ma, Y.; Hu, C.; Guo, H.; Fan, L.; Yang, S.; & Sun, W. H. Structure effect on transition mechanism of UV–visible absorption spectrum in polyimides: A density functional theory study. *Polymer*, **2018**, 148, 356-369.

150. Vishnumurthy, K. A.; Sunitha, M. S.; & Adhikari, A. V. Synthesis and characterization of thiophene-based donor–acceptor type polyimide and polyazomethines for optical limiting applications. *Polym. bull.* **2013**, 70, 147-169.

151. Tian, Y.; Song, Y.; Yao, H.; Yu, H.; Tan, H.; Song, N.; & Guan, S. Improving resistive switching characteristics of polyimide-based volatile memory devices by introducing triphenylamine branched structures. *Dyes Pigm.* **2019**,163, 190-196.

152. Gong, S.; Liu, M.; Xia, S.; & Wang, Y. Synthesis of novel soluble polyimides containing triphenylamine groups for liquid crystal vertical alignment layers. *J. Polym. Res.* **2014**, *21*, 1-11.